AD-A060 626 ILLINOIS UNIV AT CHICAGO CIRCLE DEPT OF MATERIALS ENG--ETC F/G 8/13
CYCLIC STRENGTH OF UNDISTURBED SANDS FROM NIIGATA, JAPAN.(U)
AUG 78 M L SILVER DACW39-76-M-2407

UNCLASSIFIED WES-TR-S-78-10 NL

1 OF 2
ADA
060626

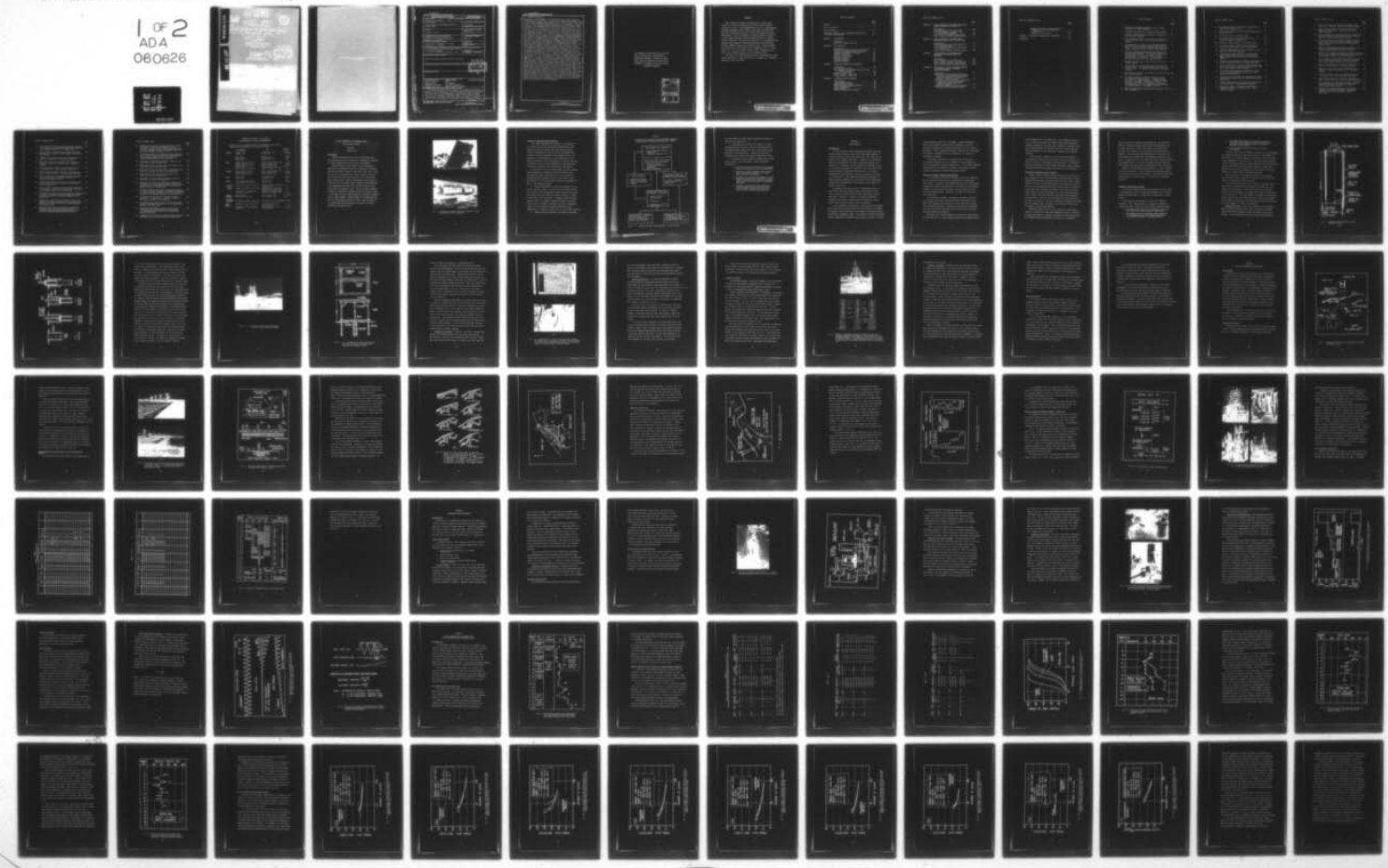

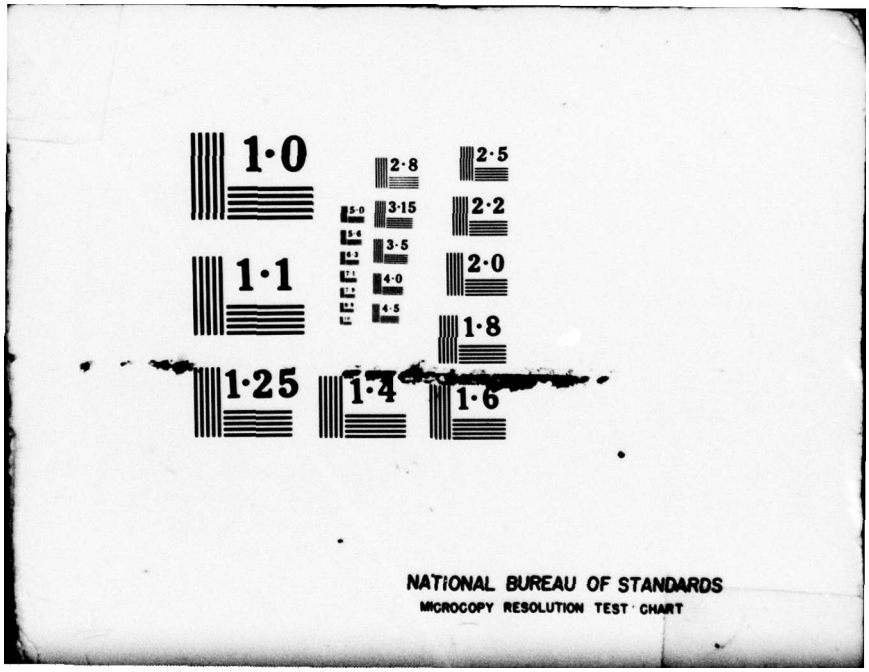
1·0
1·1
1·25
2·8
3·15
3·5
4·0
4·5
5·0
1·4
2·5
2·2
2·0
1·8
1·6
NATIONAL BUREAU OF STANDARDS
MICROCOPY RESOLUTION TEST CHART

AD A060626

DDC FILE COPY

12 LEVEL II

11 WES

TECHNICAL REPORT S-78-8

CYCLIC STRENGTH OF UNDISTURBED SANDS FROM NIIGATA, JAPAN

by

10 Marshall Lee Silver

Department of Materials Engineering
University of Illinois at Chicago Circle
Chicago, Illinois 60680

DDC
REPRODUCED
JUL 1 1978
B

11 Aug 1978

12 79 p.

9 Final rep.,

Approved for Public Release; Distribution Unlimited

Prepared for Office, Chief of Engineers, U. S. Army
Washington, D. C. 20314

Under Contract No. DACW39-76-M-2997

Monitored by Geotechnical Laboratory
U. S. Army Engineer Waterways Experiment Station
P. O. Box 631, Vicksburg, Miss. 39180

403 171

78 10 23 051

Destroy this report when no longer needed. Do not return
it to the originator.

Unclassified

SECURITY CLASSIFICATION OF THIS PAGE (When Data Entered)

REPORT DOCUMENTATION PAGE	READ INSTRUCTIONS BEFORE COMPLETING FORM
1. REPORT NUMBER: Technical Report S-78-10	2. GOVT ACCESSION NO. / 3. RECIPIENT'S CATALOG NUMBER
4. TITLE (and Subtitle): CYCLIC STRENGTH OF UNDISTURBED SANDS FROM NIIGATA, JAPAN	5. TYPE OF REPORT & PERIOD COVERED: Final report 6. PERFORMING ORG. REPORT NUMBER
7. AUTHOR(s): Marshall L. Silver	8. CONTRACT OR GRANT NUMBER(s): Contract No. DACW39-76-M-2407
9. PERFORMING ORGANIZATION NAME AND ADDRESS: Department of Materials Engineering, University of Illinois at Chicago Circle, Chicago, Illinois 60680	10. PROGRAM ELEMENT, PROJECT, TASK AREA & WORK UNIT NUMBERS: CWIS 31145
11. CONTROLLING OFFICE NAME AND ADDRESS: Office, Chief of Engineers, U. S. Army, Washington, D. C. 20314	12. REPORT DATE: August 1978 13. NUMBER OF PAGES: 174
14. MONITORING AGENCY NAME & ADDRESS (if different from Controlling Office): U. S. Army Engineer Waterways Experiment Station, Geotechnical Laboratory, P. O. Box 631, Vicksburg, Mississippi 39180	15. SECURITY CLASS. (of this report): Unclassified 15a. DECLASSIFICATION/DOWNGRADING SCHEDULE

16. DISTRIBUTION STATEMENT (of this Report)

Approved for public release; distribution unlimited

17. DISTRIBUTION STATEMENT (of the abstract entered in Block 20, if different from Report)

DDC
RECEIVED
NOV 1 1978
B

18. SUPPLEMENTARY NOTES

19. KEY WORDS (Continue on reverse side if necessary and identify by block number)

Cohesionless soils	Niigata, Japan	Undisturbed sampling
Cyclic load tests	Sands	
Dynamic loads	Soil samplers	
Earthquake engineering	Soil tests (laboratory)	
Liquefaction (soils)	Standard penetration tests	

20. ABSTRACT (Continue on reverse side if necessary and identify by block number)

Standard Penetration Tests, undisturbed field sampling, laboratory index property tests and laboratory cyclic triaxial strength tests were performed on cohesionless soils from Niigata, Japan, to determine why some soil deposits failed by liquefaction while apparently similar deposits remained stable during the 1964 earthquake. Undisturbed samples for testing were obtained from two relatively close-together sites underlain by essentially the same soil layer: a 'river site' where there was severe surface evidence of liquefaction

(Continued)

CONT'

DD FORM 1 JAN 73 1473 EDITION OF 1 NOV 65 IS OBSOLETE

Unclassified

SECURITY CLASSIFICATION OF THIS PAGE (When Data Entered)

78 10 23 051

20. ABSTRACT (Continued).

following the 1964 earthquake and a "road site" where surface evidence of liquefaction was not observed. Undisturbed soil sampling was performed with a newly-designed Japanese large diameter sampler and with an Osterberg sampler, so that U. S. and Japanese sampling procedures could be compared. Field procedures for obtaining small diameter specimens from a large diameter sample were shown to be a meaningful way to avoid sample handling problems. This is especially true if field freezing is also used to immobilize the fabric of the soil. It was found that field freezing with liquid nitrogen and storage of the samples in dry ice was a convenient way to transport and store both large and small specimens. In relatively clean, cohesionless soils which are not susceptible to frost heave, such freezing does not seem to significantly alter the soil fabric or sampled density. Comparison of standard penetration test values, index property values, and cyclic triaxial strength values for soils from the two sites showed the following: (1) In situ relative density values were low at both sites ranging between 20 percent and 60 percent. The trend was for relative density values to increase with depth; (2) Cyclic triaxial strength values for undisturbed soil specimens were not high. Cyclic stress ratios ($\sigma_{dl}/2\sigma_c'$) required to cause failure (defined as 5 percent double amplitude strain) for 20 stress cycles were on the order of 0.2 for soil specimens at an average relative density of 62 percent and on the order of 0.14 for soil specimens at an average relative density of 33 percent; (3) Sampling and testing at the river site showed low SPT values, low calculated relative density values, and low cyclic triaxial strength values. It was concluded that the river site, if unimproved, will show little resistance to liquefaction in future earthquakes; (4) Based on somewhat limited data, it appears that the cyclic triaxial strength of specimens from large diameter samples and for specimens from Osterberg samples are reasonably equivalent when test results were compared at the same value of relative density; (5) SPT values and relative density values were slightly higher for the road site than for the river site. However, the measured differences were not large. Nevertheless, sand boils, cracking and other surface indications gave clear evidence that soil at the river site liquefied and soil at the road site did not liquefy during the 1964 earthquake. This difference in behavior may have been due to higher effective stress at the road site resulting from a lower water table; (6) In reviewing historical records, it appears that most of the severe earthquake damage from liquefaction at Niigata occurred in areas that were reclaimed by dumping sand through water; and (7) In performing this study, it became clear that any form of sampling, sample handling, or specimen preparation for relatively clean cohesionless soils weakens the soil by some amount. Therefore, the test results reported may be considered as a lower bound on expected field behavior of soils from Niigata.

THE CONTENTS OF THIS REPORT ARE NOT TO BE USED FOR ADVERTISING, PUBLICATION, OR PROMOTIONAL PURPOSES. CITATION OF TRADE NAMES DOES NOT CONSTITUTE AN OFFICIAL ENDORSEMENT OR APPROVAL OF THE USE OF SUCH COMMERCIAL PRODUCTS.

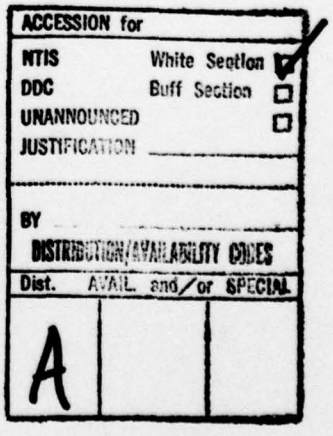

PREFACE

This report was prepared by Professor M.L. Silver, University of Illinois at Chicago Circle, under Contract DACW39-76-M-2407, as part of the on-going work at the U. S. Army Engineer Waterways Experiment Station (WES), under CWIS 31145 Work Unit entitled "Liquefaction Potential of Dams and Foundations During Earthquakes." This investigation was made possible by support of the U.S.-Japan Cooperative Science Program of the U.S. National Science Foundation. The work was directed by Dr. W.F. Marcuson III Research Civil Engineer, Earthquake Engineering and Vibrations Division (EE&VD), Geotechnical Laboratory (GL). General guidance was provided by Dr. P.F. Hadala, Chief, EE&VD, and Mr. J.P. Sale, Chief, GL. Mr. R.R.W. Beene, Office, Chief of Engineers, U.S. Army, is the technical monitor for this CWIS work unit.

Directors of the WES during this study and preparation of this report were COL G.H. Hilt, CE, and COL J.L. Cannon, CE. Technical Director was Mr. F.R. Brown.

PRECEDING PAGE BLANK-NOT FILMED

TABLE OF CONTENTS

		Page
Preface		iii
Table of Contents		v
List of Figures		viii
Conversion Factors, U. S. Customary and Metric to SI Units of Measurement		xiii
CHAPTER 1	INTRODUCTION	
	Background	1
	Outline of Research Program	3
CHAPTER 2	SOIL SAMPLING	
	Introduction	6
	Sampling and Sample Handling Requirements	7
	Selection of Samplers Used at Niigata	8
	Japanese Large Diameter Sampler	9
	Sampling Procedure	10
	Quality of the Sample	16
	Specimen Preparation	18
	Osterberg Sampler	19
	Sampling Procedure	21
	Specimen Handling	22
CHAPTER 3	FIELD SITE SELECTION AND SAMPLING	
	Introduction	24
	Flood Control Project	24
	Sand Deposition of Shinano River and 1964 Earthquake Damage	26
	Location of Test Site	32
	Boring Program - River Site	36
	Boring Program - Road Site	39
CHAPTER 4	LABORATORY TEST PROCEDURES	
	Introduction	44
	Index Property Tests	44
	Relative Density Tests	45
	Cyclic Triaxial Strength Testing	46
	Confining Pressure	54
	Cyclic Testing	54
	Testing Calculation Procedures	55

PRECEDING PAGE BLANK-NOT FILMED

TABLE OF CONTENTS (Cont.)

		Page
CHAPTER 5	CYCLIC BEHAVIOR OF SPECIMENS FROM LARGE DIAMETER SAMPLES FROM RIVER SITE	
	Introduction	58
	Soil Conditions at the River Site	58
	Index Properties at the River Site (Large Diameter Samples)	60
	Cyclic Triaxial Strength Test Results	70
	Insitu Cyclic Triaxial Strength Values	86
CHAPTER 6	CYCLIC BEHAVIOR OF SPECIMENS FROM OSTERBERG SAMPLES FROM THE RIVER SITE	
	Introduction	90
	Index Properties Values Obtained from Osterberg Specimens	91
	Cyclic Strength of Osterberg Specimens at the River Site	98
	Insitu Cyclic Triaxial Strength Values	105
CHAPTER 7	CYCLIC BEHAVIOR OF SPECIMENS FROM OSTERBERG SOIL SAMPLES FROM THE ROAD SITE	
	Introduction	107
	Soil Conditions at the Road Site	107
	Index Property Values at the Road Site	109
	Cyclic Triaxial Strength Test Results	118
	Insitu Cyclic Triaxial Strength Values	128
CHAPTER 8	COMPARISON OF CYCLIC STRENGTHS MEASURED AT DIFFERENT SITES BY DIFFERENT SAMPLING TECHNIQUES	
	Introduction	130
	Comparison of Index Property Values for Specimens from Large Diameter Samples and from Specimens from Osterberg Samples at the River Site	131
	Comparison of Cyclic Strength as Measured on Specimens from Large Diameter Samples and on Specimens from Osterberg Samples	133
	Comparison of Index Properties Between the River Site and the Road Site	138

TABLE OF CONTENTS (Cont.)

Page

Comparison of Cyclic Strength Behavior Between the River Site and the Road Site 147
Correction of SPT Values 153

CHAPTER 9 DISCUSSION, SUMMARY AND CONCLUSIONS . . . 157

REFERENCES 162

LIST OF FIGURES

		Page
1.	Liquefaction Damage Observed at Niigata, Japan, Following the 1964 Earthquake.	2
2.	Schematic Representation of Large Diameter Samples.	11
3.	Schematic Representation of Method of Operation of Large Diameter Samplers.	12
4.	(b) Cross-Section and (c) Plan View of Drilling and Driving Platform Used to Obtain Large Diameter Samples.	15
5.	(a) Appearance of a Typical Soil Specimen Showing Horizontal Soil Layering and Freedom from Disturbance. (b) Pushing Small Diameter Tubes into Large Diameter Sample to Obtain Triaxial Test Specimens.	17
6.	Picture of Osterberg Sampler and Drilling Rig and Schematic Representation Showing the Operation of the Osterberg Samplers. (a) Sampler is Set into the Bore Hole. (b) Sampling Tube is Pushed Hydraulically into the Soil. (c) The Pressure is Relieved through a Hole in the Piston Rod.	20
7.	Location Map and Plan of Flood Control Project in Niigata, Japan.	25
8.	Illustration on Diversion Dam Being Constructed in Niigata, Japan. (a) Concrete Gate Section in North Half of River. (b) Sand Fill Section in South Half of River.	27
9.	Plan and Cross-Section of Concrete and Sand Diversion Dam, Niigata, Japan.	28
10.	History of River Flow Pattern at Niigata, Japan. (a) Original Straight Channel - Shinano River on Left and Agano River on Right. (b) Channel Becomes Tortuous. (c) Channel Pattern in 1558-1573. (d) Channel in 1624-1644. (f) Channel in 1673-1688. (g) Channel in 1744-1748 (Agano River Changes Course Away from Niigata). (h) Channel in 1926.	30
11.	Map of Niigata Showing Damage Patterns Caused by the 1964 Earthquake.	31

LIST OF FIGURES (Cont.)

		Page
12.	Map Showing Location of the River Sampling Site and the Road Sampling Site.	33
13.	Cross-Section Between River and Road Boring Sites Niigata, Japan.	35
14.	Boring Plan at River and Road Sites.	37
15.	(a) Large Diameter Sampling at River Site. (b) Osterberg Sampling at Road Site.	38
16.	Records of Sample Recovery at Niigata, Japan.	42
17.	(a) Cyclic Triaxial Test Cell and (b) Cyclic Loading Equipment Used for this Investigation.	47
18.	Schematic Representation of the Components of the Cyclic Triaxial Test Equipment.	48
19.	(a) Cutting Specimen Lengths from Shelby Tube Samples Using Liquid Nitrogen. (b) Splitting Sample Tubes to Facilitate Extrusion of Frozen Samples	51
20.	Schematic Representation of Thawing, Back Pressure and Consolidation Process for Frozen Specimens.	53
21.	Typical Time History of Load, Deformation and Pore Water Pressure for a Cyclic Triaxial Strength Test on a Large Diameter Sample Specimen	56
22.	Definition of Measured Load-Deformation Values and Calculated Stress-Strain Values for Cyclic Triaxial Strength Tests.	57
23.	Soil Profile at the River Site Showing Soil Type, Method of Soil Deposition and Standard Penetration Test Values.	59
24.	Summary Showing Grain Size Distribution for Soils at the River Site - Large Diameter Samples.	64
25.	Mean Grain Size and Uniformity Coefficient as a Function of Depth at the River Site - Large Diameter Samples.	65

LIST OF FIGURES (Cont.)

		Page
26.	Insitu Void Ratio as a Function of Depth at the River Site - Specimens from Large Diameter Samples.	67
27.	Insitu Relative Density Values as a Function of Depth at the River Site - Specimens from Large Diameter Samples.	69
28.	Cyclic Strength of Undisturbed Specimens from Large Diameter Samples from the River Site for Different Depths for Consolidated Density Values.	71
29.	Effect of Density on the Cyclic Strength of Undisturbed Sand Specimens from Large Diameter Samples at the River Site at Any Depth for Consolidated Density Values.	82
30.	Summary Curve Showing the Effect of Density on the Strength of Undisturbed Specimens from Large Diameter Samples Samples at the River Site.	85
31.	Summary Curve Showing the Effect of Relative Density on the Cyclic Strength of Undisturbed Specimens from Large Diameter Samples from the Road Site.	87
32.	Insitu Values of Cyclic Triaxial Strength Failure in 20 Cycles as a Function of Depth for Specimens from Large Diameter Samples at the River Site.	89
33.	Summary Curve Showing Grain Size Distribution for Soils at the River Site - Osterberg Samples.	93
34.	Mean Grain Size and Uniformity Coefficient as a Function of Depth at the River Site - Osterberg Samples.	94
35.	Insitu Void Ratio Values as a Function of Depth at the River Site - from Osterberg Specimens.	96
36.	Insitu Relative Density Values as a Function of Depth at the River Site - from Osterberg Specimens.	97
37.	Cyclic Strength of Undisturbed Osterberg Specimens from the River Site for Different Depths for Consolidated Density Values.	99
38.	Summary Curve Showing the Effect of Relative Density on the Cyclic Strength of Undisturbed Specimens from Osterberg Samples from the River Site.	104

LIST OF FIGURES (Cont.)

		Page
39.	Insitu Values of Cyclic Triaxial Strength (Failure in 20 Cycles) as a Function of Depth for Specimens from Osterberg Samples at the River Site.	106
40.	Soil Profile at the Road Site Showing Soil Type, Method of Soil Deposition and Standard Penetration Test Values.	108
41.	Summary Curve Showing Grain Size Distribution for Soils at the Road Site - Osterberg Samples.	113
42.	Mean Grain Size and Uniformity Coefficient as a Function of Depth at the Road Site - Osterberg Samples.	114
43.	Insitu Void Ratio Values as a Function of Depth at the Road Site - from Osterberg Specimens.	116
44.	Insitu Relative Density Values as a Function of Depth at the Road Site - from Osterberg Specimens	117
45.	Cyclic Strength of Undisturbed Osterberg Specimens from the Road Site for Different Depths for Consolidated Density Values.	119
46.	Summary Curve Showing the Effect of Density on the Cyclic Triaxial Strength of Osterberg Specimens from the Road Site.	127
47.	Insitu Values of Cyclic Triaxial Strength (Failure in 20 Cycles) as a Function of Depth for Specimens from Osterberg Samples at the Road Site.	129
48.	Comparison of Insitu Void Ratio Values as a Function of Depth for Specimens from Large Diameter Samples and for Specimens from Osterberg Samples at the River Site.	132
49.	Comparison of Insitu Relative Density Values as a Function of Depth for Specimens from Large Diameter Samples and for Specimens from Osterberg Samples at the River Site.	134
50.	Comparison of the Cyclic Strength of Undisturbed Specimens from Large Diameter Samples and of Specimens from Osterberg Samples from the River Site for Different Relative Density Values.	135

LIST OF FIGURES (Cont.)

		Page
51.	Comparison of the Stress Ratio Required to Cause Failure in 20 Cycles as Measured in Cyclic Triaxial Strength Tests on Undisturbed Specimens from Large Diameter Samples and on Specimens from Osterberg Samples at the River Site.	137
52.	Comparison Showing the Effect of Relative Density on the Cyclic Triaxial Strength of Specimens from Large Diameter Samples and of Specimens from Osterberg Specimens from the River Site.	139
53.	Comparison of Standard Penetration Values at the River Site and at the Road Site.	140
54.	Comparison of Mean Particle Size with Depth at the River Site and at the Road Site.	142
55.	Comparison of Particle Uniformity Coefficient with Depth at the River Site and at the Road Site.	143
56.	Comparison of Insitu Void Ratio Values at the River Site and at the Road Site.	145
57.	Comparison of Insitu Relative Density Values at the River Site and at the Road Site.	146
58.	Comparison of the Cyclic Strength of Undisturbed Specimens from Large Diameter Samples Taken at the River Site and of Specimens Taken from Osterberg Samples Taken at the Road Site.	148
59.	Comparison Showing the Effect of Relative Density on Cyclic Triaxial Strength of Undisturbed Specimens from Large Diameter Samples at the River Site and of Specimens from Osterberg Samples at the Road Site.	149
60.	Comparison of Insitu Cyclic Triaxial Strength (Failure in 20 Cycles) as a Function of Depth at the River Site and at the Road Site.	151
61.	Distribution with Depth of Total Stress Pore Water Pressure and Effective Stress a) At the Road Site and b) At the River Site.	152
62.	Comparison with Depth of Cyclic Triaxial Axial Stress Required to Cause Failure in 20 Cycles (5% Double Amplitude Strain) for the Road Site and the River Site.	154
63.	Comparison of (a) Actual N Values and (b) Corrected N Values at the River Site and at the Road Site.	156

CONVERSION FACTORS, US CUSTOMARY AND METRIC TO SI UNITS OF MEASUREMENT

Metric and U.S. customary units of measurement used in this report can be converted to SI units as follows.

	TO CONVERT	TO	MULTIPLY BY
Length	inches (in.)	millimeters (mm)	25.40
	inches (in.)	meters (m)	0.0254
	feet (ft)	meters (m)	0.305
	miles (miles)	kilometers (km)	1.61
	yards (yd)	meters (m)	0.91
Area	square inches (sq. in.)	square centimeters (cm^2)	6.45
	square feet (sq. ft.)	square meters (m^2)	0.093
	square yards (sq. yd.)	square meters (m^2)	0.836
	acres (acre)	square meters (m^2)	4047
	square miles (sq miles)	square kilometers (km^2)	2.59
Volume	cubic inches (cu in.)	cubic centimeters (cm^3)	16.4
	cubic feet (cu ft.)	cubic meters (m^3)	0.028
	cubic yards (cu yd.)	cubic meters (m^3)	0.765
Mass	pounds (lb)	kilograms (kg)	0.453
	tons (ton)	kilograms (kg)	907.2
Force	one pound force (lbf)	newtons (N)	4.45
	one kilogram force (kgf)	newtons (N)	9.81
Pressure or Stress	pounds per square foot (psf)	newtons per square meter (N/m^2) or pascals (Pa)	47.9
	pounds per square inch (psi)	kilonewtons per square meter (kN/m^2) or kilopascals (kPa)	6.9
	kilogram force per square centimeter (kgf/cm^2)	Kilonewtons per square meter (kN/m^2) or Kilopascals (kPa)	98.07
Liquid Measure	gallon (gal)	cubic meters (m^3)	0.0038
	acre-feet (acre-ft)	cubic meters (m^3)	1233
Quantity of Flow	gallons per minute (gal/min)	cubic meters per minute (m^3/min)	0.0038
Unit Weight	pounds per cubic foot (pcf)	Kilonewtons per cubic meter (kN/m^3)	0.1572
	grams per cubic centimeter (gm/cm^3)	Kilonewtons per cubic meter (kN/m^3)	9.807

CYCLIC STRENGTH OF UNDISTURBED SANDS FROM NIIGATA, JAPAN

CHAPTER I

INTRODUCTION

Background

A better understanding of ways to investigate the liquefaction potential of natural soil deposits is required to protect people and property during earthquakes.

There has been a long history of soil instability induced by earthquakes resulting in landslides, flowslides and building damage (Newmark, 1965; Seed, 1968, Seed, 1969). Some of the most devastating of these failures recorded in recent years have been associated with soil liquefaction where during seismic shaking, cohesionless soils loose all strength and are no longer able to support overlying structures (Ambraseys and Sarma, 1969; Dixon and Burke, 1973; Kuribayashi and Tatsuoka, 1975). One of the most important examples of liquefaction damage occurred in Niigata, Japan, in 1964 where the soil under bridges and buildings liquefied causing severe damage. Intense study of the mechanism and mode of liquefaction failure at Niigata forms the basis of our present day design procedures to prevent or reduce liquefaction induced failure.

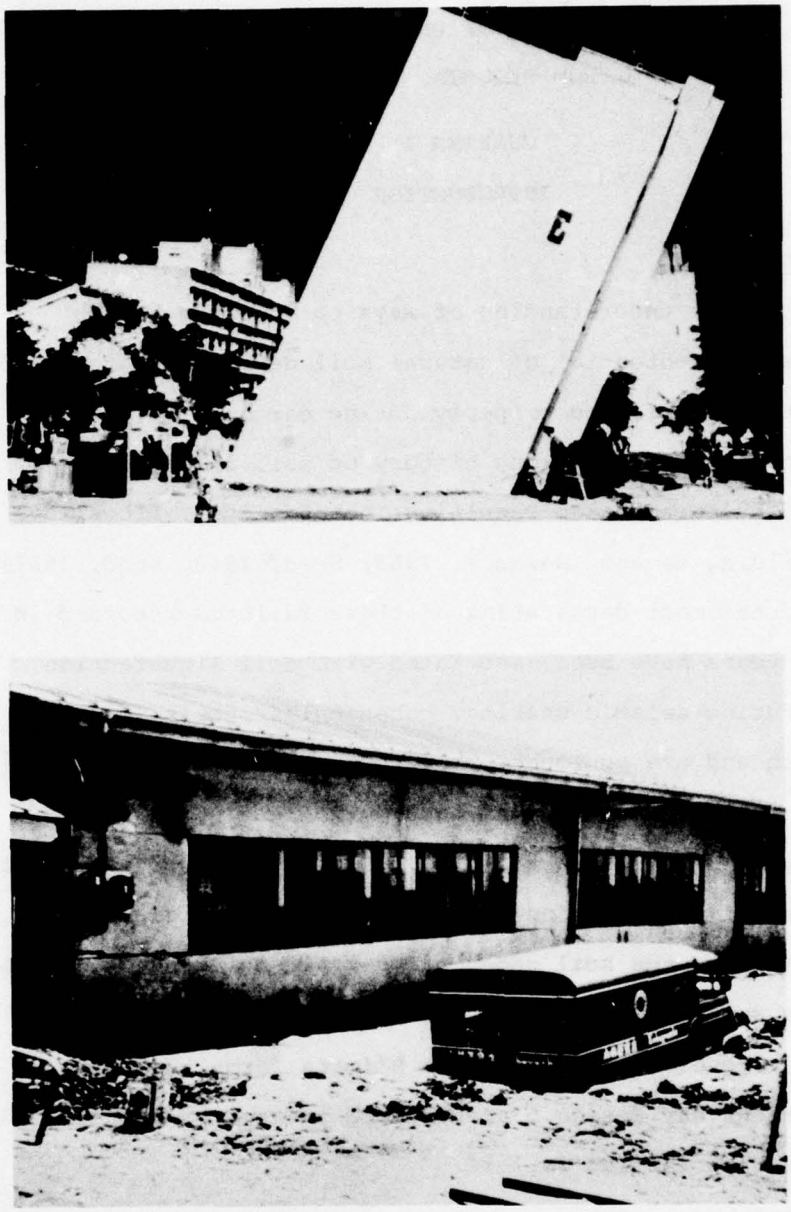

Fig. 1 Liquefaction Damage Observed at Niigata, Japan Following the 1964 Earthquake

Outline of Research Program Reported

This report describes the results of a cooperative U.S.-Japanese field and laboratory experimental program designed to study in detail why some sites in Niigata failed catastrophically during the 1964 earthquake while seemingly identical adjacent sites suffered little or no distress. An understanding of such differences in site behavior during an actual earthquake will provide important information useful for the development of improved design procedures to evaluate site safety during earthquakes.

To accomplish the goal stated above, new soil sampling, sample handling and laboratory testing procedures were developed and used to determine the cyclic strength of undisturbed sand specimens obtained from Niigata, Japan. The features of this experimental program are presented in Table 1 and summarized below.

1. Undisturbed samples of sand were obtained from two sites in Niigata, Japan: One site that experienced significant distress from liquefaction during the 1964 earthquake and another site that showed no surface evidence of liquefaction during the earthquake. A Japanese (large diameter sampler) and a U.S. sampler (Osterberg sampler) were used side by side in adjacent bore holes to provide independent checks on 1) the degree of induced disturbance during sampling and 2) values of insitu soil dry unit weight (density).

2. Sample freezing, handling, and storage techniques

TABLE 1

FLOWCHART OF RESEARCH ON UNDISTURBED SAMPLING AND TESTING OF SANDS FROM NIIGATA, JAPAN

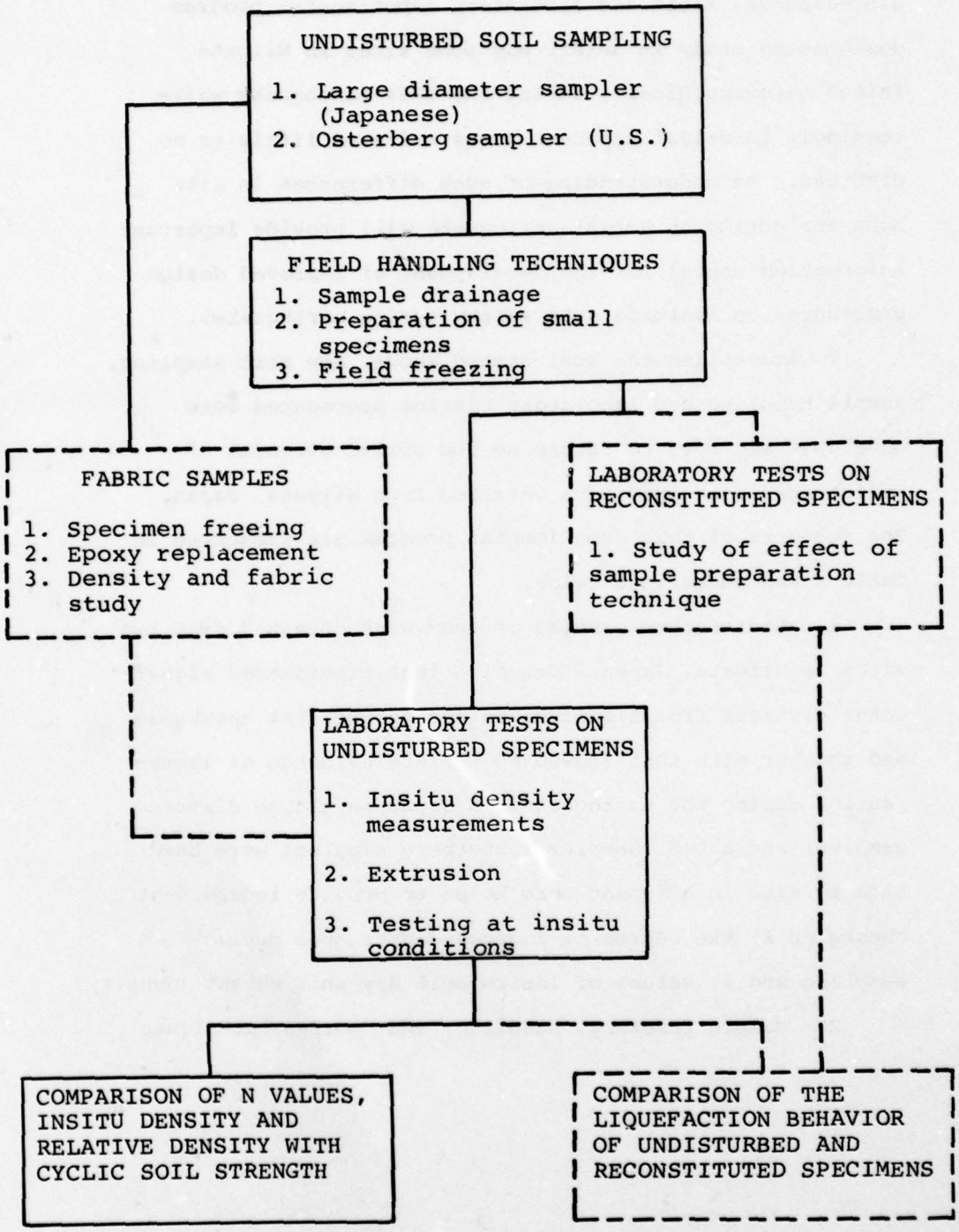

Note: - - - indicates work not described in this report

were developed to prevent sample disturbance between the field and the laboratory.

3. Specimens were obtained for studies to define undisturbed soil fabric as a step in determining how to successfully model insitu soil fabric with reconstituted specimens in the laboratory. (These results will be reported on in a future study being conducted by others).

4. Laboratory cyclic triaxial strength tests (liquefaction tests) were performed on these undisturbed specimens to:

A. Define the cyclic strength of Niigata sands that can be mobilized in future earthquakes.

B. Compare the cyclic strength in soil layers that liquefied and that did not liquefy during the 1964 earthquake.

C. Evaluate the relationship between soil index properties (grain size distribution, grain shape, relative density, specific gravity) and the cyclic soil strength of undisturbed specimens.

D. Evaluate the relationship between insitu soil characteristics (N value, relative density, insitu density) and the cyclic soil strength of undisturbed specimens.

PRECEDING PAGE BLANK-NOT FILMED

CHAPTER 2

SOIL SAMPLING

Introduction

For all classes of civil engineering projects, there has always existed a need to obtain good undisturbed samples of sand from below the water table that retain the structure and density of the sampled sand layer. Likewise, for the experimental work performed at Niigata, undisturbed samples were required 1) to determine in-place density of subsurface soils; 2) to provide specimens for laboratory static and cyclic soil strength testing (liquefaction testing) and 3) to provide specimens for fabric studies. Thus great effort was devoted to the selection of both appropriate sampling techniques and sample handling methods since the success of the experimental program would be dependent on the quality of the samples obtained *in the field*.

Throughout this report the term "undisturbed sample" is defined as a bore hole sample taken and handled with great care to minimize changes between insitu and sampled density and fabric. However, no control of possible disturbance caused by the change in stress from the anisotropic insitu state to the isotropic sampled state is possible.

It was considered advantageous to avoid placing full dependence on the use of only one field sampling technique at Niigata. For example, side by side use of two sampling techniques provides an excellent independent check on the degree of sample disturbance through comparison of measured insitu density and cyclic strength

values between the two kinds of samples. Another advantage of side by side sampling using different techniques is that it provides an opportunity of comparing Japanese and U.S. sampling procedures. Such a comparison provides a useful tool to correlate the results of Japanese and U.S. research for all classes of geotechnical problems.

This chapter describes 1) the basis used to select U.S. and Japanese samplers for use at Niigata; 2) the equipment and the field procedures used for sampling and 3) a new sample handling technique that uses freezing to prevent volume change of loose sands after sampling and before laboratory testing.

Sampling and Sample Handling Requirements

It is generally considered that many existing soil samplers do not provide satisfactory soil specimens from cohesionless soil layers. In general, many samplers densify loose cohesionless materials and loosen dense materials. The result is that samples brought to the surface do not exhibit the same density as the soil layer being sampled. Moreover, the fabric of the sand is often disturbed.

To avoid these problems, alternative techniques involving soil freezing and coring, and the digging of test shafts from which block samples are laborously cut have been used in important engineering projects. However, the cost of such techniques is quite high and can generally only be justified for the most important engineering projects.

Moreover, even if good samples are obtained from bore holes or from test pits, a further problem arises during sample handling

and transportation to the laboratory. Often sample handling is out of control of the project engineer and sample disturbance caused by dropping of the core tubes, bumping, or improper handling techniques cannot be avoided nor can the testing engineer know the magnitude of the dusturbance caused by such improper handling.

From the above discussion it can be seen that sampling techniques are required that will retain the insitu density and fabric of soils at a reasonable engineering cost. In addition, methods are required to reduce sample disturbance during shipping and storage between the sampling site and the soil laboratory.

Selection of Samplers Used at Niigata

Recent sampling trends in Japan favor the use of large diameter samplers to meet the requirements described above to obtain undisturbed specimens of sand from below the water table. Recent studies of soils at the Ohgishima land fill project near Tokyo, at the site of the Kawagishicho apartment house failures in Niigata and at other sites (Hanzawa and Matsuda, 1978) used the Bishop (1948) Sampler to obtain specimens for insitu density determinations. While it was concluded that good insitu density values were obtained, it was felt that the diameter of the specimen was too small (53 mm ID; 2.1 in ID) to preserve the fabric of the sand and that samplers with a diameter on the order of 200 mm (8 in) are needed to provide good samples.

Sampling trends in the U.S. favor the use of fixed piston samplers to obtain good undisturbed specimens of sand. Relatively large specimens are considered necessary for good testing and many samplers provide specimens 71 mm (218 in.) in diameter,

which has become a standard soil specimen size for laboratory testing. Many fixed piston samplers have been developed over the years (Hvorslev, 1949) using either an internal rod or some down hole method to hold the piston stationary during sampling. The advantages and disadvantages of different fixed piston sampling techniques have been debated extensively, however it is generally felt that down hole piston fixation requires less equipment and is a faster and cheaper sampling technique than methods that employ inner rods attached to the soil piston.

Based on the discussion presented above, two soil samplers were used at Niigata: a newly designed large diameter sampler and the Osterberg fixed piston sampler. The characteristics and field operation of these samplers is explained in subsequent sections.

Japanese Large Diameter Sampler

A new large diameter sampler was developed for this project by the Japanese to provide undisturbed specimens for 1) insitu density determinations; 2) liquefaction testing and 3) fabric studies.

A review of the fundamentals of good soil sampling (Hvorslev, 1949) indicated that a satisfactory sampler for cohesionless soils should have the following characteristics:

1. The sampler must have a large diameter to minimize side friction and resulting soil disturbance.
2. The sampler should be relatively short compared to its diameter to prevent specimen shortening and incorrect measures of in-place density.

3. The sampler should be split to make it possible to observe soil layering in the field and to make possible multiple density checks at different locations in the sample.

4. Any core restraining device must not disturb the specimen.

Figures 2 and 3 show a schematic diagram of the large diameter soil sampler developed to meet these criteria. The sampler is 200 mm (8.0 in) in inner diameter, 1000 mm (25 in) high, and has a wall thickness of 8.2 mm (0.32 in). The core barrel consists of two steel halves which are clamped together during the drilling process, but which are unlocked after sampling to expose the specimen in the field for evaluation of the quality of the soil sample and to obtain small undisturbed specimens.

The cutting bit at the bottom of the core tube contains the core catcher used to prevent the washing out of sand as the sampler is withdrawn from the bore hole.

The core catcher consists of two pieces of stainless steel screen which are folded and held within the cutting bit. The screens are connected by a cable that extends to the surface. During the coring process, the screens rest inside of the cavity in the cutting bit. After the sampler is advanced, the cables are pulled, which closes the screens securely, cutting off the sand at the bottom of the sample and restraining the sand from falling out as the sampler is lifted to the surface.

Sampling Procedure: One of the reasons why large diameter samplers have not been routinely used in the past is because large reactions are required to push the sample into the soil deposit. In the Niigata drilling, four earth anchors spaced at

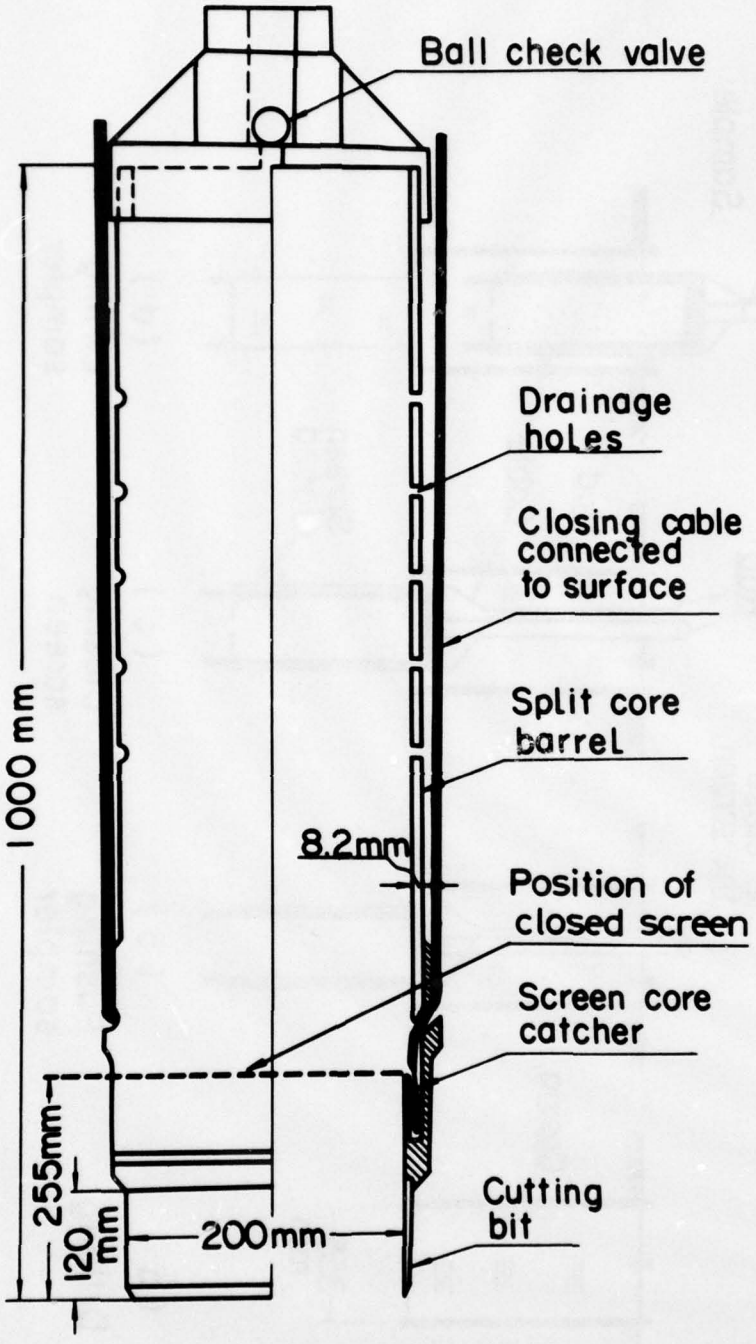

Fig. 2 Schematic Representation of Large Diameter Samples.

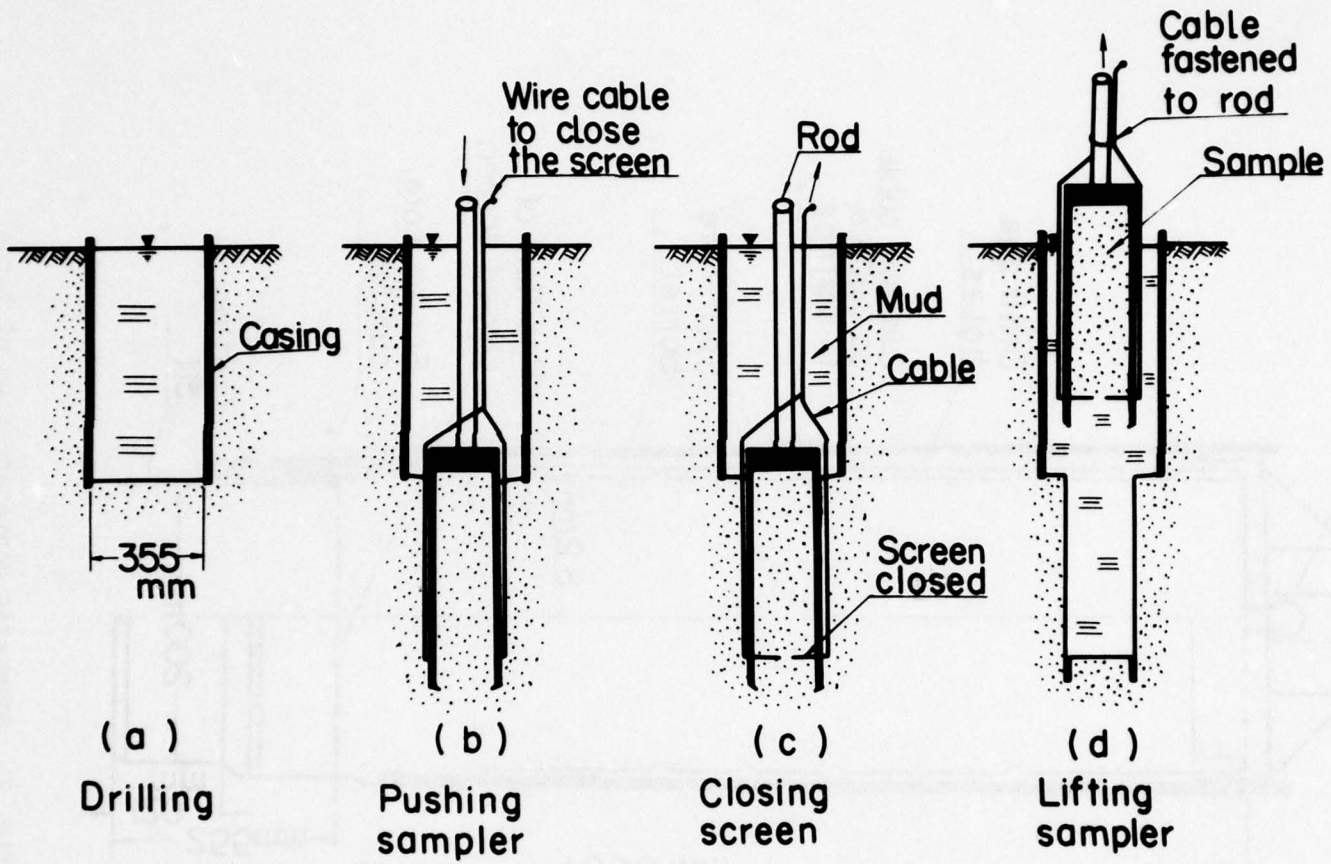

Fig. 3 Schematic Representation of Method of Operation of Large Diameter Samplers.

2 m (6.5 ft) from the drill hole, as shown in Figure 4, were used to house earth anchors. The anchors were set in drill holes at a depth of 40 m (66 ft) prior to the drilling of the bore hole. A steel framework was used to transfer the force from the anchors to the hydraulic jack used to push the soil sampler into the soil deposit. The jack itself had a capacity of 20 tonnes (10,000 lb) and was operated with a hydraulic pump

The bore hole was advanced conventionally with a fishtail bit modified with baffles that directed the drilling fluid upward away from the bottom of the hole so that sand disturbance at the bottom of the bore hole was minimized. Continuous casing was used and drilling mud was always maintained at the top of the casing. After the boring had been advanced to the required sampling depth, the casing was lowered to the bottom of the hole. The bit was then removed and the sampler was introduced into the bore hole and lowered to the bottom. At the same time the cable to the core catcher was retained at the surface, being careful not to pull on the screen during the lowering process. Once the sampler was put in place, the hydraulic jack was moved into position over the drill rod and secured to the reaction framework. Then hydraulic pressure was applied to the jack gradually so that the sampler was advanced slowly at the rate of 2 cm/min (0.8 in/min) so that excess pore pressures were not induced by the sampling operation. Moreover, the sample tube was pushed to a prescribed depth so that overdriving did not densify the soil. In general it was found that a force of 800 kg (1800 lb) was required to advance the sampler in the loosest soil while a force of 1800 kg (4000 lb)

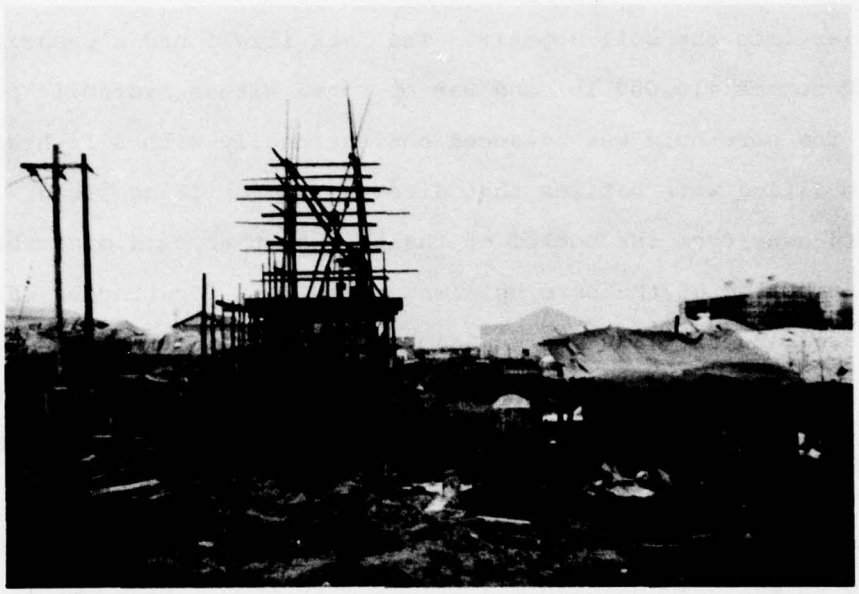

(a)

Fig. 4 (a) Picture of Driving Platform Used to Obtain Large Diameter Samples.

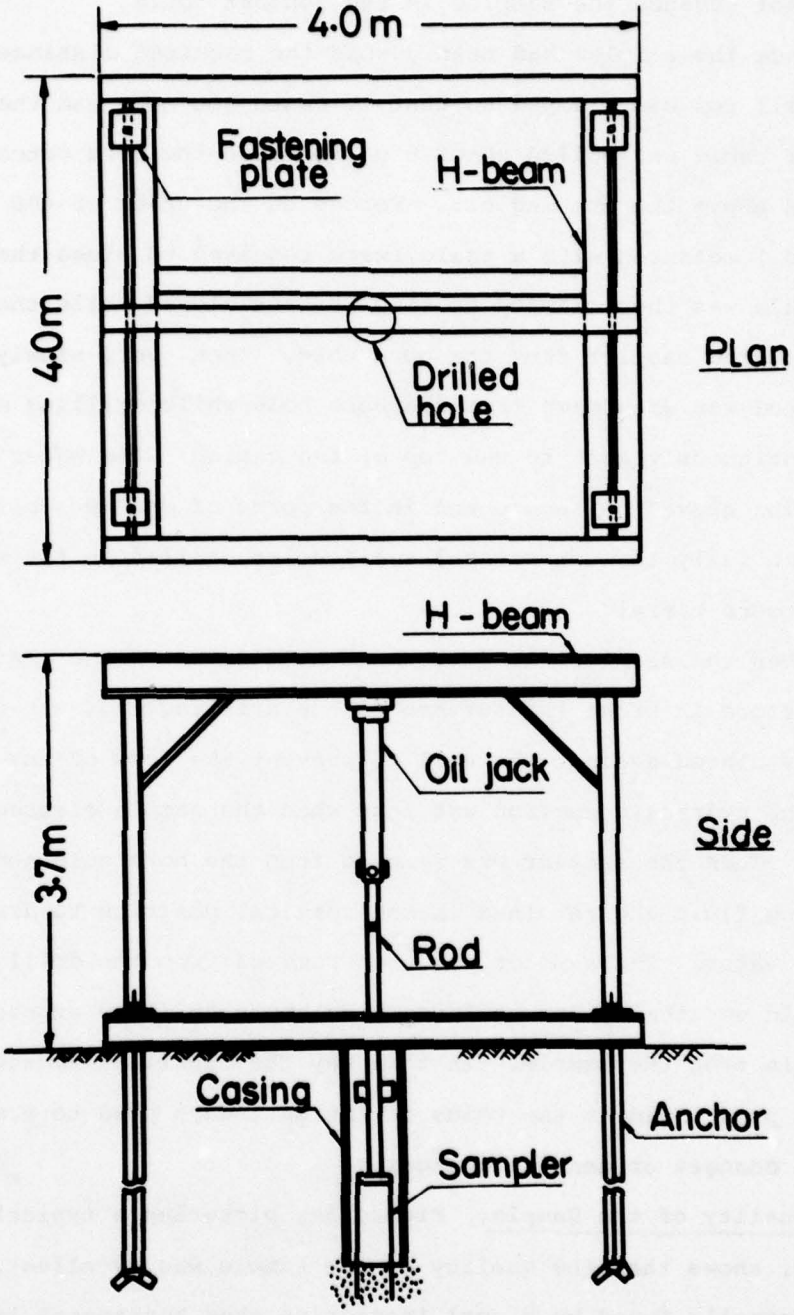

Fig. 4 (b) Cross-Section and (c) Plan View of Drilling and Driving Platform Used to Obtain Large Diameter Samples.

could not advance the sampler in the densest soils.

Once the sampler had been pushed the required distance, the drill rod was clamped so that it could not move and the core catcher cable was pulled about 8 cm to close the core catcher net located above the cutting bit. Forces on the order of 400 kg (900 lb) measured with a scale, were required to close the net. The cable was then clamped to keep the net closed while the piston withdrew the sampler from the bore hole. Then, very slowly, the drill rod was withdrawn from the bore hole while drilling mud was continuously kept to the top of the casing. The water remaining above the sample and in the pores of sand was allowed to drain fully through several small holes drilled in the wall of the core barrel.

When the sampler was just about at the top of the casing and just before it broke the surface of the drilling mud, a hand held cap was placed against the soil to prevent the loss of any sand when the hydraulic suction was lost when the sample cleared the water. Then the sampler was removed from the bore hole and the drilling fluid and retained in the vertical position to drain excess water. The sampler was then removed from the drill rod and held vertically for at least four hours to allow excess water to drain from the sample. In this way the capillary tensions of the pore fluid in the voids of the soil were used to prevent fabric changes or density changes.

Quality of the Sample: Figure 5a, picturing a typical soil sample, shows that the quality of the sample was excellent. It was generally found by visual inspection that horizontal layers were kept intact and that lenses of coarse sand, fine sand, and

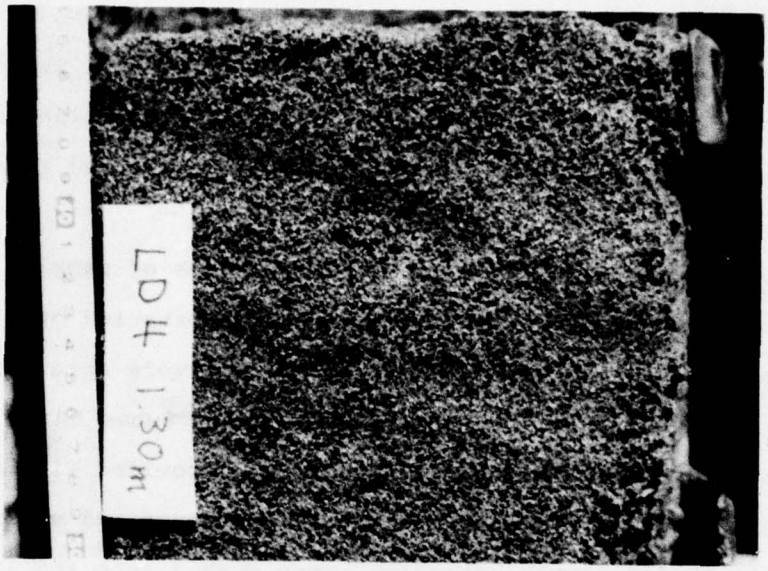

(a)

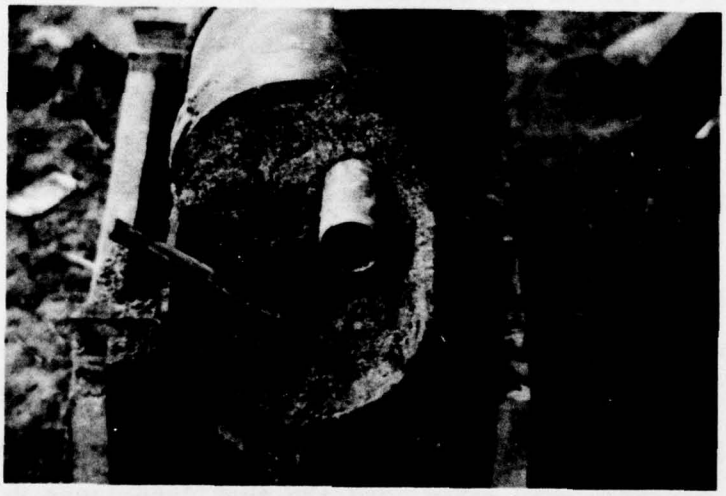

(b)

Fig. 5 (a) Appearance of a Typical Soil Specimen Showing Horizontal Soil Layering and Freedom from Disturbance (b) Pushing Small Diameter Tubes into Large Diameter Sample to Obtain Triaxial Test Specimens

silt were undisturbed, clear and sharp. Moreover, almost no side drag was evident on the sides of the core barrel. It seemed that a slight coating of bentonite mud lubricated the sides of the sampler as it was driven into the soil and prevented friction from developing.

Specimen Preparation: To avoid the problems of sample disturbance that are associated with the transportation of a large sample to the laboratory, small specimens were obtained in the field using thin 1 mm (0.039 in) thick brass tubes 50 mm (2 in) in diameter by 100 mm (4 in) long. These tubes, provided with a sharp cutting edge to minimize specimen disturbance and a longitudinal slit to aid sample extrusion, were pushed into the large diameter sample which was positioned horizontally and supported on a cradle for stability (Fig. 5b)

The core barrel of the sampler provided lateral restraint that prevented lateral displacement of the sand while the small diameter tubes were being inserted. In addition, outward movement of the back surface of the large diameter sample was prevented by a wooden plug held tightly against the rear sand surface.

To obtain the small specimens, the brass tubes were first inserted carefully into the sand at the front face of the large diameter sample. Next, the upper half of the split core barrel was pushed backward exposing the intact sand surface, pictures of the sand layering were taken, and the small specimens were carefully dug out from the large sample. This proceedure was then repeated for the next intact portion of the sample.

It was found that it was possible to obtain as many as 12 small diameter tube specimens from each large diameter sample. In addition, because of the size of the sampler, it was possible to take both vertically and horizontally oriented specimens.

Osterberg Sampler

An Osterberg sampler, a relatively simple to use hydraulically-operated piston sampler (Osterberg 1952), was used in an adjacent bore hole along side the Japanese Large Diameter sampler to obtain undisturbed specimens from Niigata, Japan.

Sampler description and operation: In operation, the sampler was lowered to the bottom of a previously drilled and cleaned out bore hole as shown in Fig. 6a, until it just made contact with the soil surface. The drill rod was clamped and water pressure was applied through the drill rod forcing down a piston to which was attached a thin wall sampling tube (Fig. 6b). A second piston (the fixed piston inside the sampling tube) was connected to the sampler head by a hollow rod. As the piston was forced down in the pressure chamber, air in the sampler tube escaped through the hollow rod and check valve. The clamped drill rod provided the reaction for pushing the tube.

When the piston had reached its full stroke and the sampling tube had penetrated its full depth into the soil, the water-pressure was automatically relieved through a hole in the hollow piston rod and through a check valve (Fig. 6c). The sampler was then turned 1-½ revolutions to engage a friction clutch that held the inside tube and outside tube together in order to break off soil at the bottom of the tube. The sampler was then slowly

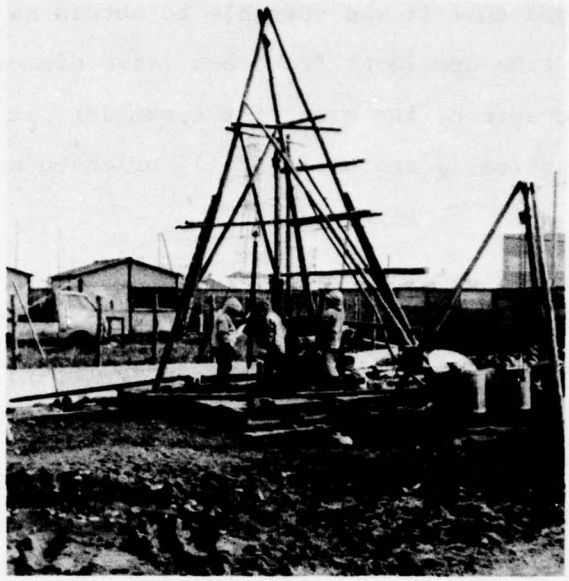

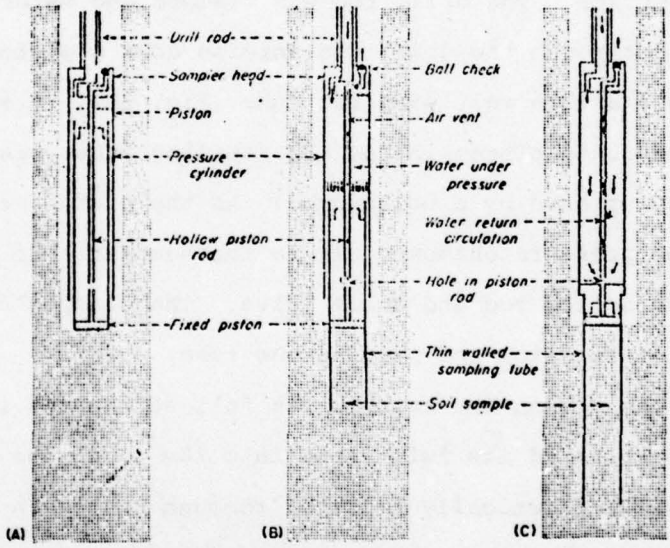

Fig. 6 Picture of Osterberg Sampler and Drilling Rig and ____ Schematic Representation Showing the Operation of the Osterberg Sampler. A) Sampler is set into the bore hole. B) Sampling tube is pushed hydraulically into the soil. C) The pressure is relieved through a hole in the piston rod.

removed from the bore hole.

Sampling Procedure: Sampling using the Osterberg sampler at Niigata was performed in a mud filled bore hole 100 mm (4.5 in) in diameter advanced with a fish tailed bit modified with baffles that directed the drilling fluid upward away from the bottom of the bore hole to reduce soil disturbance. Casing in the top 2m (6 ft) of the boring and a mud level above the ground water table were used to prevent caving of the hole.

Pressure to push the Osterberg sampler was supplied by the mud circulation pump. It was found that pressures on the order of 1000KN/m^2 (150 psi) were required to drive the piston. The reactions for the sampler was provided by clamping the drill rod to the drilling engine. Some difficulty was experienced when taking deep samples in materials with Standard Penetration Test (SPT) resistance on the order of N=20 when the reaction was found to be insufficient and the drilling machine was lifted off the ground. (A large truck mounted drilling rig would have provided more reaction but such equipment does not exist in Japan because it can not be used in the narrow streets found in Japanese urban areas). However, no difficulty in providing a satisfactory reaction was encountered when taking samples in the relatively loose materials that were found to predominate at Niigata.

While the sampler was being withdrawn from the bore hole, fresh drilling mud was introduced into the bore hole to prevent caving. When the sampling tube just cleared the mud surface a small amount of soil was removed from the core-tube and an expandable O-ring packer was introduced into the tube and locked to prevent the loss of sand.

Then, a small portable battery operated drill was used to make a small hole below the piston to break the vacuum developed by the sampler and to make it easier to remove the sample tube. After removing the sample tube, the dimensions of the sample were obtained.

The bottom packer was equiped with small vertical drainage holes and thus when the vacuum under the piston was released, water from the soil voids was free to flow out of the sample. Samples were drained for 24 hours in a vertical position to prepare them for the frozen sample handling technique described in the next section.

Specimen Handling

To further protect the density and insitu fabric of the Osterberg samples and the large diameter samples they were quickly frozen in liquid nitrogen in the field and stored in dry ice while they were transported back to the laboratory. In the laboratory the samples were stored in a commercial ice cream freezer until tested.

This freezing technique turned out to be a reasonably simple way to handle the loose sands found at Niigata. Importantly, it was found that this freezing technique did not change the dimensions of the specimens. This is because drainage was used to clear the soil voids of excess water and only provided enough water at the grain to grain contacts to provide particle binding when the specimen was frozen. In general, experience using this freezing technique has shown that the following precautions must be followed to avoid specimen disturbance:

1. The sample must be carefully drained and no free water must remain in the soil voids. Thus freezing can best be performed on relatively clean cohesionless materials since the presence of fines of clay or silt does not allow for satisfactory drainage. Freezing of soil when the voids are full of water can produce volume increase due to the expansion of water induced by freezing.

2. A quick freezing technique is required to avoid sample disturbance. Liquid nitrogen provides an excellent freezing source and dry ice can be used while transporting the specimens.

The quality of the frozen specimens was checked by noting the specimen volume both before and after freezing. No measurable difference was noted. It was also found that the spit brass tubes of the large diameter specimens did not open up as a result of freezing and that the specimen length remained constant further confirming that freezing did not disturb the specimens.

CHAPTER 3

FIELD SITE SELECTION AND SAMPLING

Introduction

To achieve the goals of this program of 1) assessing the stability in future earthquakes of sites that have liquefied in past earthquakes and 2) comparing the cyclic strength of sites that did and did not show evidence of liquefaction under strong ground shaking in past earthquakes, careful consideration was given to the selection of a representative sampling site in Niigata. Fortunately, such a site was found on the banks of the Shinano River adjacent to a new flood control diversion dam being constructed by the Office of the Shinano River project of the Japanese Ministry of Construction. Thus, investigations carried out at this site provided information for an additional goal of predicting the stability of the diversion dam during earthquakes.

The following pages 1) describe the features of the diversion dam, 2) give the history of deposition in Niigata and at the site, 3) physically describe the site and 4) summarize the field sampling and boring program.

Flood Control Project

The purpose of the flood control project in Niigata, shown in Fig. 7, being undertaken by the Japanese Ministry of Construction, is to prevent flood waters of the Shinano River from

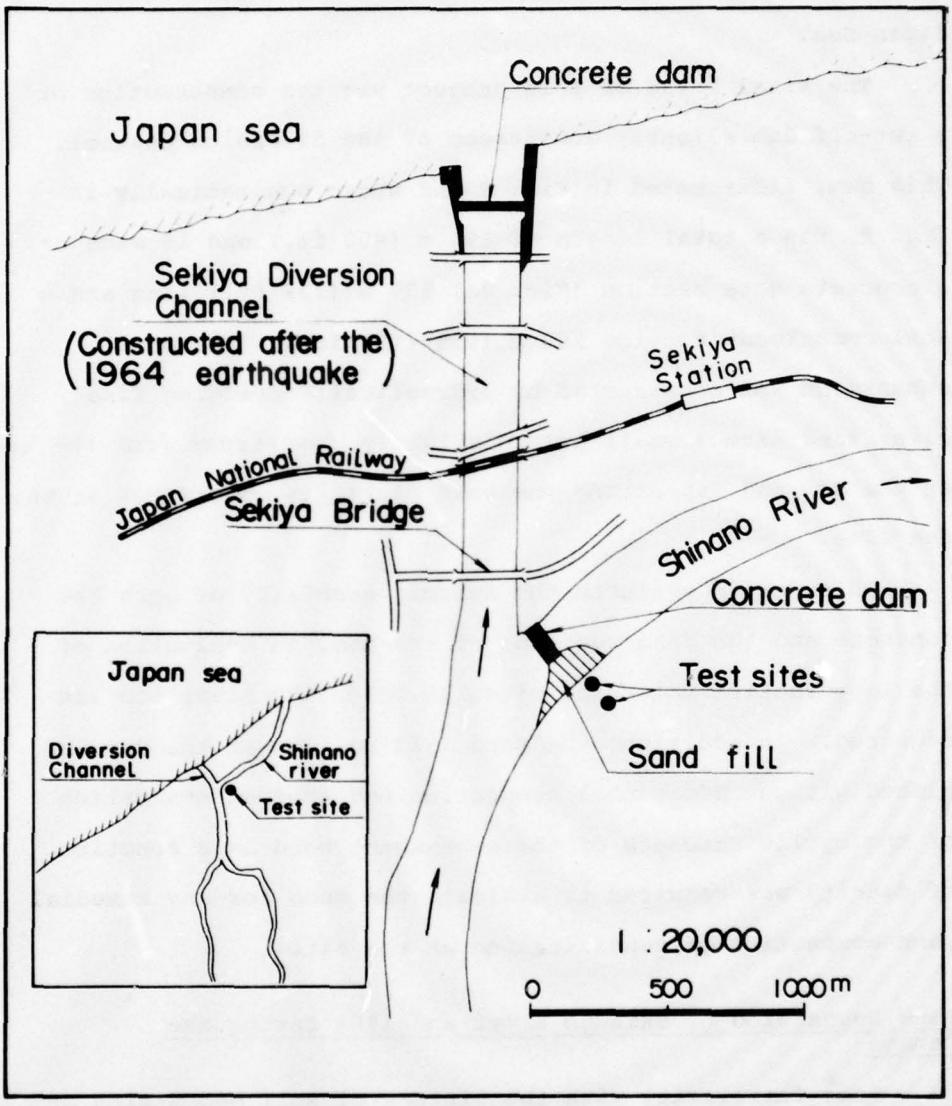

Fig. 7 Location Map and Plan of Flood Control Project in Niigata, Japan.

passing through downtown Niigata. The initial pahse of this project was the construction of a diversion channel in 1971 connecting the river upstream from downtown Niigata with the Japan Sea.

The final phase of this project was the construction of a cut-off dam slightly downstream of the diversion channel. This dam, illustrated in Fig. 8 and shown schematically in Fig. 9, has a total length of 290 m (950 ft.) and is made of a concrete gate section (Fig. 8a) 130 m (426 ft.) long and a soil embankment section 160 m (525 ft.) long. The soil embankment was constructed by hydraulically dredging fine river sand from a small island slightly downstream from the site of the dam and depositing the sand pluvially underwater at the dam site.

In order to evaluate the seismic stability of both the concrete and the sand sections of the dam, an evaluation of the liquefaction potential of soils below the river bed was required. In addition, the sand fill portion of the dam was placed without additional compaction and thus an evaluation of the cyclic strength of the embankment sand as a function of density was required to evaluate the need for any remedial sand compaction or densification at the site.

Sand Deposition of Shinano River and 1964 Earthquake Damage

Some familiarity with the history of soil deposition at

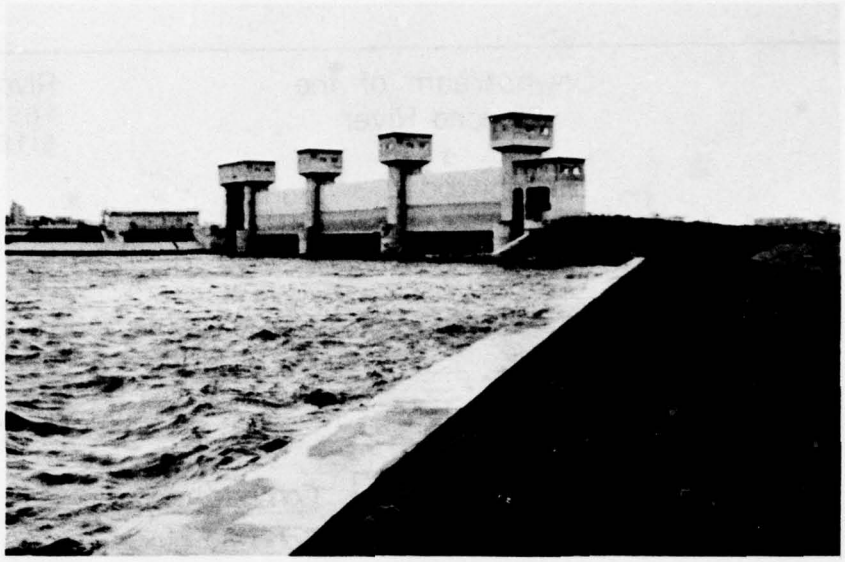

(a)

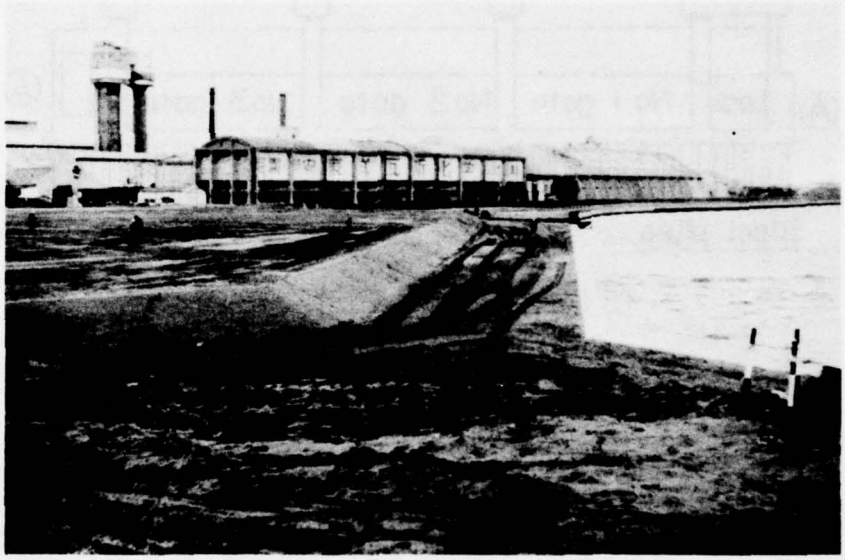

(b)

Fig. 8 Illustration of Diversion Dam being constructed in Niigata, Japan. a) Concrete gate section in north half of river. b) Sand fill section in south half of river.

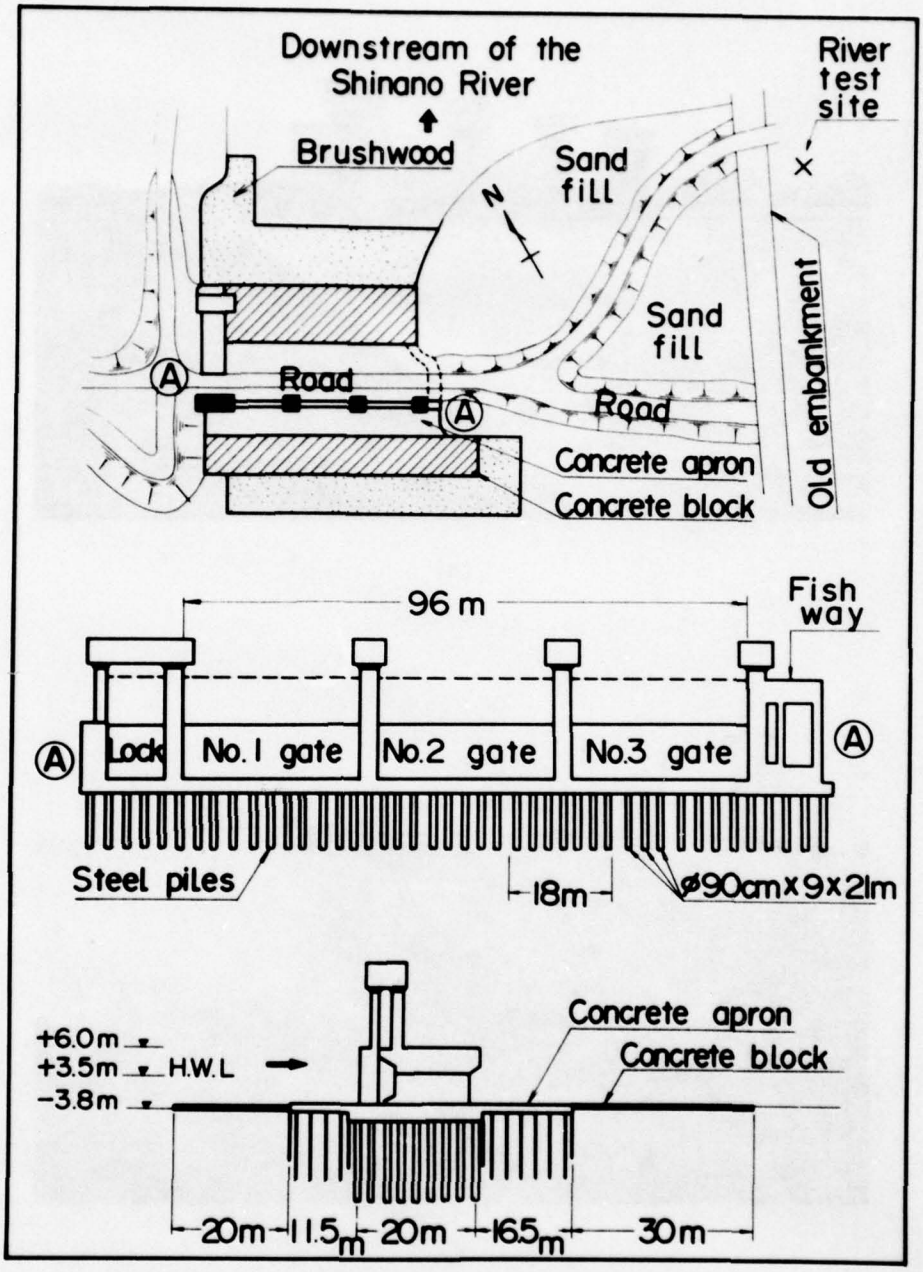

Fig. 9 Plan and Cross-Section of Concrete and Sand Diversion Dam, Niigata, Japan.

Niigata is useful in order to understand differences in the characteristics of underlying soil layers and to understand the damage patterns that occurred in the 1964 earthquake. Such a picture is presented in Fig. 10 which graphically shows river flow patterns in Niigata for the past 300 years.

It may be seen that both the Shinano River and the Agano River have consistently meandered over the site, resulting in alternate cycles of scour and deposition of silt and sand. (Fig. 10 A to E). By the middle of the 18th century, the area consisted of low-lying marshes, sand bars, scour holes, and braided streams (Fig. 10G).

Beginning in the middle of the 18th century, agriculture was encouraged in the area and reclamation of low-lying land was undertaken by dumping sand in water. This reclamation process was accelerated following the Meiji restoration in 1864 when Niigata became an important sea port specializing in trade with Russia. Thus, by 1926 the Shinano River was channelized, deep scower holes were filled, and adjacent low-lying swamps were reclaimed (Fig. 10H).

Fig. 11 shows damage patterns in Niigata that resulted from the 1964 earthquake. In general, no significant damage was noted in Zone A (a beach sand deposit), light damage was noted in Zone B (an older stream deposit), and heavy to calistrophic damage was noted in Zone C (a new reclaimed deposit), which was immediately adjacent to the Shinano River. By

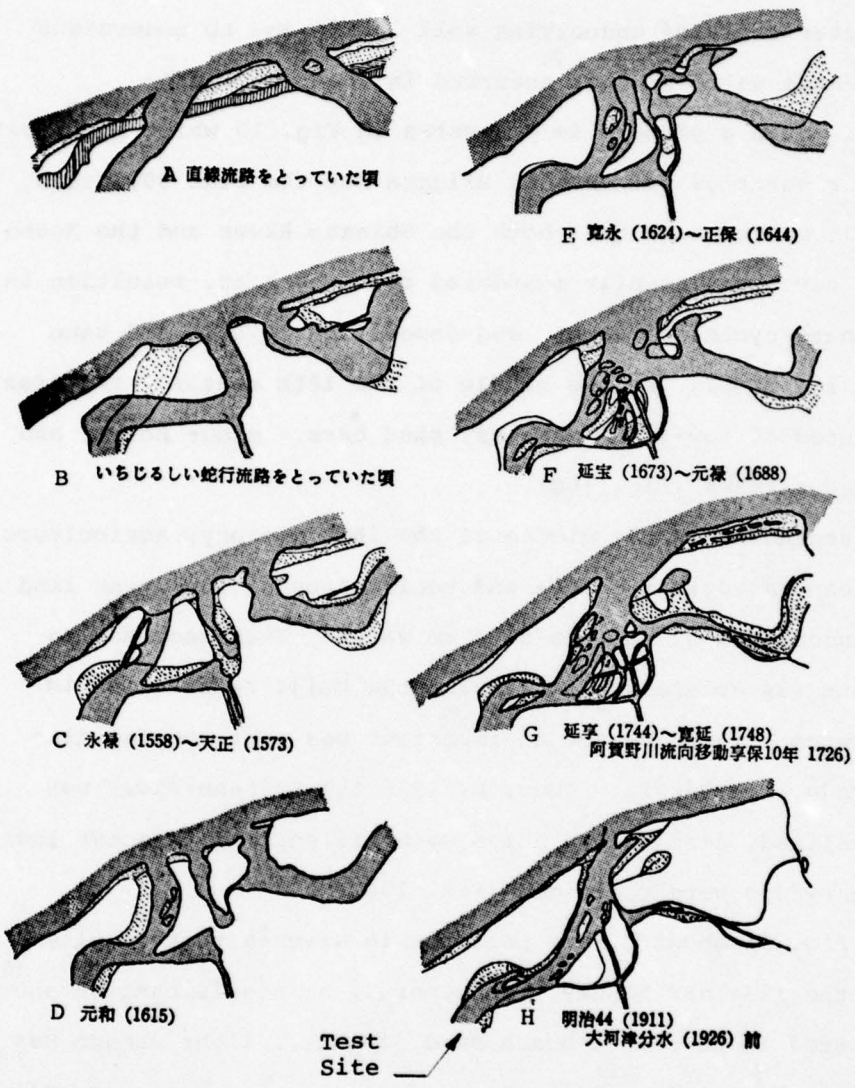

Fig. 10 History of river flow pattern at Niigatta, Japan. A) Orignial straight channel - Shinano River on left and Agano River on right. B) Channel becomes tortuous. C) Channel pattern in 1558-1573. D) Channel in 1615. E) Channel in 1624-1644. F) Channel in 1673-1688. G) Channel in 1744-1748 (Agano river changes course away from Niigata). H) Channel in 1926

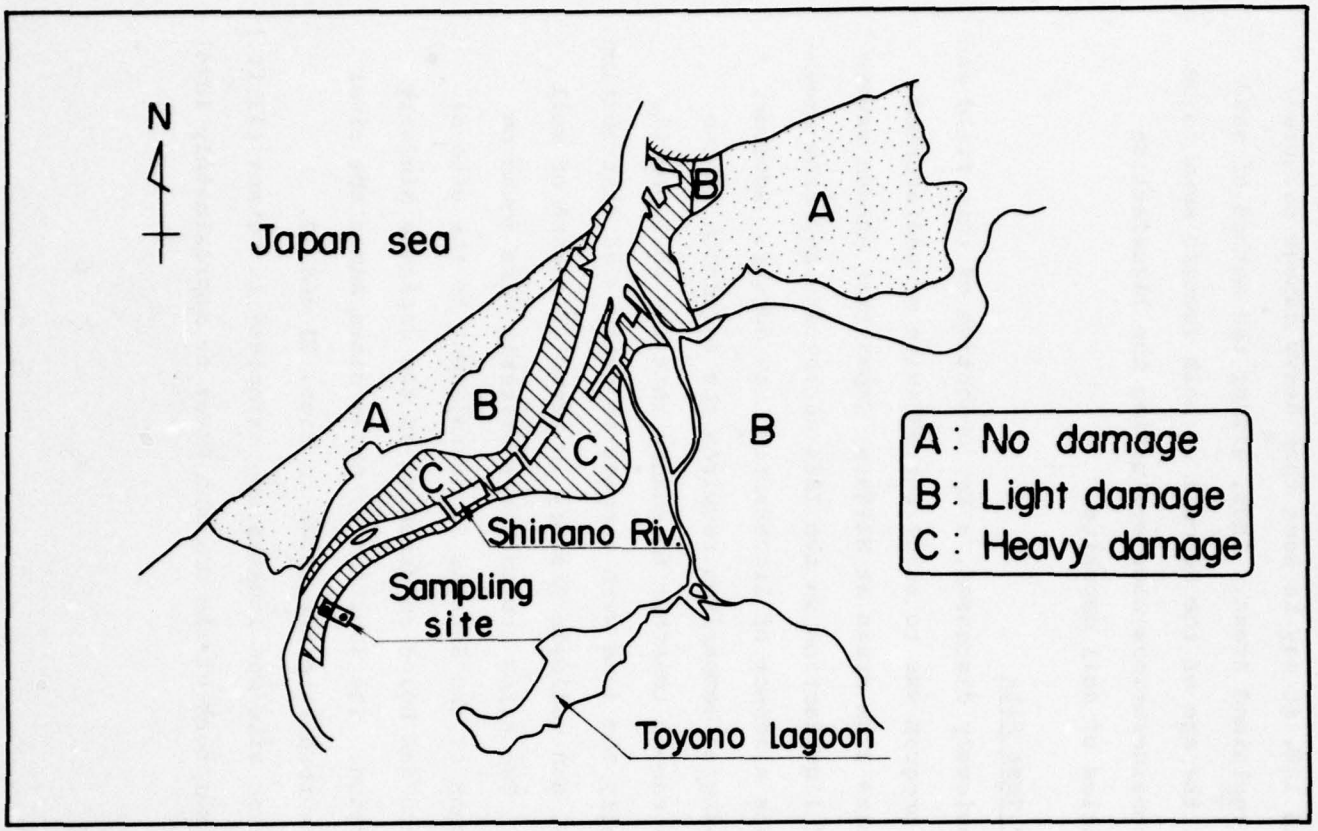

Fig. 11 Map of Niigata Showing Damage Patterns Caused by the 1964 Earthquake.

comparing the shape of the heavy damage in Zone C (Fig. 11) with the shape of the Shinano River channelization shown in Fig. 10G and 10H, it may be seen that heavy damage occurred in heavily reclaimed areas. Thus, either the method of sand deposition, the age of the deposit or both factors seem to be important considerations when evaluating the liquefaction characteristics of soil deposits.

Location of Test Site

As previously discussed, a key objective of this field and laboratory program was to study the behavior of undisturbed soil specimens from areas at Niigata, Japan that showed severe evidence of liquefaction in the 1964 earthquake and from areas where surface evidence of liquefaction was absent. However, such a meaningful comparison requires the selection of two sites close enough together to ensure that the soil profile is essentially the same with respect to grain size distribution, grain shape, and geologic history in terms of method of soil deposition. Two sites meeting this criteria were found on the south bank of the Shinano River adjacent to the site of the diversion dam being constructed by the Japanese Ministry of Construction. The location of these sites, named the river site and the road site, are shown in Figs. 11 and 12.

The river site was located approximately 10 meters (33 ft.) from the right bank of the Shinano River on approximately level

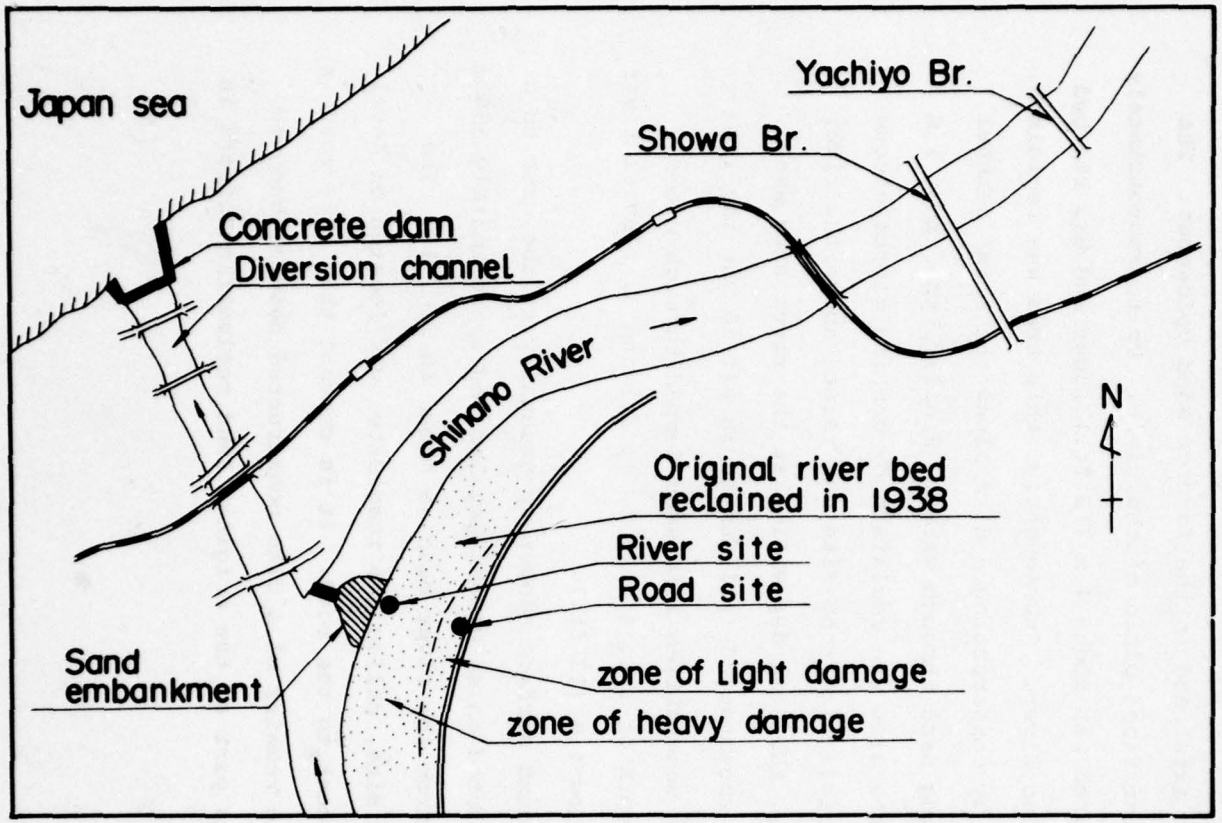

Fig. 12 Map Showing Location of the River Sampling Site and the Raod Sampling Site.

ground (Fig. 13). Following the 1964 earthquakes, damage surveys reported severe evidence of liquefaction at this location in the form of surface cracking (approximately parallel to the river axis) and in the form of sand volcanoes. The area was in the flood plain of the river. Up to approximately 1955, this area was about 4 m (13 ft.) lower and was the bed of the Shinano River. Subsequently, this area was reclaimed, most likely by constructing a dike along the river channel and by dumping sand through water. Finally, the upper 1 m (3 ft.) of the site was reclaimed by dumping miscellaneous borrow materials after the site was raised above the river level. Thus, the soil deposition at the river site was probably 1) uncompacted fill dumped in air in the top 1 m (3 ft.); 2) undensified fine sand dumped through water between a depth of 1 to 4 m (3 to 13 ft) and 3) fluvial river deposits below 4 m (13 ft.).

The ground surface slopes up gradually to the east to a road constructed on an embankment located approximately 350 m (1150 ft) from the river bank as shown in Fig. 13. The second test site, called the road site, was located on level ground adjacent to the road. It is thought that this road is actually the remains of a dike constructed several hundred years ago as part of the original land reclamation effort in Niigata.

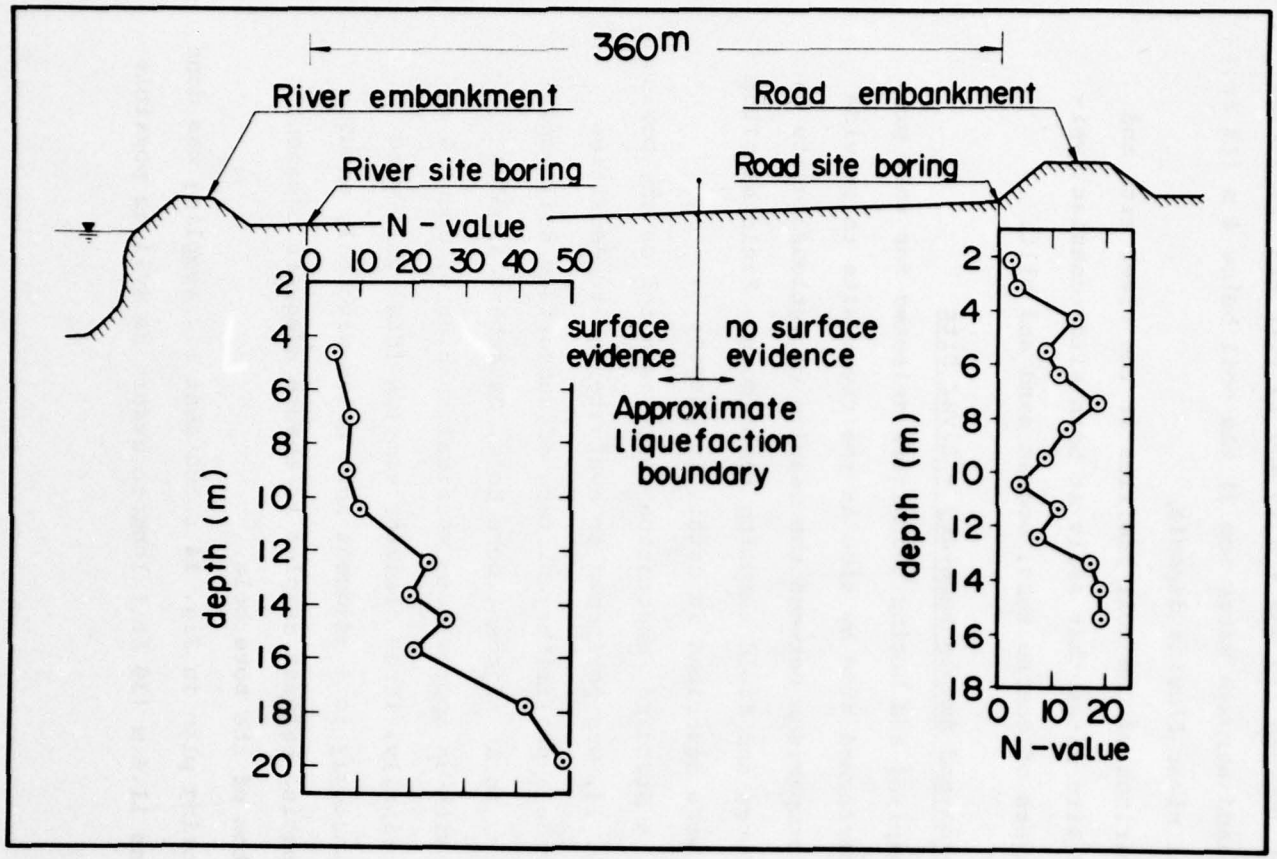

Fig. 13 Cross-Section between River and Road Boring Sites Niigata, Japan.

It is believed that at the road site 1) the top 1.5 m (5 ft.) was deposited above the water surface by dumping fill; 2) the layer between 1.5 and 4 m (5 and 13 ft.) was deposited by dumping sand through water and 3) the soil below 4 m (13 ft.) is a natural river fluvial deposit.

A comparison of the soil profiles at the river site and at the road site shows that soils at both sites consist typically of layers of coarse sand, medium sand and silt.

Boring Program and Sample Recovery - River Site

All sampling and boring techniques selected for this program were performed side by side at the river site to provide a basis of comparison between the results of various insitu test procedures and field sampling techniques. Field sampling procedures were described in detail in Chapter 2.

First, a Standard Penetration Test, as noted on the boring plan in Fig. 14, was performed to evaluate insitu densities and to provide a preliminary picture of subsurface soil conditions. Then, in an adjacent bore hole, Osterberg samples were taken with an approximate vertical spacing of about 4 m (13 ft.). Finally, large diameter samples (Fig. 15) were taken continuously in 4 adjacent bore holes with only enough vertical spacing between samples to ensure adequate cleanout of the bottom of the bore hole.

The boring plan in Fig. 14 shows that all sampling was done along a line 11.6 m (30 ft.) long to ensure as well as possible

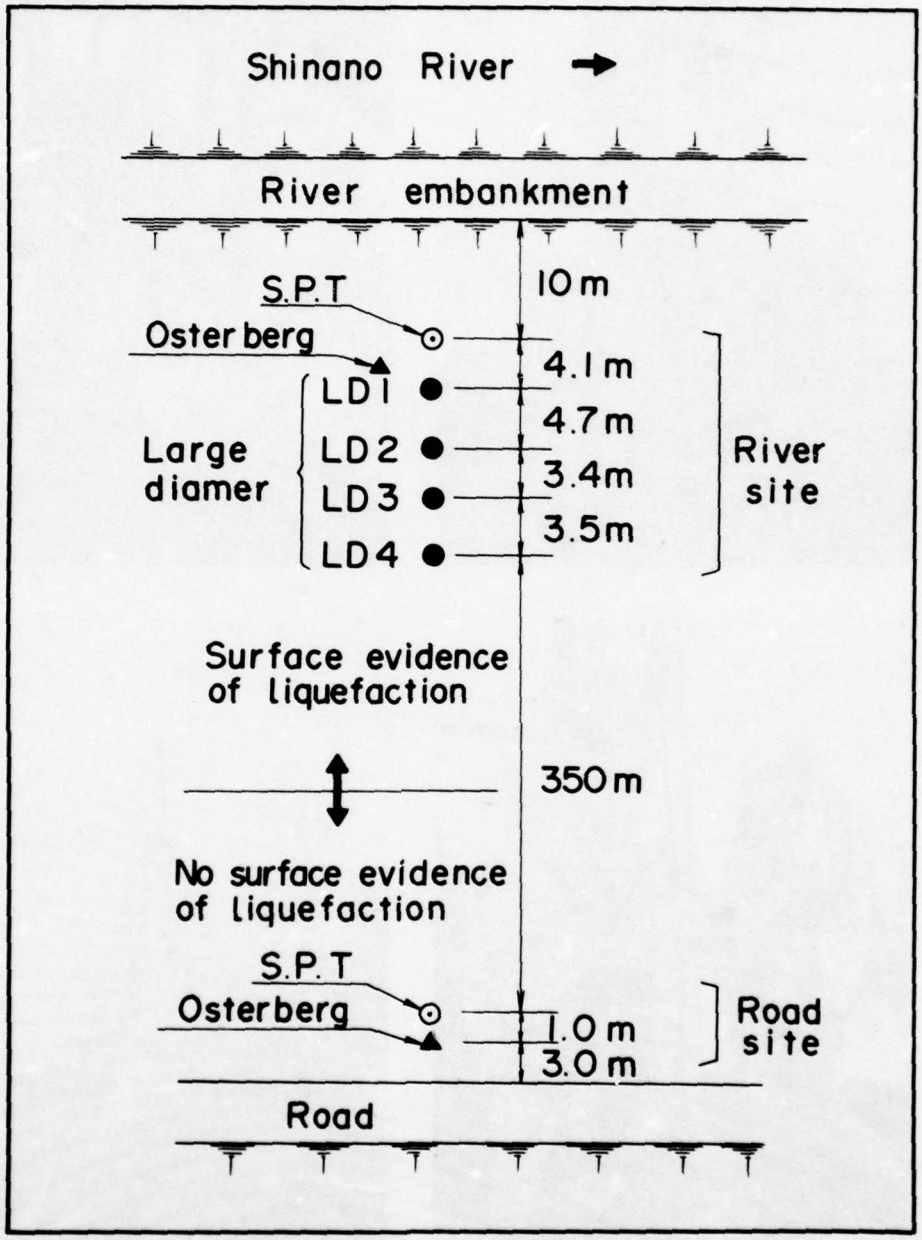

Fig. 14 Boring Plan at River and Road Sites.

(a)

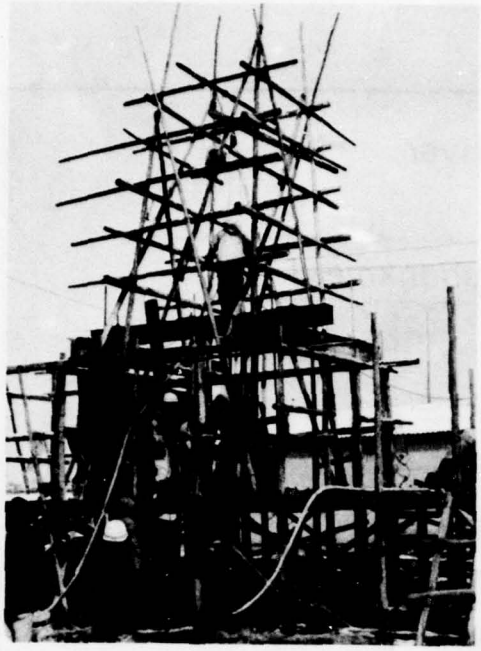

(b)

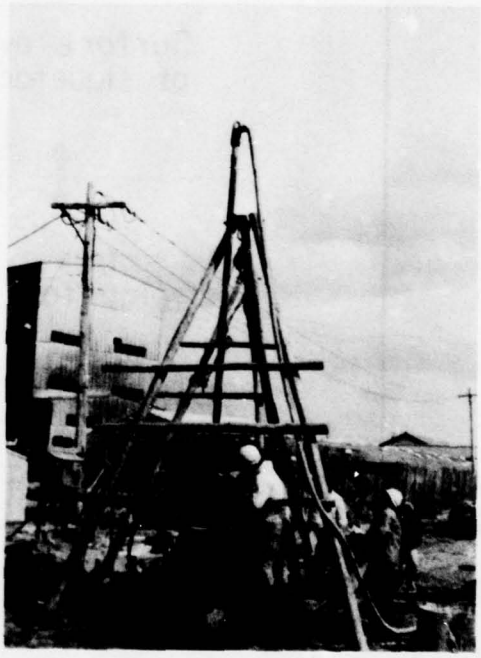

Fig. 15 a) Large Diameter Sampling at River Site
b) Osterberg Sampling at Road Site.

that the same soils were sampled in each boring.

A summary of the results of the sampling program at the river site is tabulated in Table 2 and graphically shown in Fig. 16 with an estimate of sample quality. In general the quality of the 6 Osterberg samples taken at the river site were considered to be good and recovery was high.

The quality of the large diameter samples ranged from no recovery to excellent. The first boring, LD1, had to be abandoned at a depth of 6 m (20 ft.) because of an obstruction. Recovery of samples in Boring LD2 was initially poor but improved rapidly as experience was gained with the new large diameter sampling technique. Recovery was excellent in boring LD3 to a depth of 7 m, where unexpected difficulty in recovery was found. Finally, even better sample recovery was noted in boring LD4 showing that sampling techniques had been mastered. Nevertheless, sampling results was difficult past 8 m. Inspection of the partially recovered samples at deeper depths showed the existence of a layer of uniformly graded loose coarse sand lacking any fine material whatsoever. This seemed to explain the reason for sampling difficulty since this type of material is difficult to sample using any technique.

Boring Program - Road Site

The boring and sampling program at the road site was similar to that at the river site except that in the interests of economy, large diameter samples were not taken. A Standard

TABLE 2

SUMMARY OF SAMPLE RECOVERY
Niigata, Japan

	Boring No.	Sample No.	Type of Sample	Depth (cm)	Distance Pushed (cm)	Sample Quality	No. of Specimens		
	LD 1	1	LD	1.10-1.80	70	good	5		
	LD 1	2	LD	2.65-3.35	70	good	6		
	LD 1	3	LD	4.15-4.85	46	lost	0		
	LD 1	4	LD	5.15-5.65	50	very disturbed	2		
	LD 2	1	LD	2.15-2.85	70	good	6		
	LD 2	2	LD	3.20-3.90	70	not good	3		
	LD 2	3	LD	4.15-4.85	70	lost	0		
	LD 2	4	LD	5.15-5.66	51	lost	0		
	LD 2	5	LD	6.15-6.64	48.5	lost	0		
	LD 2	6	LD	7.15-7.74	58.5	lost	0		
	LD 2	7	LD	8.15-8.85	70	good	5		
	LD 2	8	LD	9.15-9.85	70	good	4		
	LD 2	9	LD	10.15-10.85	70	lost	0		
	LD 2	10	LD	11.15-11.64	49	poor	2		
	LD 3	1	LD	3.10-3.90	80	very good	6 H2		
	LD 3	2	LD	4.10-4.90	80	very good	6 H2		
	LD 3	3	LD	5.10-5.90	80	good	5		
	LD 3	4	LD	6.10-6.90	80	very good	7 H2		
	LD 3	5	LD	7.10-7.72	62	lost	0		
	LD 3	6	LD	9.10-9.74	64	lost	0		
	LD 3	7	LD	10.10-10.87	76.5	lost	0		
	LD 3	8	LD	11.15-11.69	53.5	poor	2		

TABLE 2 (Cont.)

	Boring No.	Sample No.	Type of Sample	Depth (cm)	Distance Pushed (cm)	Sample Quality	No. of Specimens		
	LD 3	9	OB	12.00-12.90	90	poor			
	LD 3	10	OB	13.00-13.90	90	very good			
	LD 4	1	LD	1.15-1.95	80	very good	9		
	LD 4	2	LD	2.15-2.95	80	good	6		
	LD 4	3	LD	3.20-4.01	81	very good	8		
	LD 4	4	LD	4.15-4.95	80	very good	9		
	LD 4	5	LD	5.15-5.95	80	good	7		
	LD 4	6	LD	6.15-6.98	83	good	7		
	LD 4	7	LD	7.15-7.95	80	good	8		
	LD 4	8	LD	9.15-9.95	80	poor	3		
	LD 4	9	LD	10.15-10.95	80	poor	1		

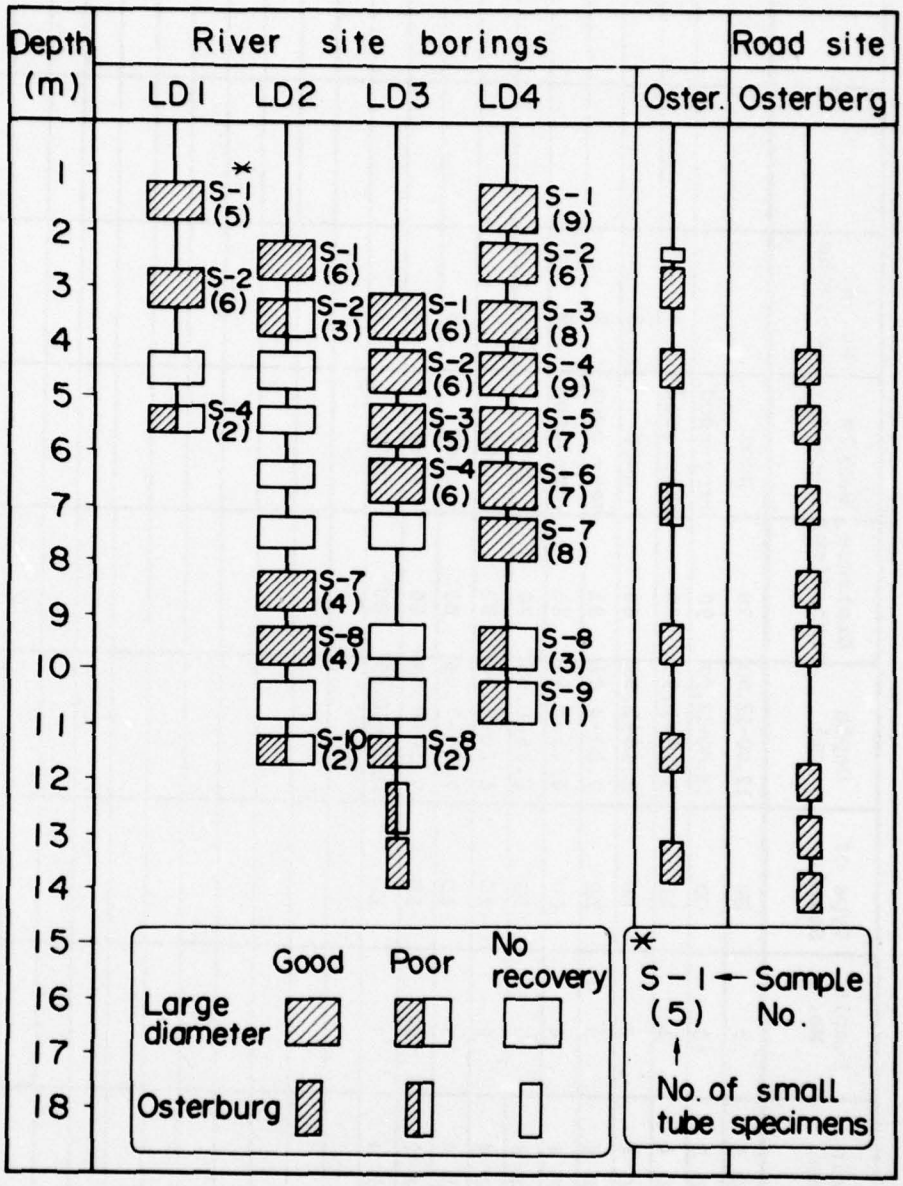

Fig. 16 Records of sample recovery at Niigata, Japan.

Penetration test was first used to define soil densities and the subsurface soil profile. Then, in an adjacent bore hole as shown in Fig. 14, nearly continuous Osterberg samples were taken to a depth of 14 m (46 ft.). Recovery and the quality of these samples were high as shown on Fig. 16 which summarizes the field sampling program at the road site.

CHAPTER 4

LABORATORY TEST PROCEDURES

Introduction

Each of the soil specimens obtained from the field were tested in Japan to evaluate index property values and to determine cyclic triaxial strength behavior. These test procedures, described in detail in subsequent pages, generally followed U.S. practice and thus the test results may be evaluated in the same way as test results obtained from U.S. laboratories.

Index Property Tests

A complete series of index property tests were performed on each specimen from the large diameter sample and on each Osterberg test specimen as follows:

1. Initial and consolidated dry unit weight determination
2. Specific gravity tests
3. Grain size distribution
4. Limiting minimum and maximum density tests (relative density)

Dry unit weight - Values of initial dry unit weight were determined by measuring the dimensions of the thawed specimen confined in the triaxial cell under a small vacuum of -20 KN/m^2 (-400 lb/ft^2). Three circumference (Pi tape) measurements were made at the top, middle and bottom of the specimen and averaged to obtain the specimen diameter after making a suitable correction for membrane thickness. Specimen height was determined

with a vernier caliper. The weight of the solid portion of the specimen was determined at the completion of the triaxial test by carefully washing the specimen into a beaker and drying it in an oven for 24 hours.

A comparison of specimen dimensions before and after thawing under the $-20\ KN/m^2$ ($-400\ lb/ft^2$) vacuum showed that an average volume decrease of approximately 1% occurred for all specimens. This is significantly less than the 9% volume change associated with the thawing of water showing that ice lenses were probably not present and that water did not fill the specimen voids before freezing. The absence of ice lenses and of continuous water in the specimen voids is an indirect indication that freezing did not disrupt the fabric of the specimen.

Values of consolidated dry unit weigth were calculated from measurements of axial deformation and specimen volume change during consolidation after saturation at a low effective stress of $20\ KN/m^2$ (500 psf). In general, volumetric strains on the order of 5% were measured for the majority of the specimens.

Grain size and specific gravity - Specimen grain size distributions and specific gravity values were determined using Japanese standards (Japanese Society of SM and FE, 1976) which are for most practical purposes similar to ASTM (1976) procedures.

Relative Density Tests

Both maximum and minimum density tests were performed on

each specimen obtained in the field. Minimum density values were obtained by carefully spooning oven dry sand into a mold with zero height of drop. A number of minimum density values were obtained for each specimen and the minimum value was reported.

Maximum density values were determined by subjecting a surcharged dry soil specimen to vertical vibration. Subsequent investigations, however, showed that these density values were higher than values that would be measured in the U.S. using techniques such as the ASTM D2049 procedure. Therefore, relative density values given in this report were corrected upward to make them comparable with values used in U.S. Geotechnical Engineering practice.

Cyclic Triaxial Strength Testing

The triaxial cells and cyclic loading apparatus used in this investigation are shown in Figs. 17 and 18. The equipment meets the standards for cyclic soil strength equipment presented by Silver (1976). For example, the cells are provided with low friction bellofram seals and an external chamber that makes it possible to maintain exact alignment between the specimen plattens. The saturation and pore pressure system provided

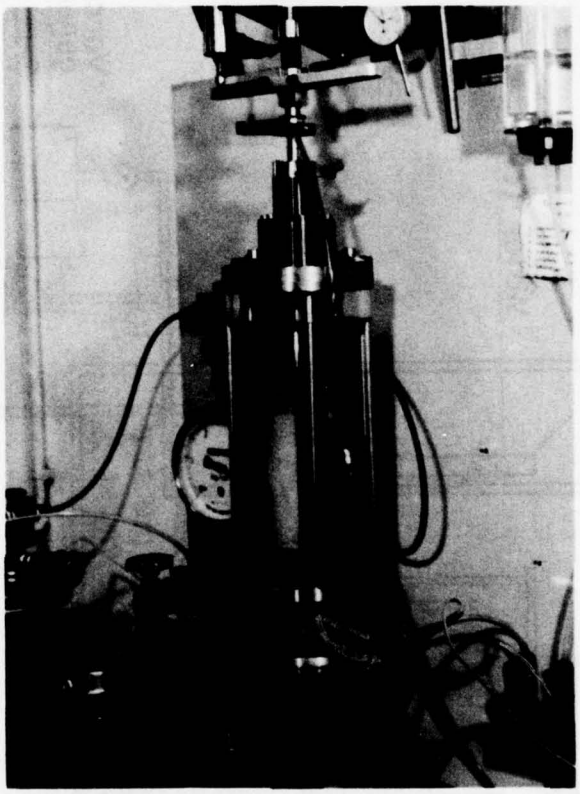

Fig. 17 (a) Cyclic Triaxial Test Cell and Cyclic Loading Equipment Used for This Investigation

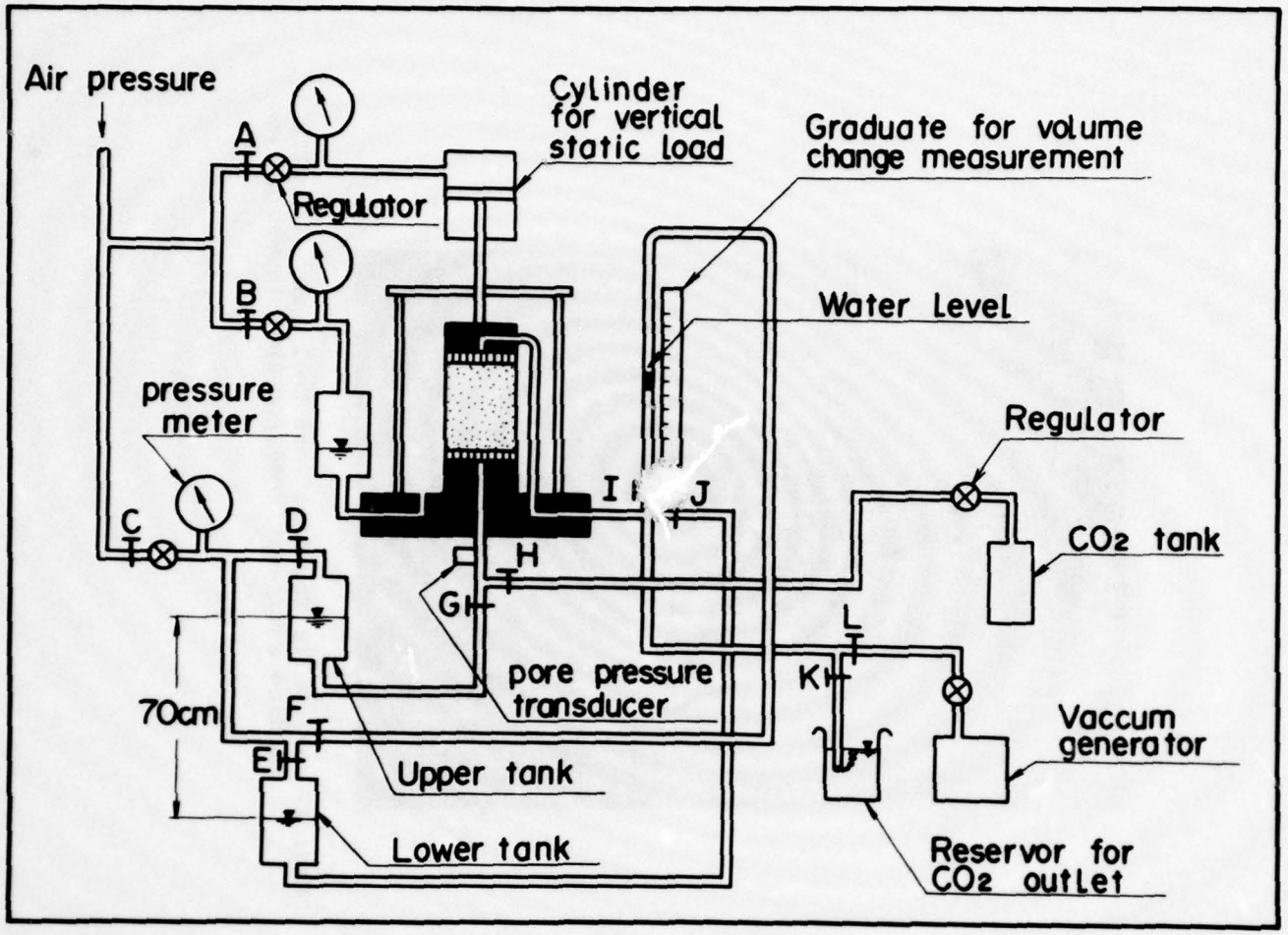

Fig. 18 Schematic Representation of the Components of the Cyclic Triaxial Test Equipment.

top and bottom platten drainage and flushing.

A semi-conductor pore pressure transducer was mounted rigidly in the base of the triaxial cell, minimizing the volume of the pore pressure measurement system. B values were measured with a digital voltmeter readout system capable of reading $\pm$ 5 x 10^{-5} KN/m^2 (2 lb/ft^2).

Cyclic loads were applied by a servo-hydraulic loading apparatus employing a rubber linkage to enhance system stability. Time histories of load, deformation and pore pressure were amplified and readout using a light beam galvanometer oscillograph.

Preparation of frozen samples - All frozen samples, both small specimens from the large diameter sampler and 0.8 m (2.6 ft.) long thin wall shelby tubes from the Osterberg sampler were transported frozen packed in dry ice to the laboratory. There they were stored in an ice cream freezer at -10°C until tested.

Small diameter specimens were prepared for cyclic triaxial strength testing by first trimming loose sand from the specimen ends to eliminate any weak zones at the specimen top and bottom and to ensure that the specimen ends were parallel. Stones were then placed on the ends of the specimen which was extruded from the split brass liner by pushing down on a mandrel.

Osterberg specimens were prepared in a similar way except that because they were shipped to the laboratory frozen in 0.8 m (2.6 ft.) long lengths, the first step was to saw the

tube into 15 cm (6 in) long lengths using the electric hacksaw. shown in Fig. 19a. Then a band saw was used to split the tube lengthwise while a clamp kept the tube from springing open (Fig. 19b). For both cutting procedures, liquid nitrogen was used as the cutting fluid to prevent the specimen from thawing. After splitting, the clamp around the tube was slowly opened making it possible to remove the intact specimen. The specimen was then placed still frozen in a frame where the ends were trimmed flat and parallel.

Specimen measurements - The still frozen small specimen or Osterberg specimen was placed on the triaxial bottom platten, the top platten was lowered to make contact with the top stone and a split membrane expander was used to place a triaxial membrane around the specimen which was subsequently sealed with O-rings. A small vacuum of -20 kN/m^2 (-400 lb/ft^2) was applied to maintain the shape of the sample and initial frozen specimen dimensions were obtained to calculate the initial frozen unit weight. All diameter measurements were taken with a circumference rule (Pi tape) at the top, middle, and bottom of the specimen. Specimen height was measured with a vernier caliper. Appropriate corrections were made for the membrane thickness.

After the sample was allowed to completely thaw out for two hours under the applied vacuum, dimensions were again taken to calculate the thawed unit weight. The triaxial cell was then assembled around the sample, water was introduced into the triaxial chamber, and the vacuum was gradually reduced to

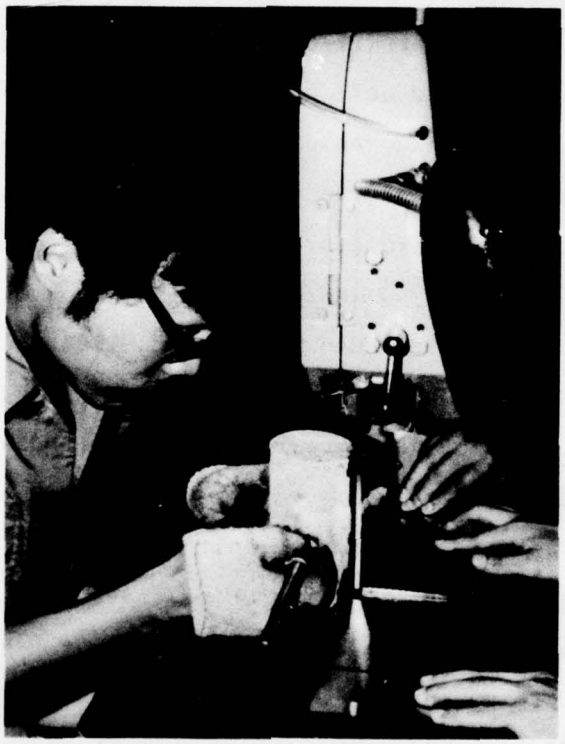

Fig. 19 (a) Cutting Specimen Lengths from Shelby Tube Samples Using Liquid Nitrogen (b) Splitting Sample Tubes to Facilitate Extrusion of Frozen Sample

zero while simultaneously increasing the cell pressure to a value of 20 KN/m^2 (400 lb/ft^2).

Saturation and consolidation - The specimen preparation, saturation and consolidation procedure is schematically represented in Fig. 20. It may be seen that after the specimen was allowed to thaw, CO_2 was used to aid the saturation by allowing it to flow from the bottom platten through the specimen to the top platten for approximately 1 hour. In this way, CO_2 was used to replace air from the soil voids. Since CO_2 is significantly more soluble in water than air, saturation time was greatly reduced.

Saturation and back pressure procedures closely followed those suggested by Silver (1976). Saturation was accomplished by concurrently applying cell pressure and back pressure to the specimen while maintianing an effective confining pressure of 20 KN/m^2 (400lb/ft^2). B value checks were made at intervals to monitor the saturation process. All tests were conducted at back pressure values of 26 kN/m^2 (2000 lb/ft^2) and the resulting B values in all cases exceeded 0.96. Consolidation was subsequently carried out by increasing the cell pressure while maintaining a constant value of back pressure and while monitoring axial deformation and specimen volume change with time so that the specimen consolidated unit weight could be determined. During both the back pressuring and consolidation process, correction loads were applied to the piston to compensate for the uplift force on the load rod which was rigidly connected to the top platten.

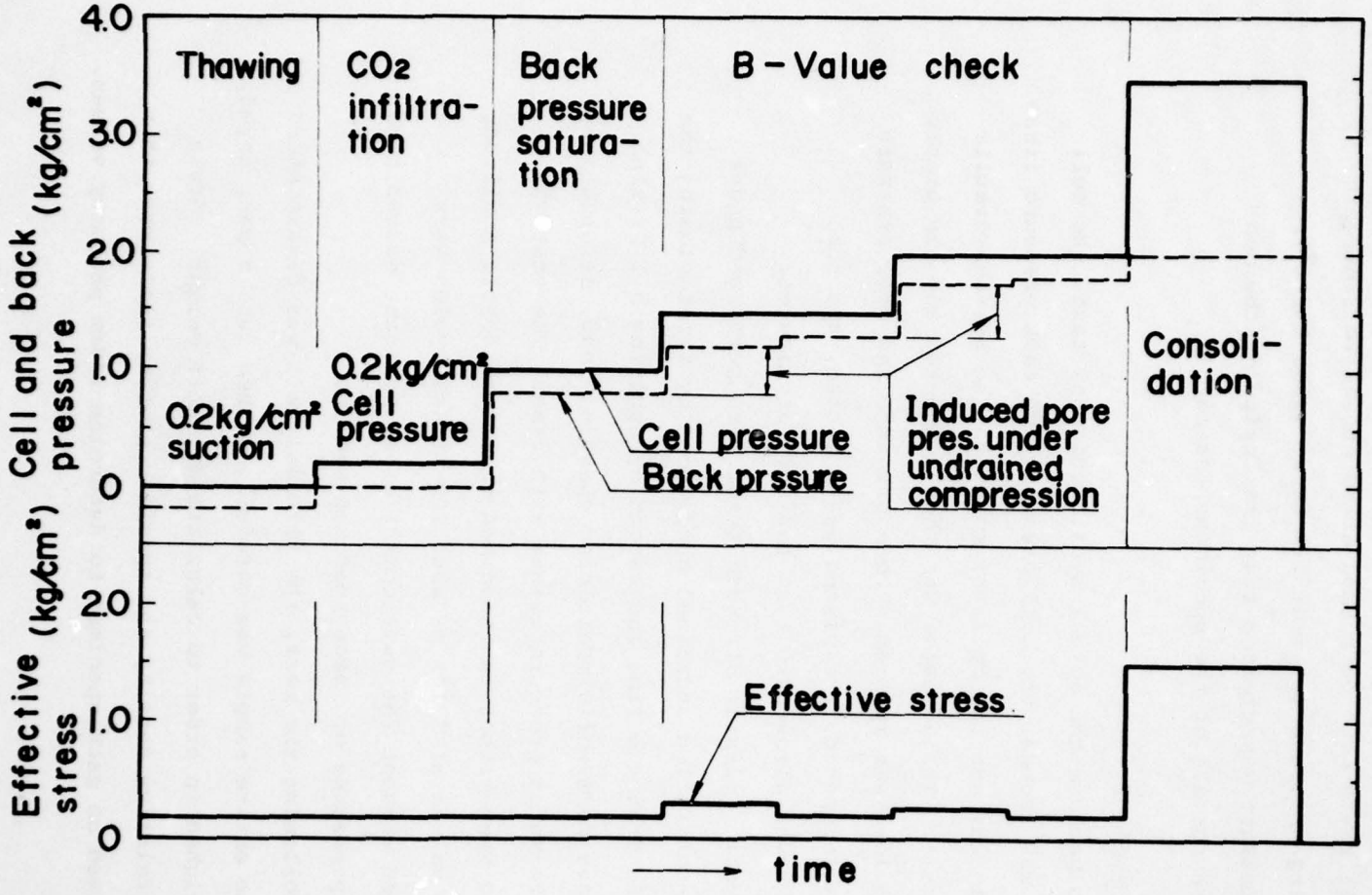

Fig. 20 Schematic Representation of Thawing, Back Pressure and Consolidation Process for Frozen Specimens.

Confining Pressure

All tests were performed at an effective isotropic confining pressure (σ'_o) of 147 KN/m^2 (3000 lb/ft^2). This pressure was greater than the insitu overburden pressure for all of the specimens tested.

Cyclic Testing

To perform the actual cyclic triaxial test, the cell piston was locked, the cell pressure and back pressure lines were closed, and the cell was moved to the servo-hydraulic test frame. The actuator was then connected and the proper seating load was applied. Pore pressure and cell pressure lines were opened, the piston was unlocked, and the specimen was allowed to rest for several minutes.

Cyclic triaxial strength tests were performed under stress-controlled undrained conditions by first closing the specimen drainage line and second by applying a 1 Hz sine load wave form while monitoring changing load, deformation, and pore water pressure values with time. The test was stopped when either the specimen exhibited double amplitude strain values of ± 10% or when 200 stress cycles were exceeded without the development of significant excess pore water pressures or large specimen strains.

Following the test, the triaxial cell was disassembled and the entire sample was carefully washed into a pan, dryed, and weighed in order to calculate dry unit weight. Grain size, relative density and specific gravity tests were then performed on each specimen to determine index property values.

Test calculation procedures - A typical time history plot of load deformation and pore pressure with time for a cyclic strength test performed on a small specimen from the large diameter sample is shown in Fig. 21. It may be seen that there is no significant load fall off when large specimen strains developed. This constant amplitude load wave form was recorded for all tests and thus the test results meet the test limits proposed by Silver (1976).

Values of cyclic stress and strain for each cycle were calculated using the definitions presented in Fig. 22. For convenience, values of cyclic vertical stress applied to the specimen were normalized by calculating the applied cyclic stress ratio SR

$$SR = \frac{\sigma_{d\ell}}{2\sigma'_o}$$

where $\sigma_{d\ell}$ is the single amplitude cyclic axial stress and σ'_o is the initial effective confining pressure. Values of cyclic stress ratio (SR) versus the number of cycles to initial liquefaction (defined as the cycle where the pore water pressure first equals the cell pressure) 5% and 10% double amplitude strain were then plotted to define the cyclic strength of undisturbed specimens of Niigata sand.

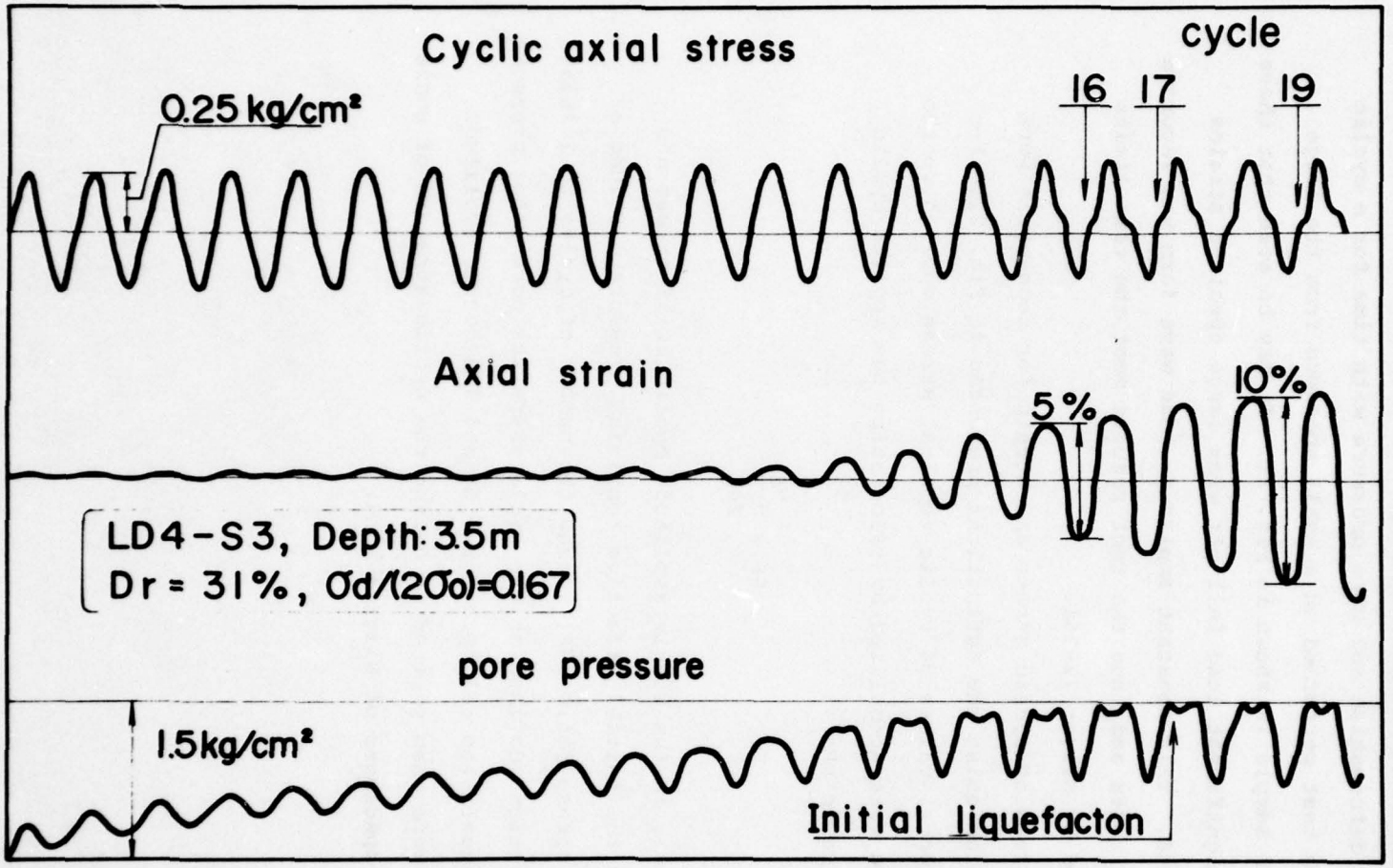

Fig. 21 Typical Time History of Load, Deformation and Pore Water Pressure for a Cyclic Triaxial Strength Test on a Large Diameter Sample Specimen.

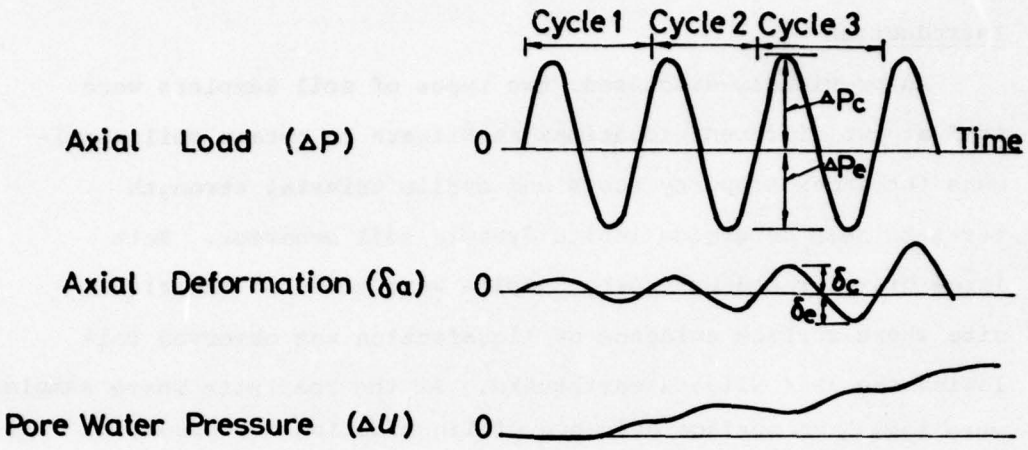

Definition of Calculated Stress and Strain Values

$$\sigma_{dl}\,(\text{Single Amplitude}) = \frac{\Delta P_c + \Delta P_e}{2A_c}$$

$$\epsilon_a\,(\text{Double Amplitude}) = \frac{\delta_c + \delta_e}{L_c}$$

Where $\Delta P_c, \Delta P_e, \delta_c, \delta_e$ are Defined in Figures Above

A_c is the Consolidated Specimen Area

L_c is the Consolidated Specimen Length

Fig. 22 Definition of Measured Load-Deformation Values and Calculated Stress Strain Values for Cyclic Triaxial Strength Tests.

CHAPTER 5

CYCLIC BEHAVIOR OF SPECIMENS FROM LARGE DIAMETER SAMPLES FROM RIVER SITE

Introduction

As previously discussed, two types of soil samplers were used at two different locations in Niigata to obtain soil specimens for index property tests and cyclic triaxial strength tests to help determine insitu dynamic soil behavior. Both large diameter and Osterberg samples were taken at the river site where surface evidence of liquefaction was observed following the 1964 Niigata earthquake. At the road site where samples were taken, no surface evidence of liquefaction was observed.

This chapter describes index property test results and cyclic triaxial strength test results for tests performed on specimens of sand obtained by pushing small diameter tubes into the large diameter samples. Subsequent chapters will describe test results for Osterberg samples, from both the river site and the road site.

Soil Conditions at the River Site

Soil conditions at the river site are shown in Fig. 23 which plots soil type, soil formation, and N values obtained from standard penetration tests. The site consists of approximately 1 m (3 ft) of surface soil. This is underlain by a 3 m (10ft) thick layer of medium sand which was deposited through reclamation of the site from the flood plain of the Shinano River. Below the reclaimed layer is an alluvium

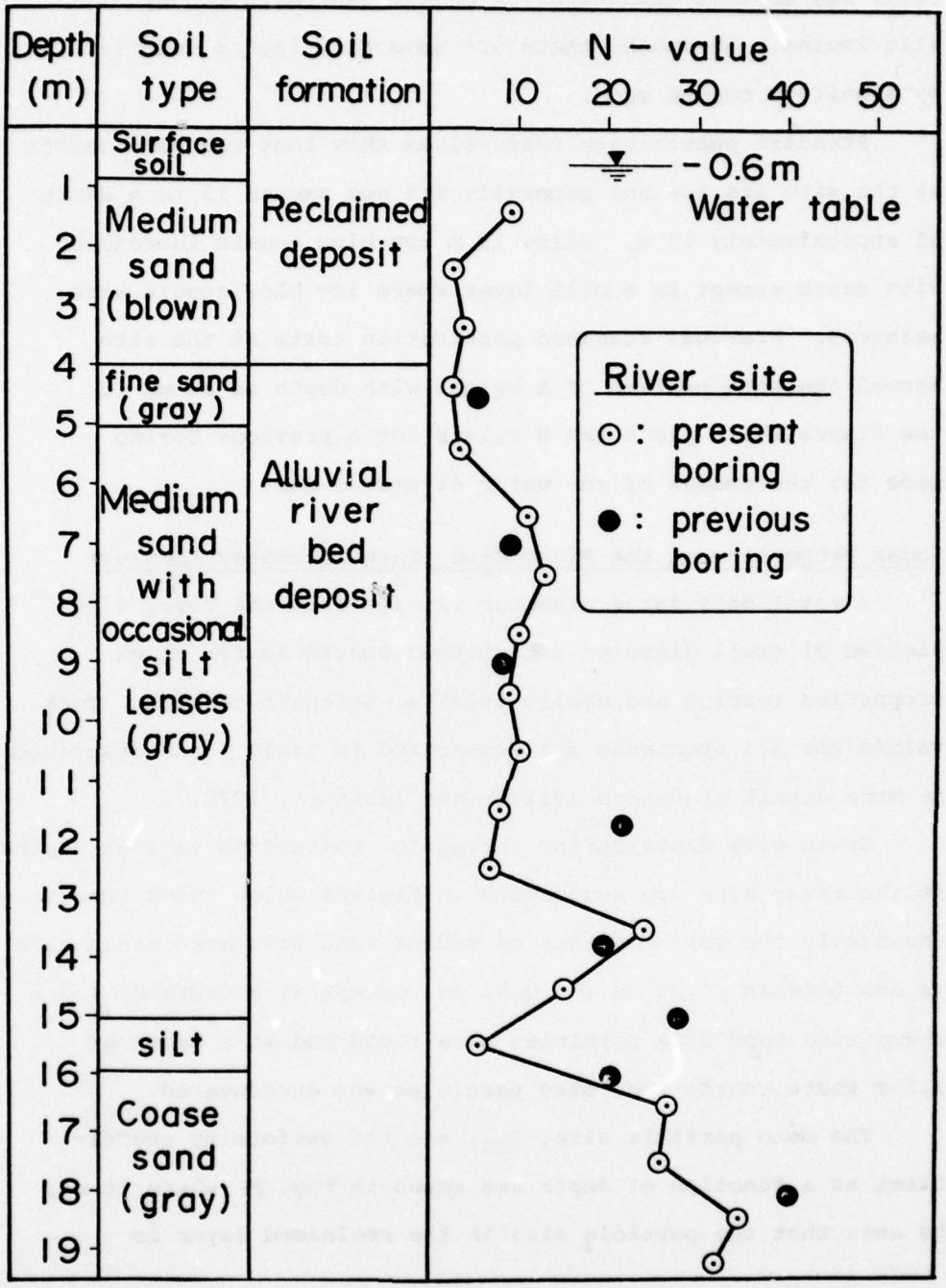

Fig. 23 Soil Profile at the River Site showing Soil Type, Method of Soil Deposition and Standard Penetration Test Values

river bed deposit consisting of medium sand with occasional silt lenses. At depth, there are some silt layers underlain by a uniform coarse sand.

Standard penetration test values show that the blow counts at the site are low and generally did not exceed 15 to a depth of approximately 13 m. Below 13 m the blow counts increased with depth except in a silt layer where low blow counts were measured. Previous standard penetration tests at the site showed the same pattern of N values with depth as shown in the Figure which plots the N values for a previous boring made for the design of the water diversion dam.

Index Properties at the River Site (Large Diameter Samples)

A total of 9 large diameter samples from the river site yielded 31 small diameter undisturbed specimens for index properties testing and cyclic triaxial strength testing. Test values for all specimens are summarized in Table 3 and described in more detail elsewhere (Silver and Ishihara, 1978).

Grain size distribution curves for soils from various depths at the river site are summarized in Fig. 24 which shows that predominantly the soil consists of medium sand with mean grain size values between 0.35 mm and 0.55 mm, except at a depth of 4.5 m where fine sand size particles were found and at a depth of 9.5 m where coarse sand size particles was encountered.

The mean particle size, D_{50}, and the uniformity coefficient as a function of depth are shown in Fig. 25 where it may be seen that the particle size in the reclaimed layer is

TABLE 3
INDEX PROPERTY VALUES AND CYCLIC TRIAXIAL TEST VALUES FOR
SPECIMENS FROM LARGE DIAMETER SAMPLES FROM THE RIVER SITE - NIIGATA, JAPAN

Sample No.	Depth (m)	Gradation		Specific Gravity	Void Ratio		Limiting Void Ratio		Relative Density		$\frac{\sigma_{dl}}{2\sigma_o'}$	No. of Cycles		
		D_{50} (mm)	U_c		e_c	e	e_{max}	e_{min}	D_{rc}(%)	D_r(%)		init.	5%	10%
LD4-52	2.5	0.36	2.7	2.669	0.782	0.808	1.020	0.649	64	57	0.219	8	7	12
"	"	"	"	"	0.816	0.842	"	"	56	48	0.154	55	56	64
"	"	"	"	"	0.804	0.836	"	"	58	50	0.192	3	4	3
"	"	"	"	"	0.785	0.812	"	"	63	56	0.229	10	9	10
LD4-53	3.5	0.37	2.5	2.675	0.948	0.983	1.067	0.615	26	19	0.219	7	5	8
"	"	"	"	"	0.926	0.964	"	"	31	23	0.117	17	16	19
"	"	"	"	"	0.912	0.941	"	"	34	28	0.112	110	109	113
LD3-52	4.5	0.18	1.8	2.651	0.811	0.909	1.257	0.658	61	58	0.338	19	18	21
"	"	"	"	"	0.835	0.856	"	"	70	67	0.397	11	4	11
"	"	"	"	"	0.863	0.885	"	"	66	62	0.330	10	5	12
"	"	"	"	"	0.947	0.974	"	"	52	48	0.282	-	6	12

e, D_r = Initial void ratio or relative density of undisturbed specimens.

e_c, D_{rc} = Consolidated void ratio or relative density of undisturbed specimens.

All tests performed at an effective confining pressure (σ'_o) of 1.5 Kg/cm^2 (3000 lb/ft^2)

TABLE 3 (Cont.)

Sample No.	Depth (m)	Gradation		Specific Gravity	Void Ratio		Limiting Void Ratio		Relative Density		$\sigma_{d\ell}$	Number of Cycles		
		D_{50} (mm)	U_c		e_c	e	e_{max}	e_{min}	D_{rc}(%)	D_r(%)	$2\sigma_o'$	init.	5%	10%
LD3-53	5.5	0.35	2.0	2.663	0.879	0.913	1.069	0.572	38	31	0.208	3	2	3
"	"	"	"	"	0.925	0.965	"	"	29	21	0.157	6	6	7
"	"	"	"	"	0.934	0.971	"	"	27	20	0.102	62	62	64
"	"	"	"	"	0.865	0.902	"	"	41	33	0.142	24	24	25
LD3-54	6.5	0.46	2.0	2.661	0.821	0.853	1.058	0.530	45	38	0.148	7	7	8
"	"	"	"	"	0.768	0.802	"	"	55	49	0.111	50	50	52
"	"	"	"	"	0.816	0.850	"	"	46	39	0.123	16	16	17
"	"	"	"	"	0.810	0.847	"	"	47	40	0.194	2	2	3
LD4-57	7.5	0.45	2.1	2.675	0.792	0.823	0.974	0.554	43	37	0.225	5	4	5
"	"	"	"	"	0.730	0.755	"	"	58	53	0.183	16	14	19
"	"	"	"	"	0.718	0.842	"	"	61	32	0.173	25	23	29
"	"	"	"	"	0.714	0.745	"	"	62	54	0.149	57	57	60

TABLE 3 (Cont.)

Sample No.	Depth (m)	Gradation		Specific Gravity	Void Ratio		Limiting Void Ratios		Relative Density		σ_{dl}	Number of Cycles		
		D_{50} (mm)	U_c		e_c	e	e_{max}	e_{min}	D_{rc} (%)	D_r (%)	$2\sigma_o'$	init.	5%	10%
LD2-57	8.5	0.55	2.7	2.672	0.835	0.872	0.988	0.552	36	26	0.141	10	10	10
"	"	"	"	"	0.758	0.808	"	"	52	42	0.176	7	6	7
"	"	"	"	"	0.807	0.849	"	"	42	31	0.122	21	21	22
LD2-58	9.5	0.7	3.0	2.650	0.794	0.830	0.997	0.477	39	32	0.209	4	3	4
"	"	"	"	"	0.696	0.728	"	"	58	53	0.200	22	17	20
"	"	"	"	"	0.805	0.852	"	"	37	28	0.167	3	3	3
LD2-510	11.5	0.68	3.0	2.678	0.781	0.809	1.022							
"	"	"	"	"	0.755	0.781	"							

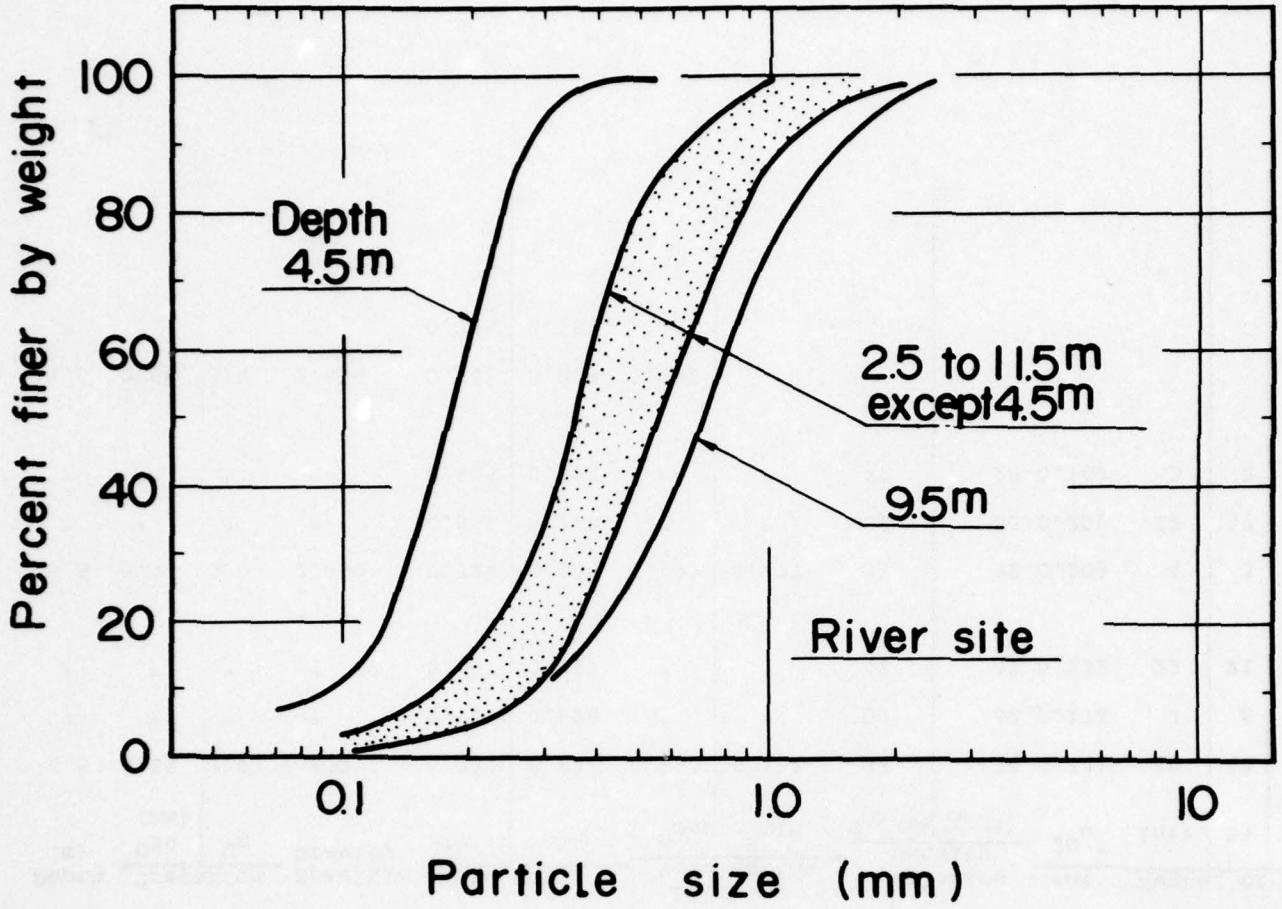

Fig. 24 Summary Showing Grain Size Distribution for Soils at the River Site - Large Diameter Samples.

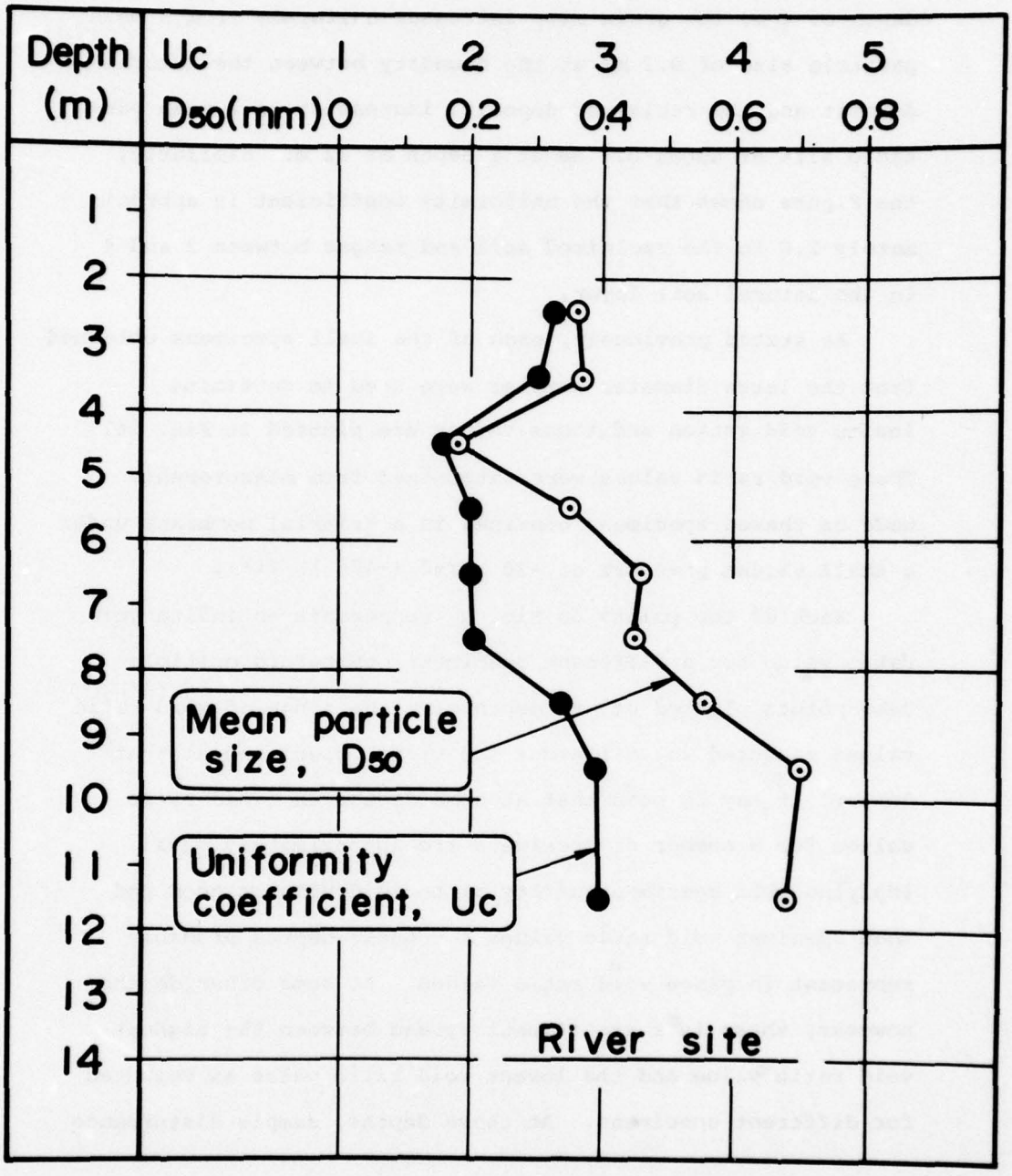

Fig. 25 Mean Grain Size and Uniformity Coefficient as a Function of Depth at the River Site - Large Diameter Samples.

approximately 0.3 mm. In the natural soil, beginning at a depth of 4 m, the grain size increases uniformly from a mean particle size of 0.2 mm at the boundary between the natural deposit and the reclaimed deposit, increasing to a mean particle size of about 0.7 mm at a depth of 12 m. Similarly, the Figure shows that the uniformity coefficient is approximately 2.8 in the reclaimed soil and ranges between 2 and 4 in the natural soil layer.

As stated previously, each of the small specimens obtained from the large diameter sampler were used to determine insitu void ratios and these values are plotted in Fig. 26. These void ratio values were determined from measurements made on thawed specimens confined in a triaxial membrane under a small vacuum pressure of -20 kN/m2 (-400 lb/ft^2).

Each of the points on Fig. 26 represents an insitu void ratio value for a different specimen; therefore multiple data points plotted at any depth give the range of void ratio values measured for different individual specimens at that depth. It may be seen that at some depths the void ratio values for a number of specimens are approximately equal, implying that specimen quality at these depths is good and that specimen void ratio values for these depths probably represent in place void ratio values. At some other depths, however, there is a significant spread between the highest void ratio value and the lowest void ratio value as measured for different specimens. At these depths, sample disturbance

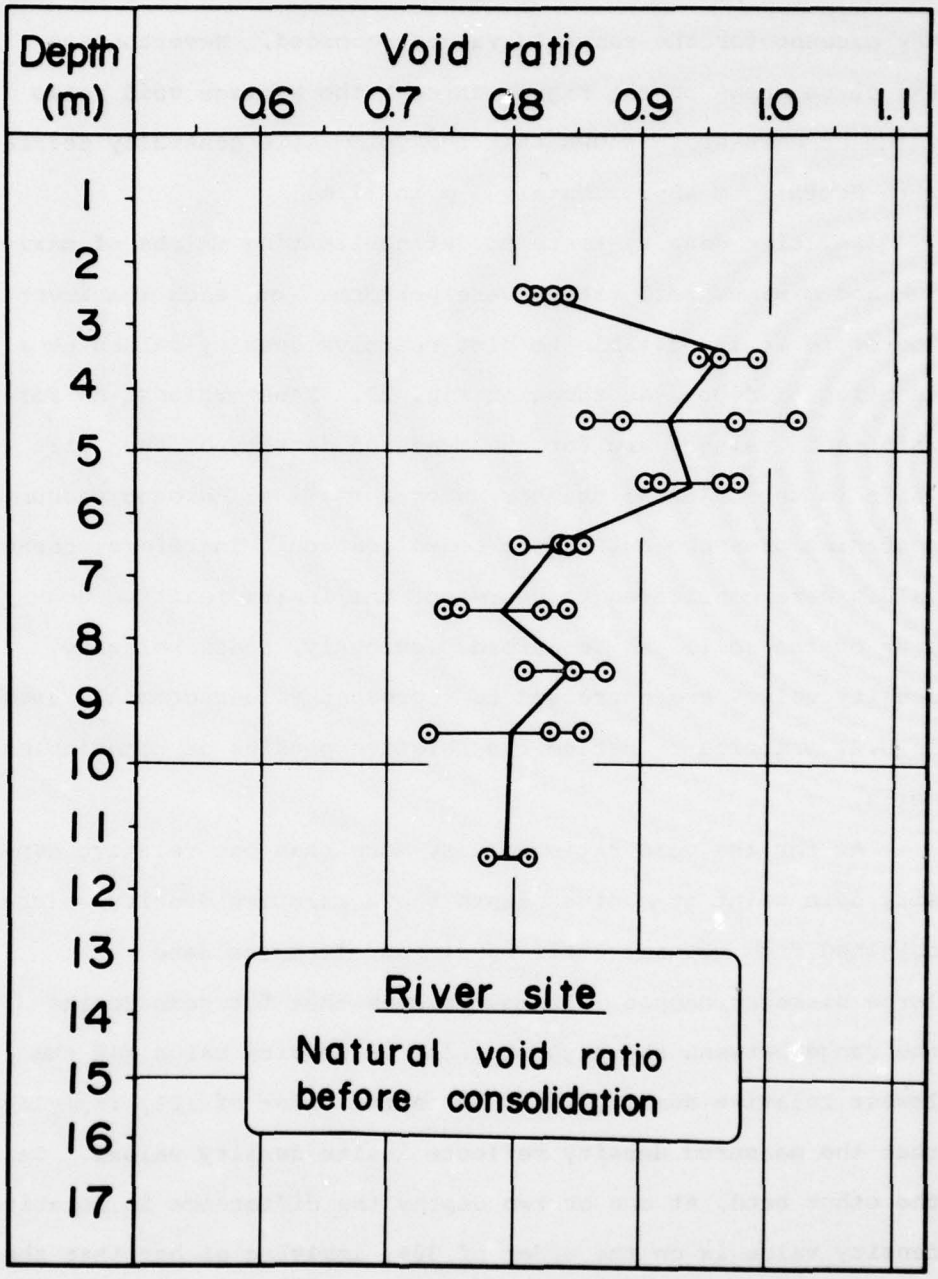

Fig. 26 Insitu Void Ratio as a Function of Depth at the River Site - Specimens from Large Diameter Samples.

and handling problems or the natural variation in soil density may account for the range in values recorded. Nevertheless, the curve drawn on the Figure through the average void ratio value at each depth shows that the void ratio generally decreases with depth from approximately 3 m to 12 m.

Relative density tests to define limiting values of maximum and minimum void ratios were performed on each specimen; therefore it is possible to plot relative density values as a function of depth, as shown on Fig. 27. These values, as for void ratio values, are for the measured density of the soil while in the triaxial chamber under a small all around vacuum confining pressure but before consolidation. Therefore, these values were considered to represent the insitu relative density of the soil. As described previously, these relative density values are corrected to represent values commonly used in U.S. practice to define the relative packing of cohesionless soils.

As for the void ratio values, more than one relative density data point at a given depth shows relative density values obtained from several small specimens from the same large diameter sample. It may be seen that for some depths the range between the highest relative density value and the lowest relative density value is on the order of 10%, implying that the measured density reflects insitu density values. On the other hand, at one or two depths the difference in relative density value is on the order of 30%, implying either that the

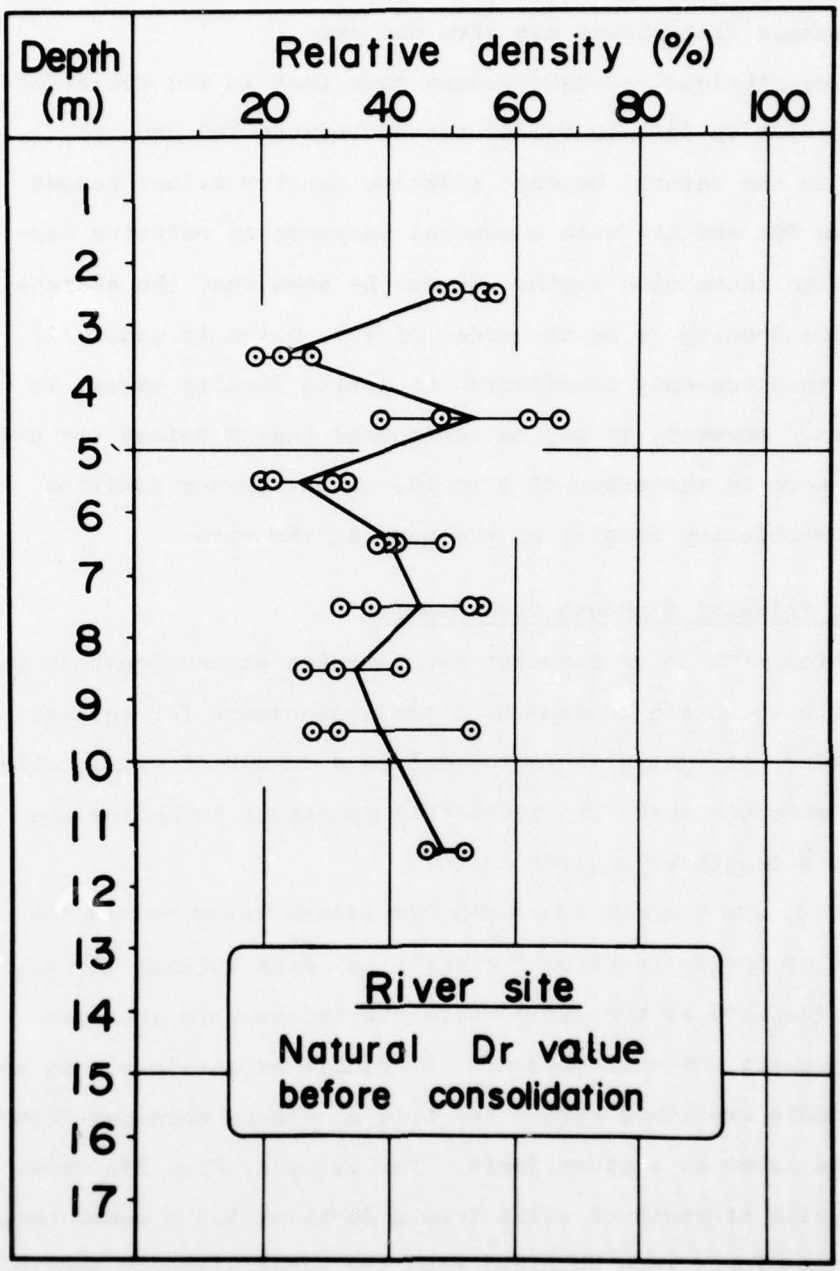

Fig. 27 Insitu Relative Density Values as a Function of Depth at the River Site - Specimens from Large Diameter Samples.

natural variation in soil density is large at that depth or that sample disturbance may have occurred.

Nevertheless, average values show that in the reclaimed sand, relative density values ranged between 20% and 50%, while in the natural deposit relative density values ranged between 30% and 50% with a general increase in relative density with increasing depth. It may be seen that the average relative density is on the order of 40%, which is generally lower than commonly considered for insitu density values at Niigata. However, it may be remembered that N values for the layer were on the order of 5 to 10, which further confirms the low relative density of the sand at the site.

Cyclic Triaxial Strength Test Results

From each large diameter sample taken at any depth it was possible to obtain as many as 9 small specimens for testing. Therefore, it was possible to perform a number of cyclic triaxial strength tests on undisturbed specimens to define the cyclic strength at a given depth.

Fig. 28a through 28i shows the stress ratio versus the number of cycles required for soils to reach initial liquefaction, (defined as the cycle where the excess pore pressure first equals the cell pressure) 5% double amplitude strain and 10% double amplitude strain for soil specimens obtained from samples taken at a given depth. For example, Fig. 29a shows the cyclic strength of soils from a depth of 2.5 m where three small specimens were obtained from the large diameter sample.

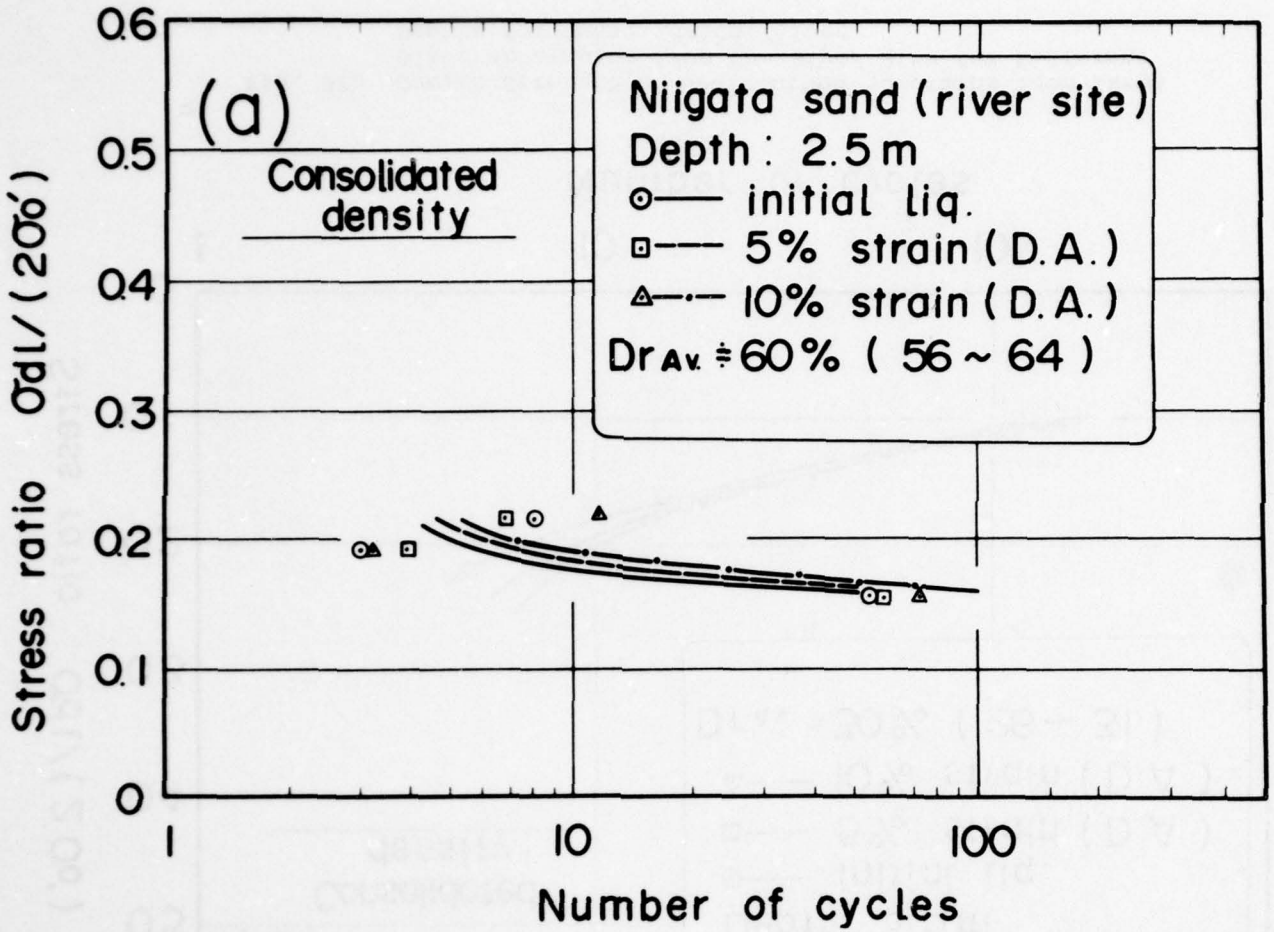

Fig. 28a Cyclic Strength of Undisturbed Specimens from Large Diameter Samples from the River Site for Different Depths for Consolidated Density Values.

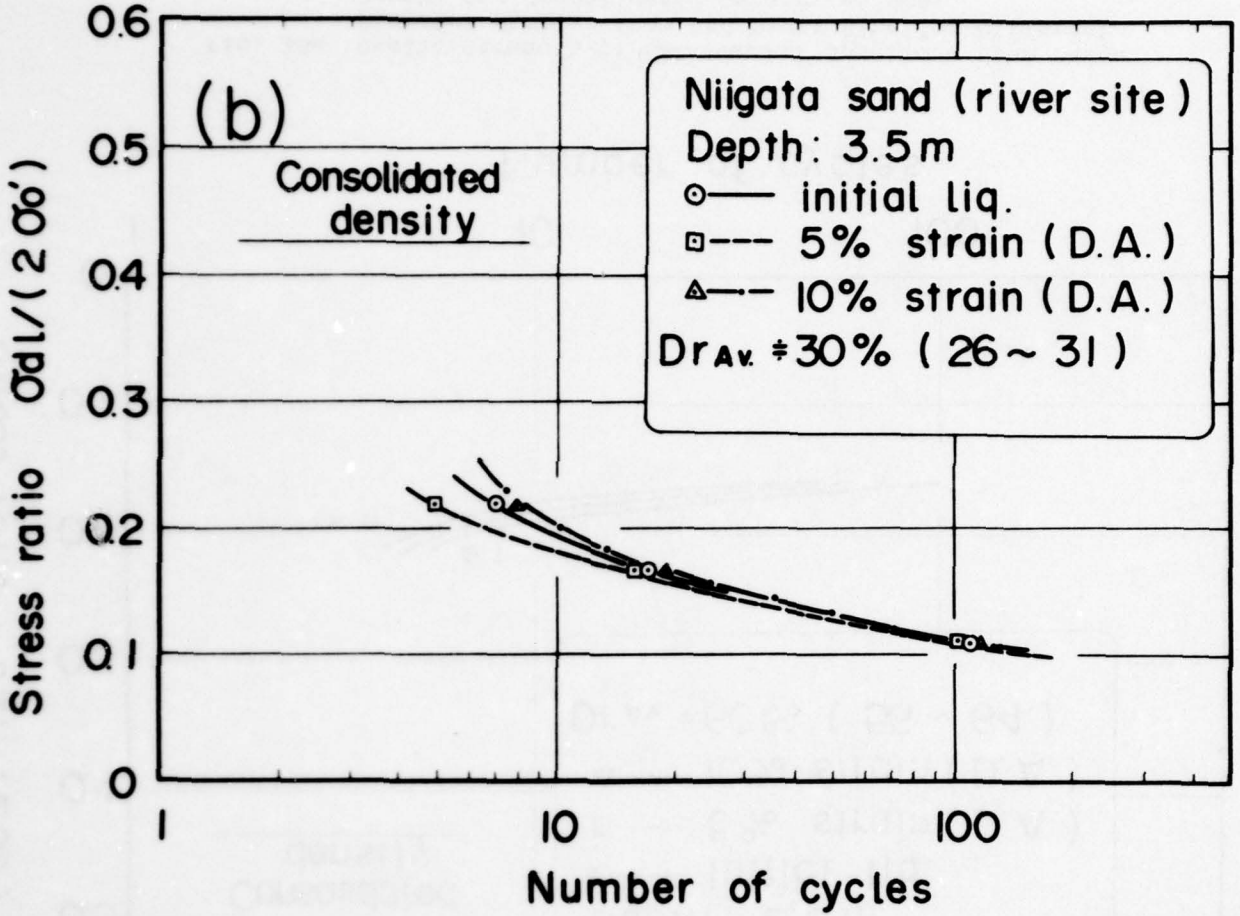

Fig. 28b Cyclic Strength of Undisturbed Specimens from Large Diameter Samples from the River Site for Different Depths for Consolidated Values.

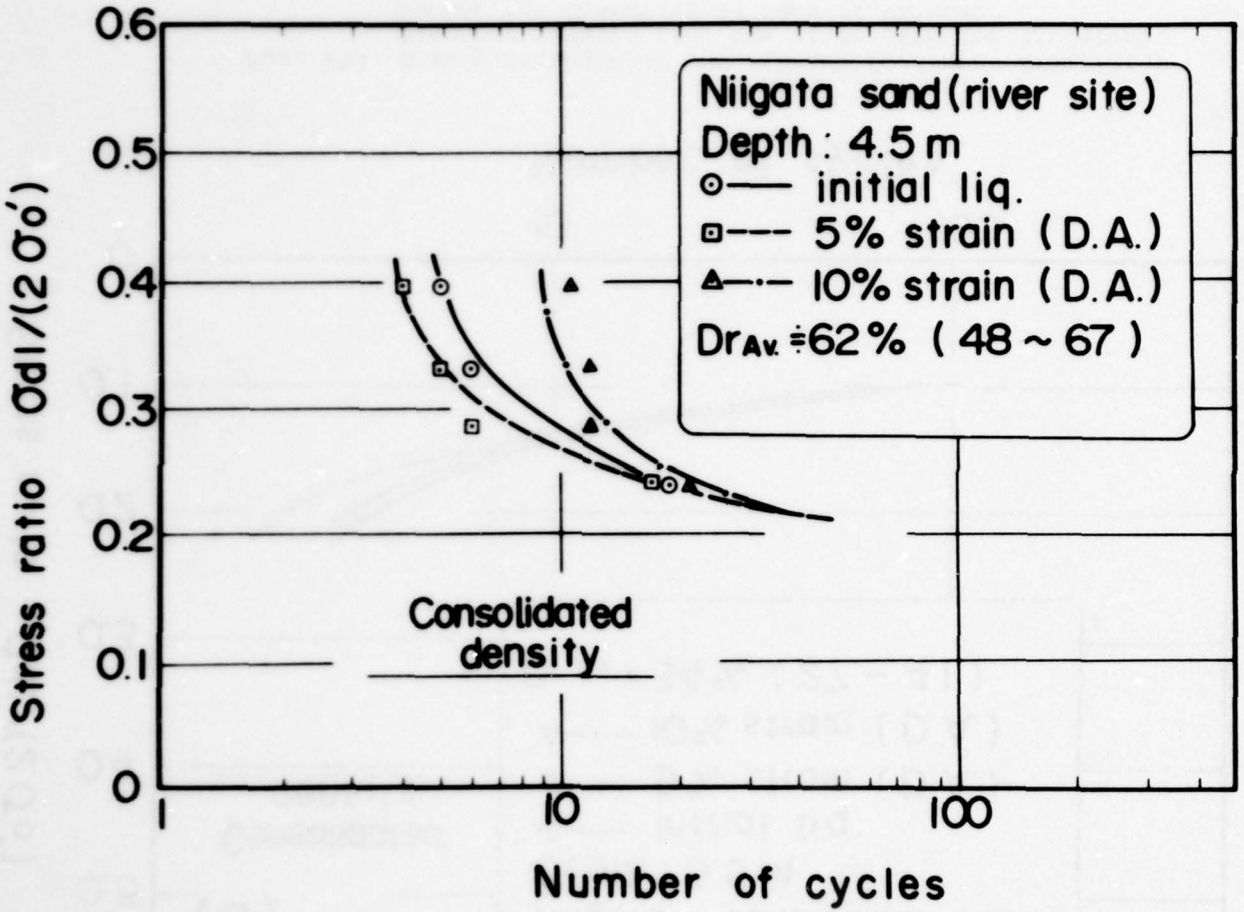

Fig. 28c Cyclic Strength of Undisturbed Specimens from Large Diameter Samples from the River Site for Different Depths for Consolidated Density Values.

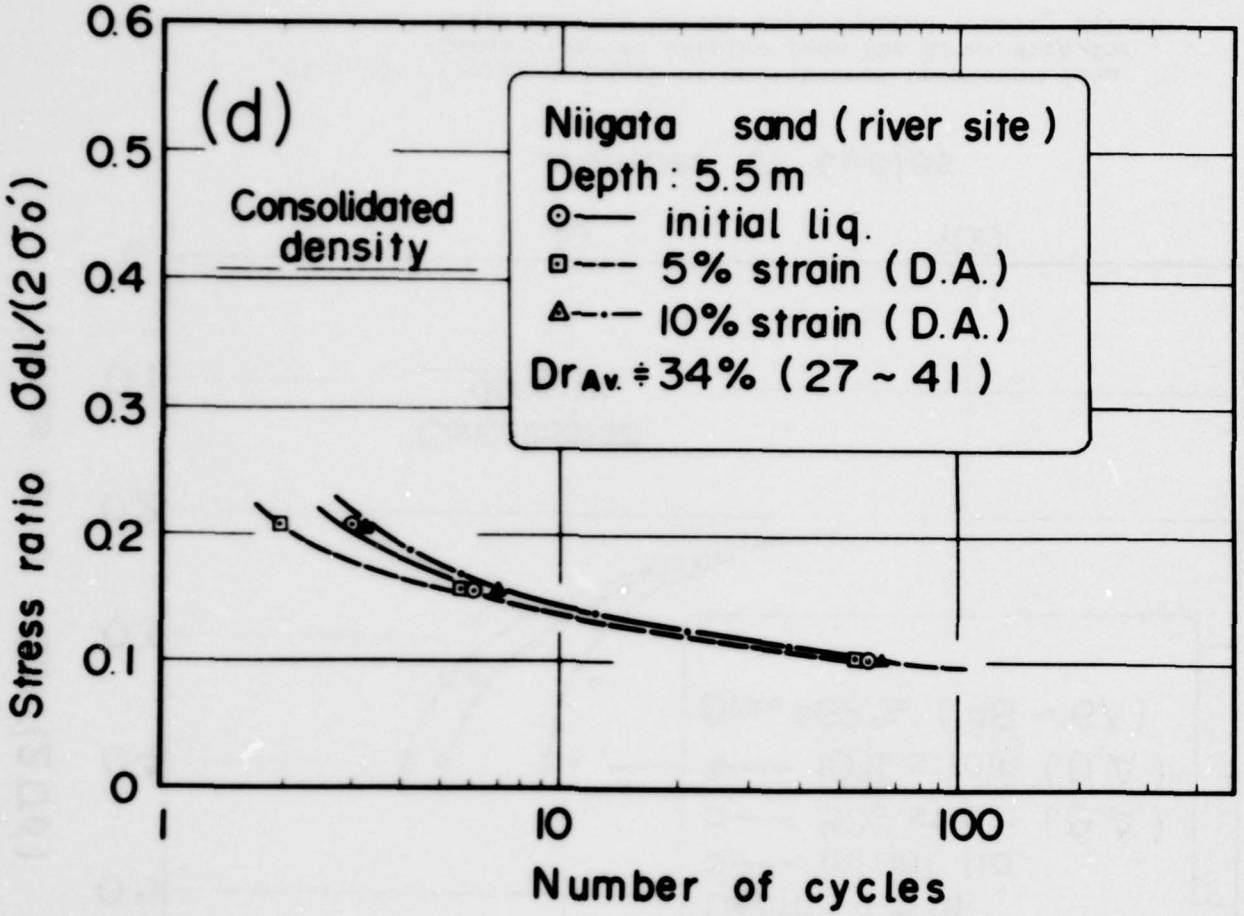

Fig. 28d Cyclic Strength of Undisturbed Specimens from Large Diameter Samples from the River Site for Different Depths for Consolidated Density Values.

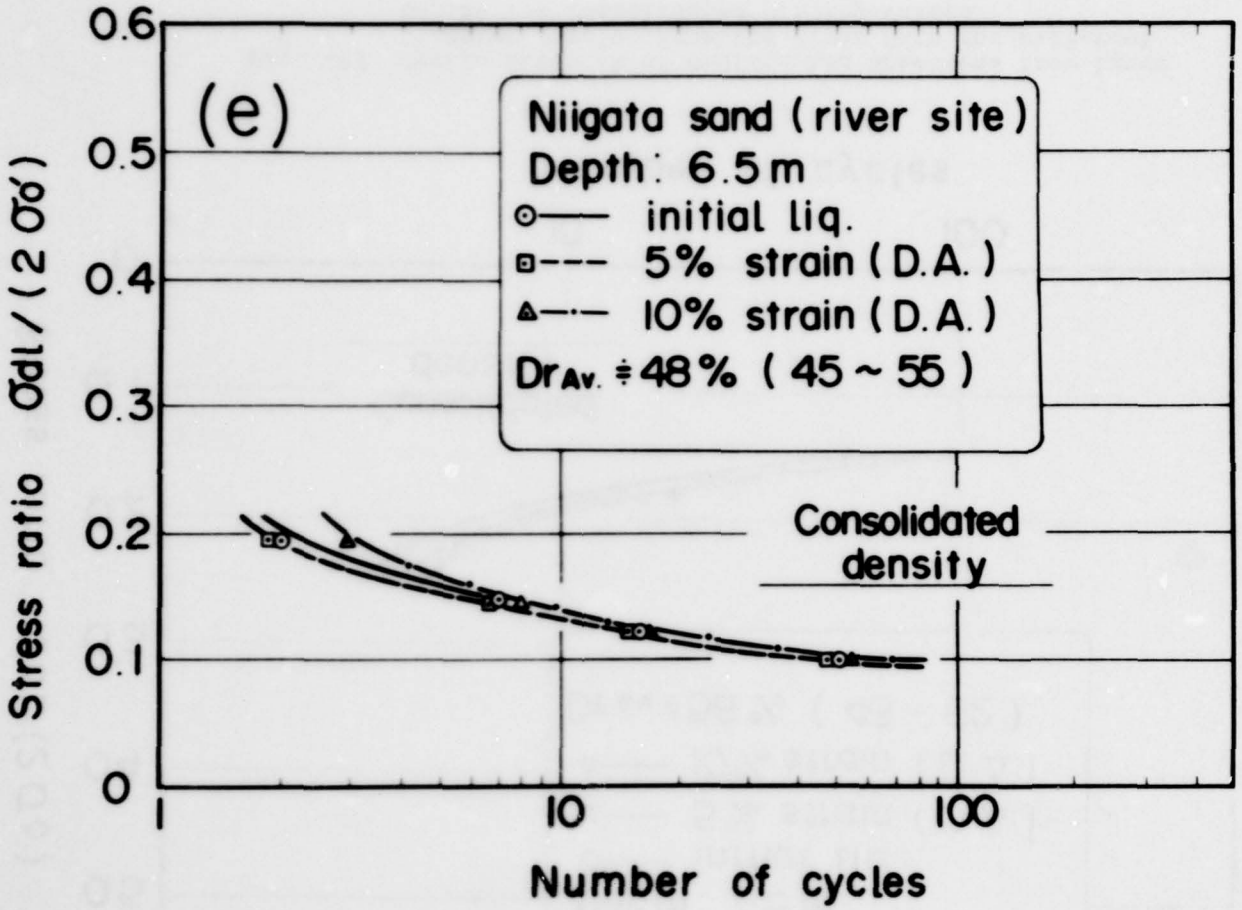

Fig. 28e Cyclic Strength of Undisturbed Specimens from Large Diameter Samples from the River Site for Different Depths for Consolidated Density Values.

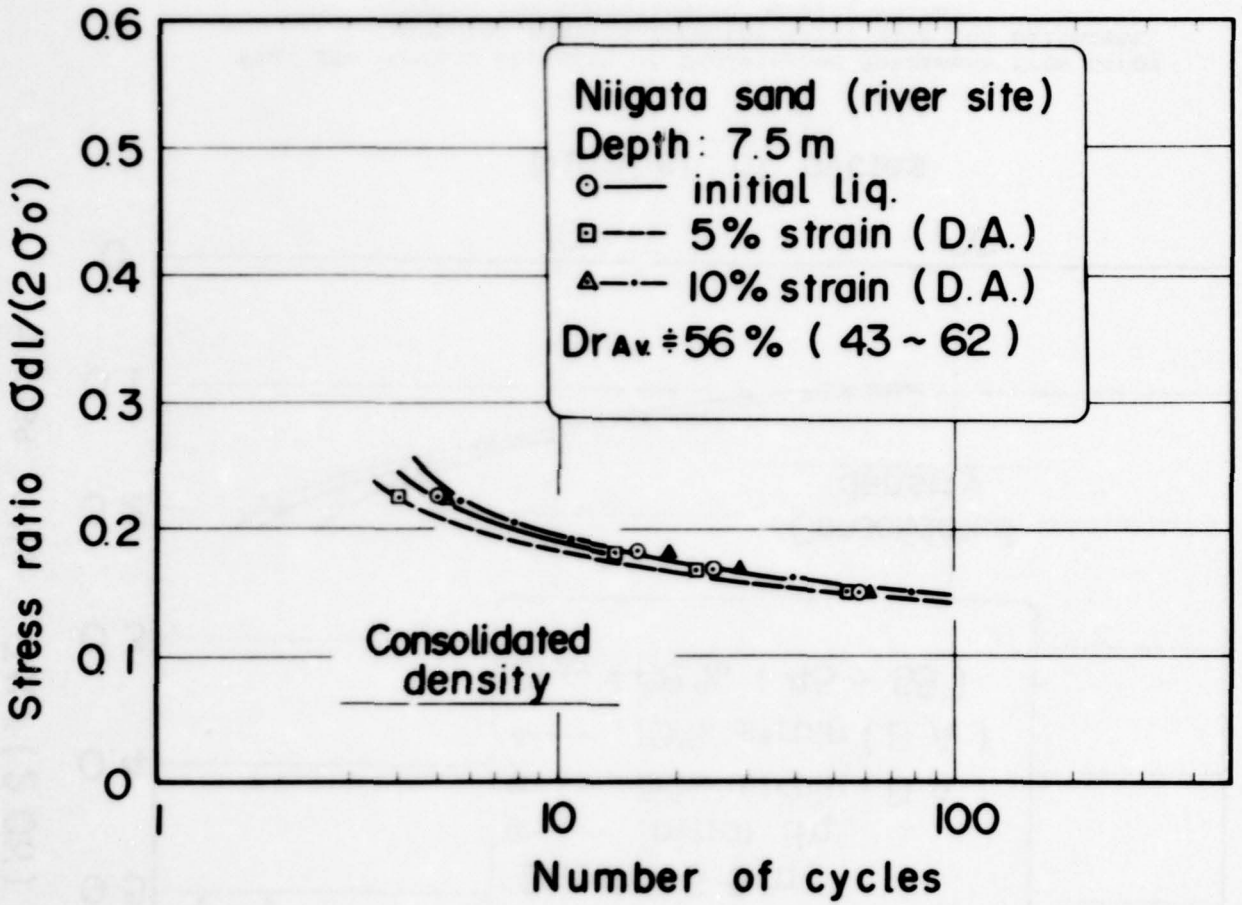

Fig. 28f Cyclic Strength of Undisturbed Specimens from Large Diameter Samples from the River Site for Different Depths for Consolidated Density Values.

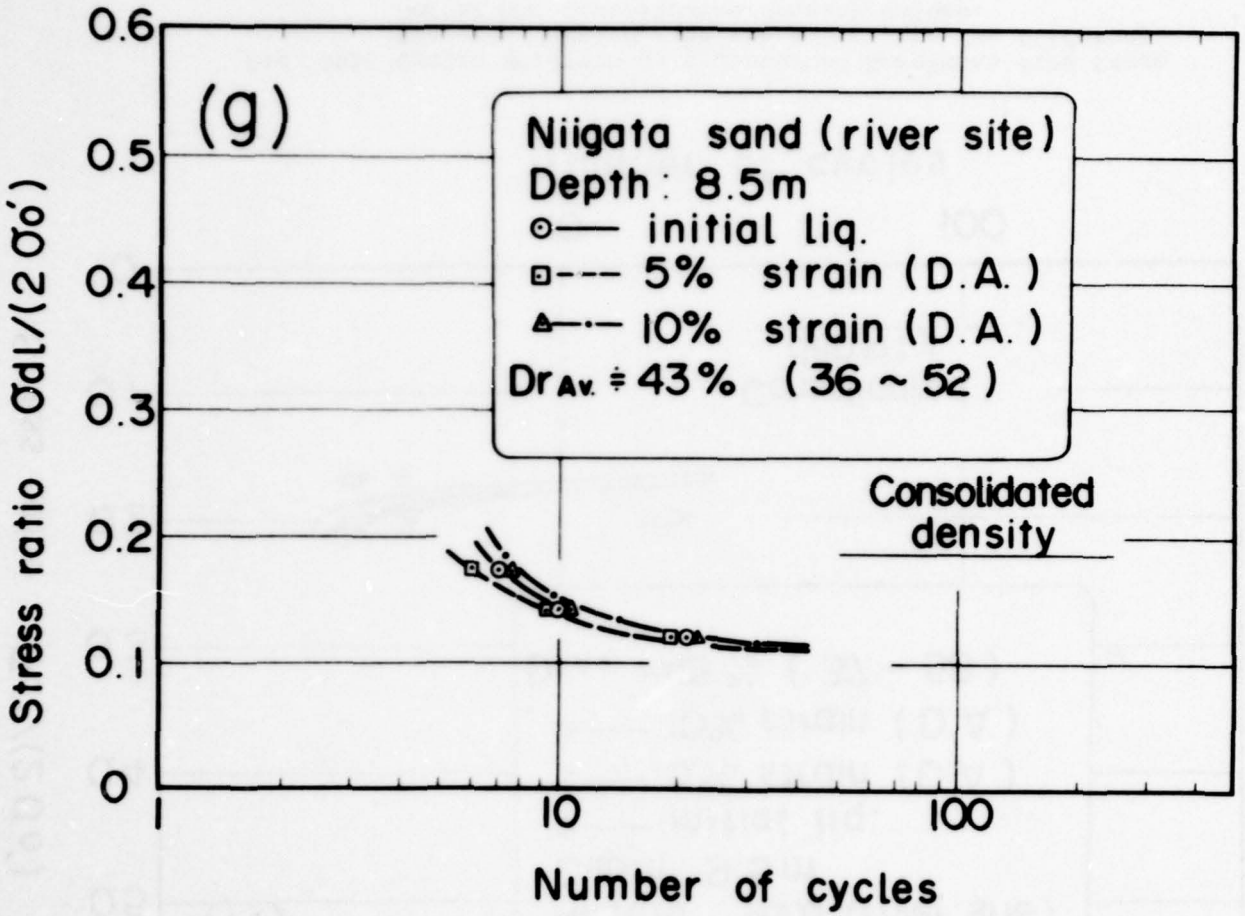

Fig. 28g Cyclic Strength of Undisturbed Specimens from Large Diameter Samples from the River Site for Different Depths for Consolidated Density Values.

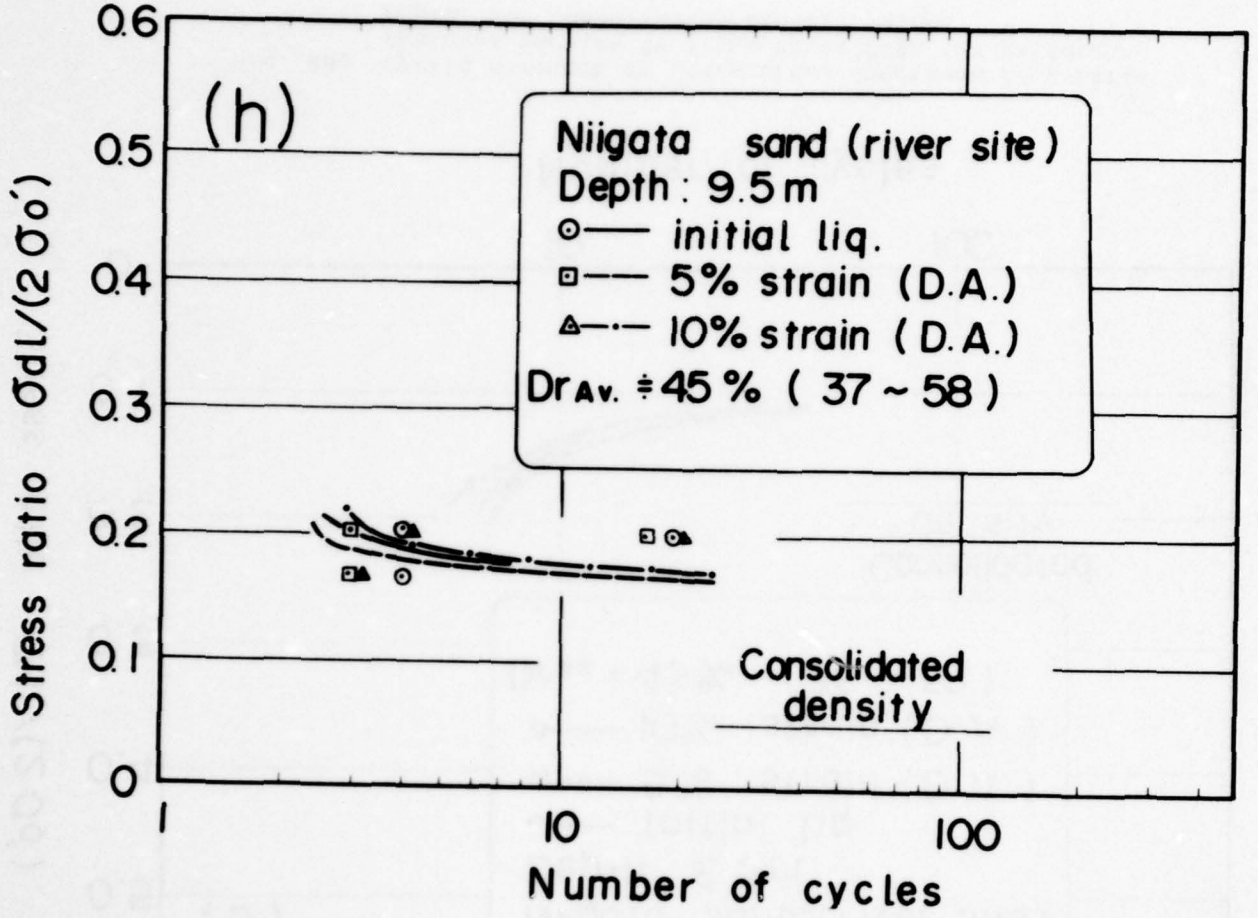

Fig. 28h Cyclic Strength of Undisturbed Specimens from Large Diameter Samples from the River Site for Different Depths for Consolidated Density Values.

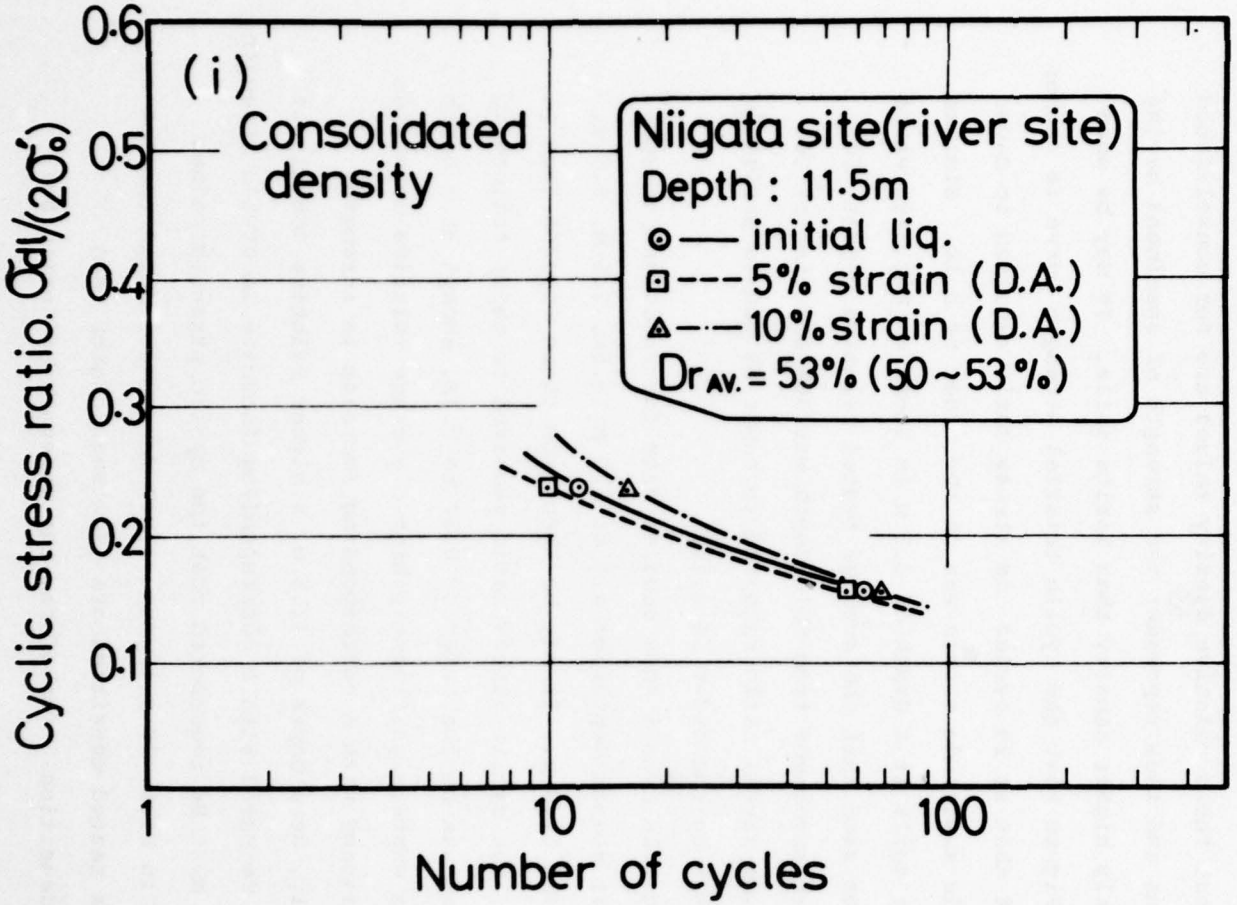

Fig. 28i Cyclic Strength of Undisturbed Specimens from Large Diameter Samples from the River Site for Different Depths for Consolidated Density Values.

The relative density of these specimens ranges between 56% and 64%; therefore the average relative density for specimens at this depth was 60% as shown on the Figure. It should be noted that these relative density values are for consolidated specimens and thus represent the strength of specimens having a slightly higher density than insitu soils. It may be seen on the Figure that the cyclic triaxial strength curve is rather flat and that at 20 cycles the stress ratio required to cause 5% double amplitude strain was on the order of 0.18. Similar data for soils at a depth of 3.5 m is shown on Fig. 28b where it may be seen that the average tested relative density for the three specimens from this depth was 30% and that at 20 cycles the stress ratio required to cause 5% double amplitude strain was on the order of 0.16.

Figs. 28 c to i show similar data for specimens at successively deeper depths of 4.5 m, 5.5 m, 6.5m, 7.5 m, 8.5 m, 9.5 m, and 11.5 m. It may be seen from these figures that in general, the cyclic stress ratio required to cause failure in 20 cycles was on the order of 0.14 to 0.18, except at a depth of 4.5 m where significantly higher average relative densities were measured with a corresponding increase in strength. Similarly, at a depth of 11.5 m, a higher relative density of 53% was measured with a corresponding increase in cyclic strength.

It must be remembered that the cyclic strength values plotted in Figs. 28 a through i are for consolidated specimens. Thus the tested densities are somewhat higher than insitu densities. Therefore, the strength of insitu soil

specimens as measured in the cyclic triaxial strength test would be slightly lower than the values given in these curves, even though the shapes of the curves should be the same.

To show the effect of relative density on the strength of these undisturbed soil specimens, the data in Fig. 28a through f has been replotted in Fig. 29. To develop these figures, the cyclic stress ratio required to cause 5% double amplitude strain was plotted for specimens at any depth with relative density values in a given range. Thus, Fig. 29a plots the cyclic strength of specimens with relative density values between 25% and 40% and thus shows the cyclic strength of specimens at an average relative density of 33%. Similarly, Fig. 29b shows the cyclic strength for specimens at any depth at the site having relative density values ranging between 41% and 55% and thus shows the strength for specimens at an average relative density of 48%. Fig. 29c shows the same data for specimens having relative density values between 56% and 70%, giving an average relative density value of about 62%.

It may be seen that there is some scatter in the test results and that the scatter is higher for specimens that failed in less than 10 cycles; but it may be seen that the scatter decreases significantly for specimens that failed in more than 10 cycles. The summary curve shown in Fig 30 obtained from the data in Fig 29 is a reasonable approximation of the strength of the undisturbed specimens tested.

AD-A060 626 ILLINOIS UNIV AT CHICAGO CIRCLE DEPT OF MATERIALS ENG--ETC F/G 8/13
CYCLIC STRENGTH OF UNDISTURBED SANDS FROM NIIGATA, JAPAN.(U)
AUG 78 M L SILVER DACW39-76-M-2407

UNCLASSIFIED WES-TR-S-78-10 NL

2 OF 2
ADA
060626

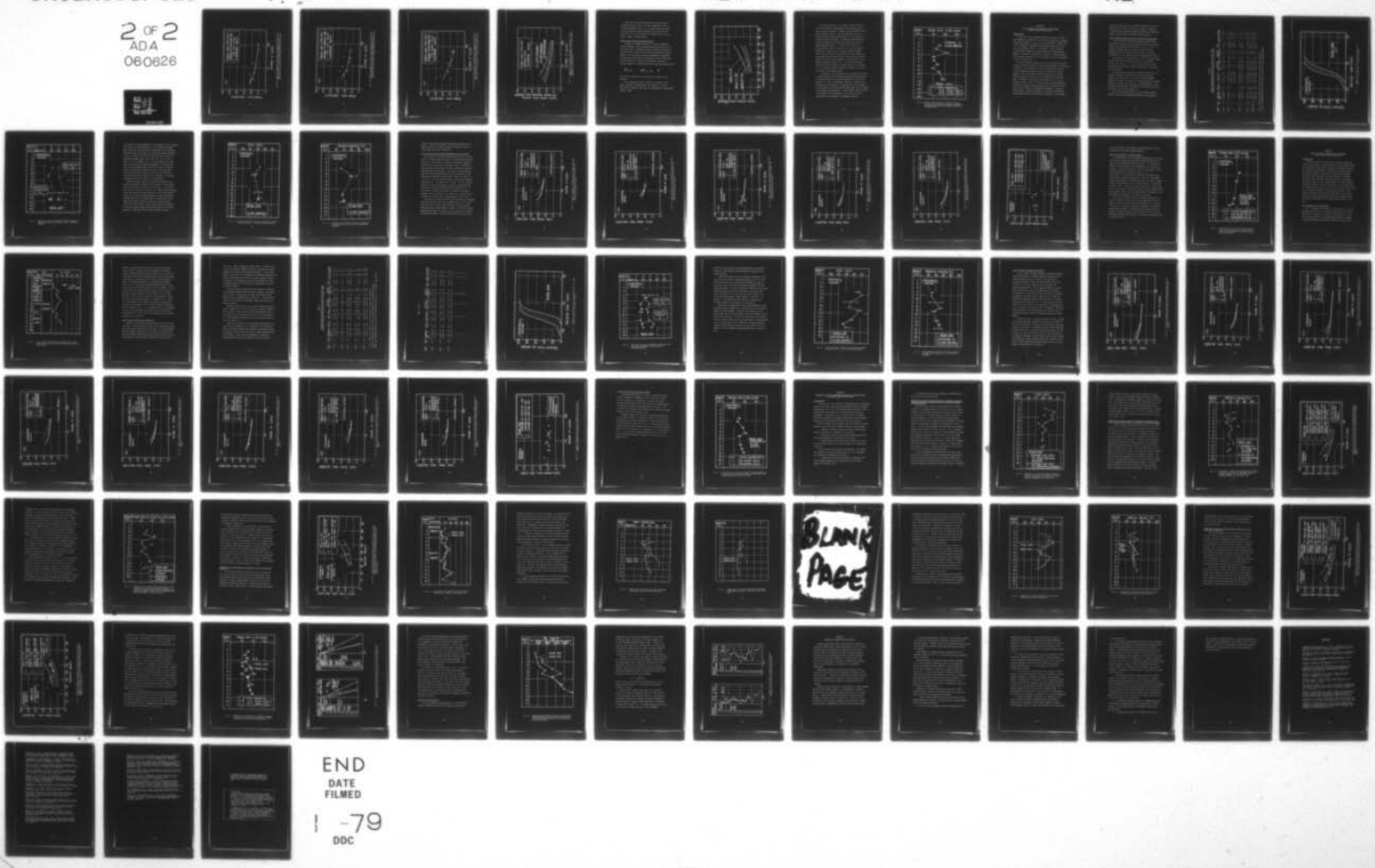

END
DATE
FILMED
1 -79
DDC

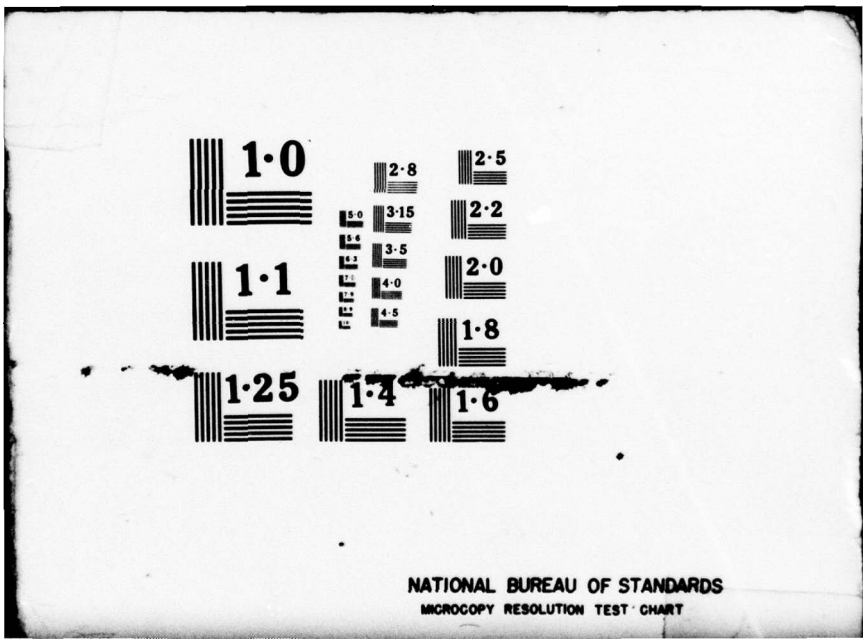
1·0
1·1
1·25
2·8
3·15
3·5
4·0
4·5
1·4
2·5
2·2
2·0
1·8
1·6
NATIONAL BUREAU OF STANDARDS
MICROCOPY RESOLUTION TEST CHART

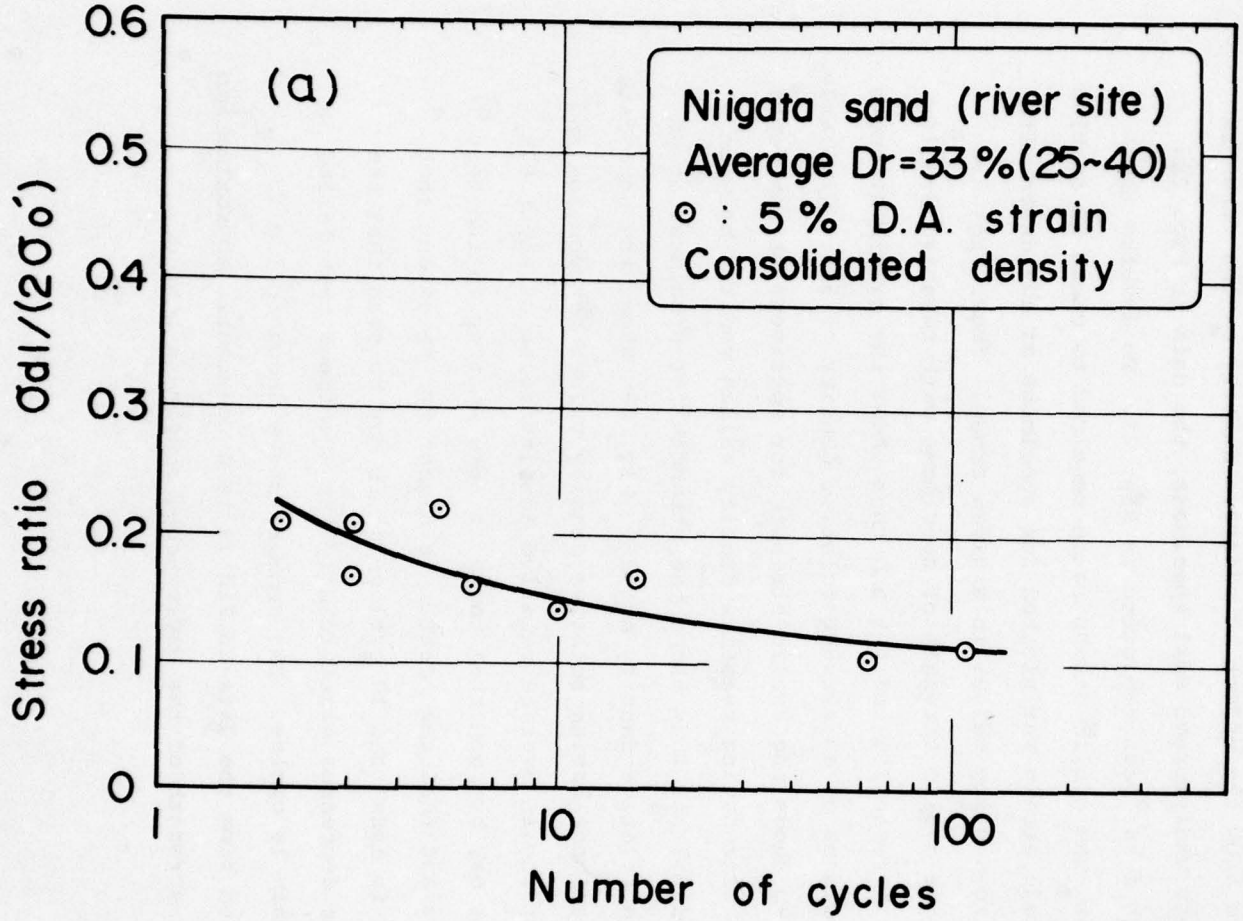

Fig. 29a Effect of Density on the Cyclic Strength of Undisturbed Sand Specimens from Large Diameter Samples at the River Site at Any Depth for Consolidated Density Values

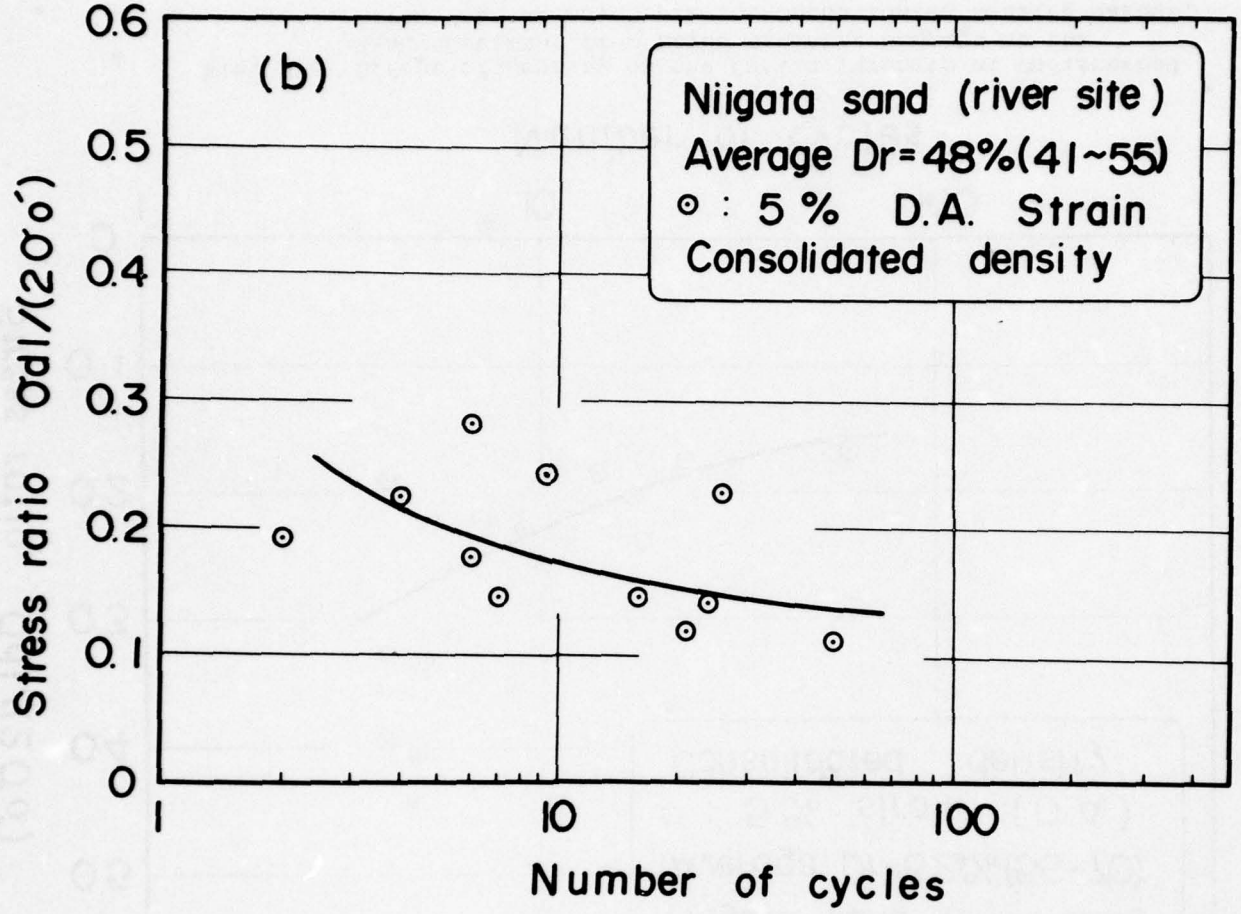

Fig. 29b Effect of Density on the Cyclic Strength of Undisturbed Sand Specimens from Large Diameter Samples at the River Site at Any Depth for Consolidated Density Values.

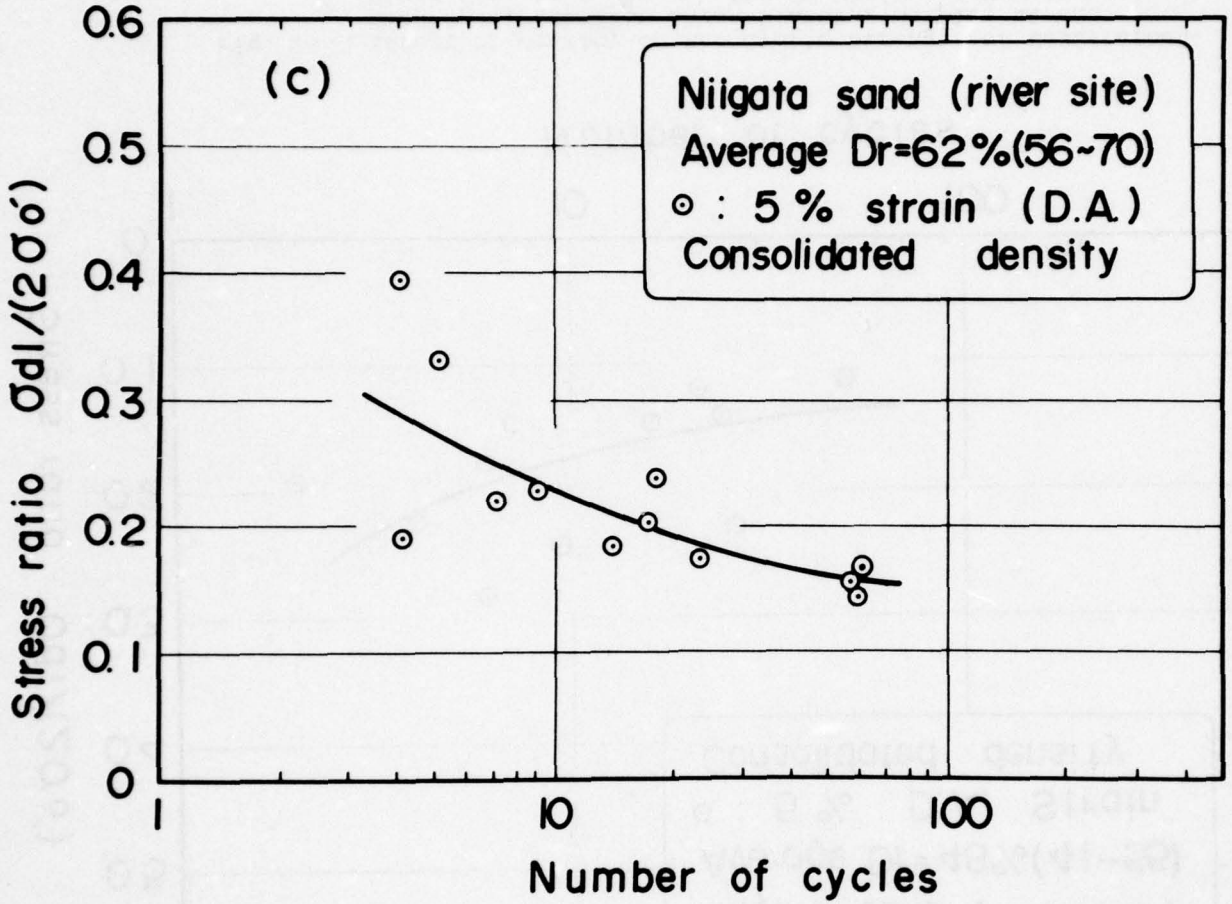

Fig. 29c Effect of Density on the Cyclic Strength of Undisturbed Sand Specimens from Large Diameter Samples at the River Site at Any Depth for Consolidated Density Values.

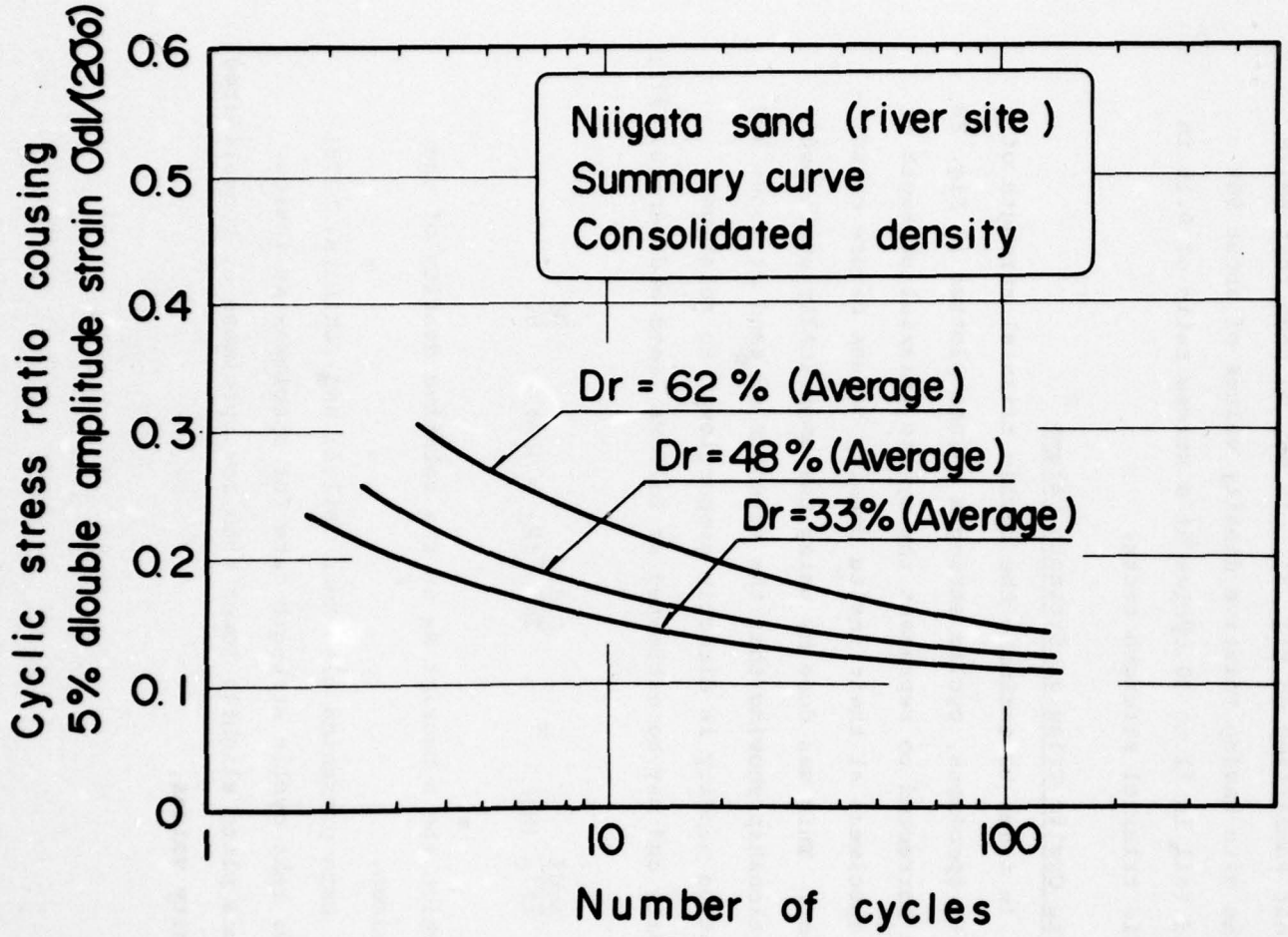

Fig. 30 Summary Curve Showing the Effect of Density on the Strength of Undisturbed Specimens from Large Diameter Samples at the River Site.

The effect of relative density on the stress ratio required to cause failure (5% double amplitude strain) is further summarized on Fig. 31. It may be seen that soils at the site having relative density values of about 50% would fail in 11 to 30 cycles at a stress ratio of 0.15 in cyclic triaxial strength tests.

Insitu Cyclic Triaxial Strength Values

In order to estimate the cyclic triaxial strength of insitu specimens, cyclic strength values plotted in Fig. 28 were corrected to represent the cyclic triaxial strength of the specimens at their insitu density values before consolidation. This was done by using the empirically confirmed relationship showing that the strength of sand at about 50% relative density is directly proportional to relative density and may be estimated as follows (Seed and Idriss, 1971):

$$\frac{\Delta\sigma d\ell}{2\sigma'_c}(R_d) = \frac{\Delta\sigma d\ell}{2\sigma'_c}(R_d = 50\%) \quad \frac{R_d}{50}$$

in which the subscript R_d is the relative density of the specimen.

Data presented elsewhere (Silver and Ishihara, 1978) shows that cyclic strength data for specimens at insitu values plots slightly lower than for specimens at consolidated density values.

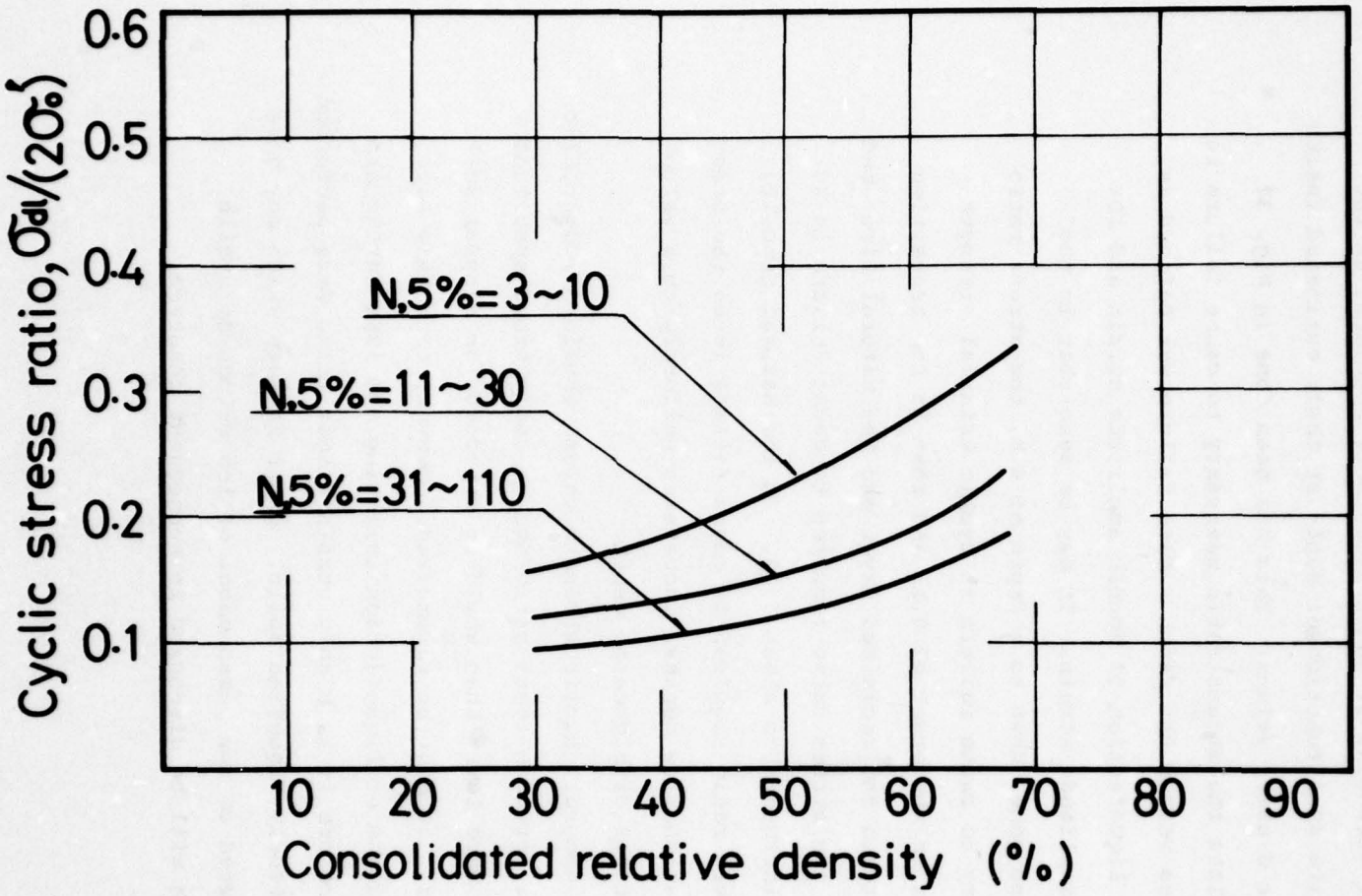

Fig. 31 Summary Curve Showing the Effect of Relative Density on the Cyclic Strength of Undisturbed Specimens from Large Diameter Samples from the Road Site.

For design purposes, it is useful to show the cyclic triaxial strengths of undisturbed soil specimens at the river site as a function of depth at their estimated insitu relative density values. This has been done in Fig. 32 which plots the stress ratio necessary to cause failure in 20 cycles versus the depth. Here failure was defined as initial liquefaction, 5% double amplitude strain and 10% double amplitude strain. It may be seen that in the reclaimed zone, down to a depth of 4 m, the stress ratio necessary to cause failure in cyclic triaxial strength tests is on the order of 0.15 and that in the transition zone between the reclaimed layer and the natural river bed deposit the stress ratio required to cause failure in 20 cycles increases to about 0.22. In the natural deposit, the stress ratio required to cause failure is on the order of 0.1 at shallow depths, increasing uniformly to a value of about 0.2 with greater depth.

In general, cyclic strength values obtained from cyclic triaxial strength tests performed on undisturbed specimens of sand were lower than would be expected for natural soil deposits. It must be remembered, however, that this site showed signs of liquefaction following the 1964 earthquake and therefore it is highly possible that tests were performed on previously liquefied soils. Other factors which may have contributed to the measurement of low values of cyclic strength will be discussed in subsequent chapters.

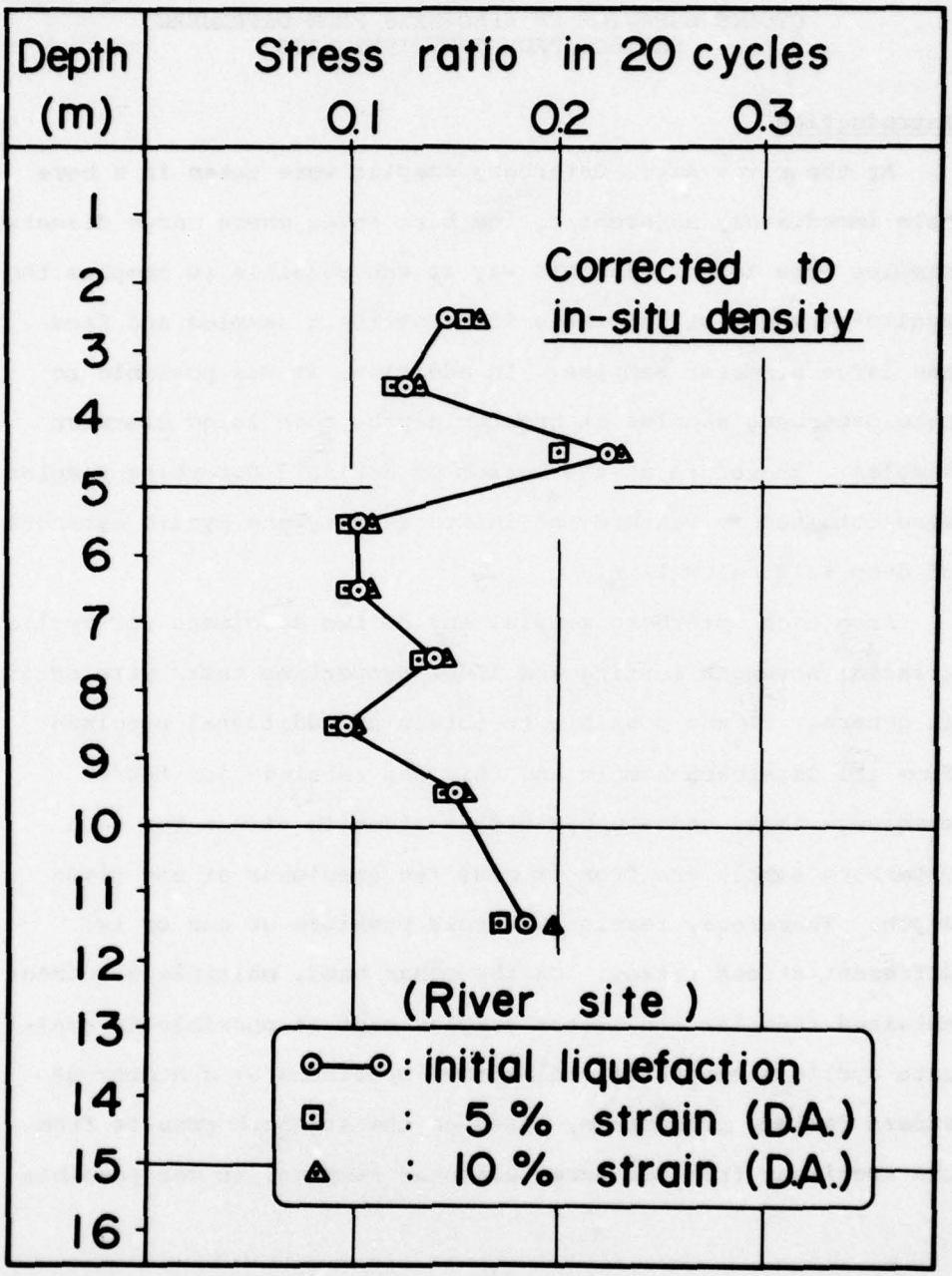

Fig. 32 Insitu Values of Cyclic Triaxial Strength Failure in 20 Cycles as a Function of Depth for Specimens from Large Diameter Samples at the River Site.

CHAPTER 6

CYCLIC BEHAVIOR OF SPECIMENS FROM OSTERBERG SAMPLES FROM THE RIVER SITE

Introduction

At the river site, Osterberg samples were taken in a bore hole immediately adjacent to the bore holes where large diameter samples were taken. In this way it was possible to compare the cyclic strength of specimens from Osterberg samples and from the large diameter samples. In addition, it was possible to take Osterberg samples at greater depths than large diameter samples; therefore at the bottom of Boring 3 Osterberg samples were obtained to measure the insitu density and cyclic strength of deep soil below 12 m.

From each Osterberg sample, one or two specimens for cyclic triaxial strength testing and index properties tests were obtained. In general, it was possible to obtain an additional specimen from the Osterberg sample and this was retained for fabric studies. Thus, undisturbed cyclic strength values for each Osterberg sample are from at most two specimens at any given depth. Therefore, testing was only possible at one or two different stress ratios. On the other hand, multiple specimens obtained from large diameter samples made it possible to evaluate cyclic strength of undisturbed specimens at a number of stress ratios. Therefore, based on the strength results from the specimens from the large diameter samples, it was possible

to select stress ratios for Osterberg specimens that would cause failure in about 10-20 cycles, making it possible to compare cyclic strength between specimens from Osterberg samples and specimens from large diameter samples.

Index Properties Values Obtained from Osterberg Specimens

The soil profile from which Osterberg samples were obtained was exactly the same profile in which large diameter samples were obtained and was shown in Fig. 23. Five Osterberg samples taken at the road site provided 10 specimens for index property tests and cyclic triaxial strength tests. All test results are summarized on Table 4.

The particle size distribution for the Osterberg samples at the river site is summarized in Fig. 33 for depths between 4.5 m and 13.5 m. It may be seen that the grain size distributions form a rather narrow band in the medium sand size range.

The mean particle size and uniformity coefficient as a function of depth at the river site for the Osterberg samples is shown in Fig. 34. As for the large diameter samples, the grain size tends to increase slightly with depth and has a mean particle size, D_{50}, of approximately 0.4 mm. Similarly, the uniformity coefficient is relatively constant with depth and is on the order of 2.

As for the specimens from the large diameter samples, density values for the Osterberg samples were obtained by

TABLE 4

INDEX PROPERTY VALUES AND CYCLIC TRIAXIAL TEST VALUES
OSTERBERG SPECIMENS FROM THE RIVER SITE, NIIGATA, JAPAN

Sample No.	Depth (m)	Gradation		Specific Gravity	Void Ratio		Limiting Void Ratios		Relative Density		$\frac{\sigma d\ell}{2\sigma_o'}$	No. of Cycles		
		D_{50} (mm)	U_c		e_c	e	e_{max}	e_{min}	D_{rc} (%)	D_r (%)		init.	5%	10%
B1-S3	4.5	0.40	2.14	2.62	0.822	0.842	0.997	0.498	35	31	0.270	7	7	13
B1-S4	6.7	0.40	1.60	2.65	0.774	0.790	1.005	0.622	60	56	0.216	10	10	17
"	"	"	"	"	0.704	0.727	"	"	79	73	0.227	9	7	10
"	"	"	"	"	0.769	0.788	"	"	62	57	0.108	∞	∞	∞
B1-S6	11.5	0.46	1.89	2.67	0.854	0.879	1.050	0.539	38	34	0.195	3	3	4
"	"	0.65	3.04	2.68	0.747	0.769	0.933	0.491	42	37	0.251	3	3	5
B1-S7	13.5	0.39	1.72	2.68	0.787	0.809	0.929	0.514	34	29	0.144	14	14	15
"	"	0.57	2.14	2.67	0.781	0.806	0.942	0.599	47	40	0.218	3	2	3
LD3-S10	13.2	0.41	1.77	2.68	0.798	0.816	1.018	0.547	47	43	0.177	12	11	15
"	"	0.40	2.00	2.68	0.840	0.866	1.016	0.622	45	38	0.219	3	3	4

e, D_r = Initial void ratio and relative density of undisturbed specimens.

e_c, D_{rc} = Consolidated void ratio and relative density of undisturbed specimens.

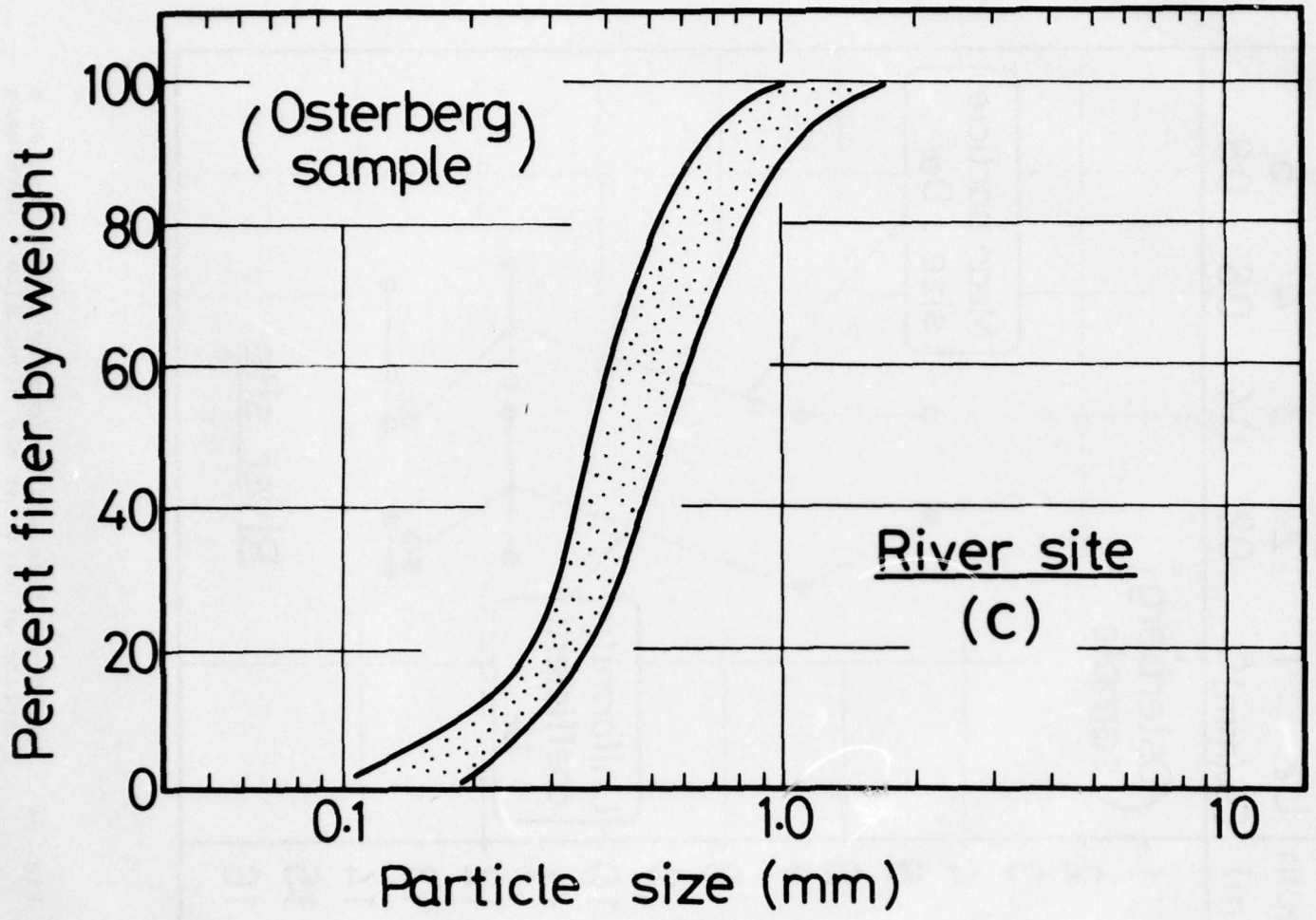

Fig. 33 Summary Curve Showing Grain Size Distribution for Soils at the River Site - Osterberg Samples.

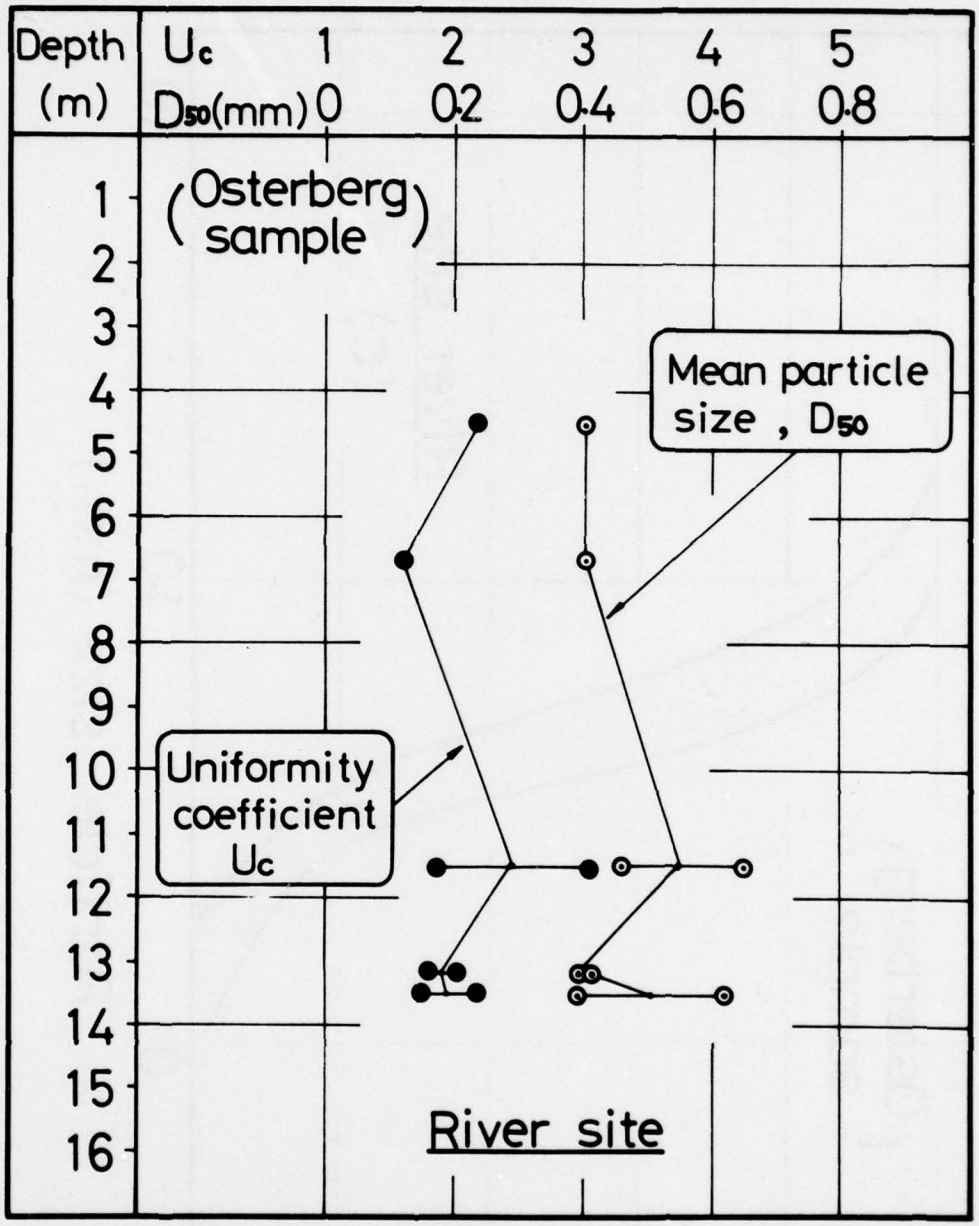

Fig. 34 Mean Grain Size and Uniformity Coefficient as a Function of Depth at the River Site - Osterberg Samples.

1) extruding a frozen specimen, 2) by confining it in a triaxial cell under a low vacuum pressure, 3) by letting the sample thaw out, and 4) by measuring the dimensions of the specimen. Calculated void ratio values as a function of depth are shown in Fig. 35, where it may be seen that void ratio values for Osterberg specimens were on the order of 0.7 to 0.8 from a depth of 4 m to a depth of 14 m. At some depths it was possible to make several density measurements on different portions of the Osterberg sample and this is shown by the horizontal line connecting void ratio values at a given depth. It may be seen that, in general, the void ratio values are relatively uniform and there is not a great deal of variation in measured void ratio values at a given depth.

Relative density values as a function of depth for the Osterberg specimens is shown in Fig. 36 where it may be seen that relative density values from a depth of 4 m to a depth of 14 m are on the order of 30% to 60%. These relative density values were obtained in the same way as the relative density values for the large diameter specimens, where a maximum and minimum density test was performed on each specimen and corresponding relative density values were calculated using insitu void ratio values. Again, there is less variability in relative density values at any given depth than in values measured for specimens from the large diameter samples.

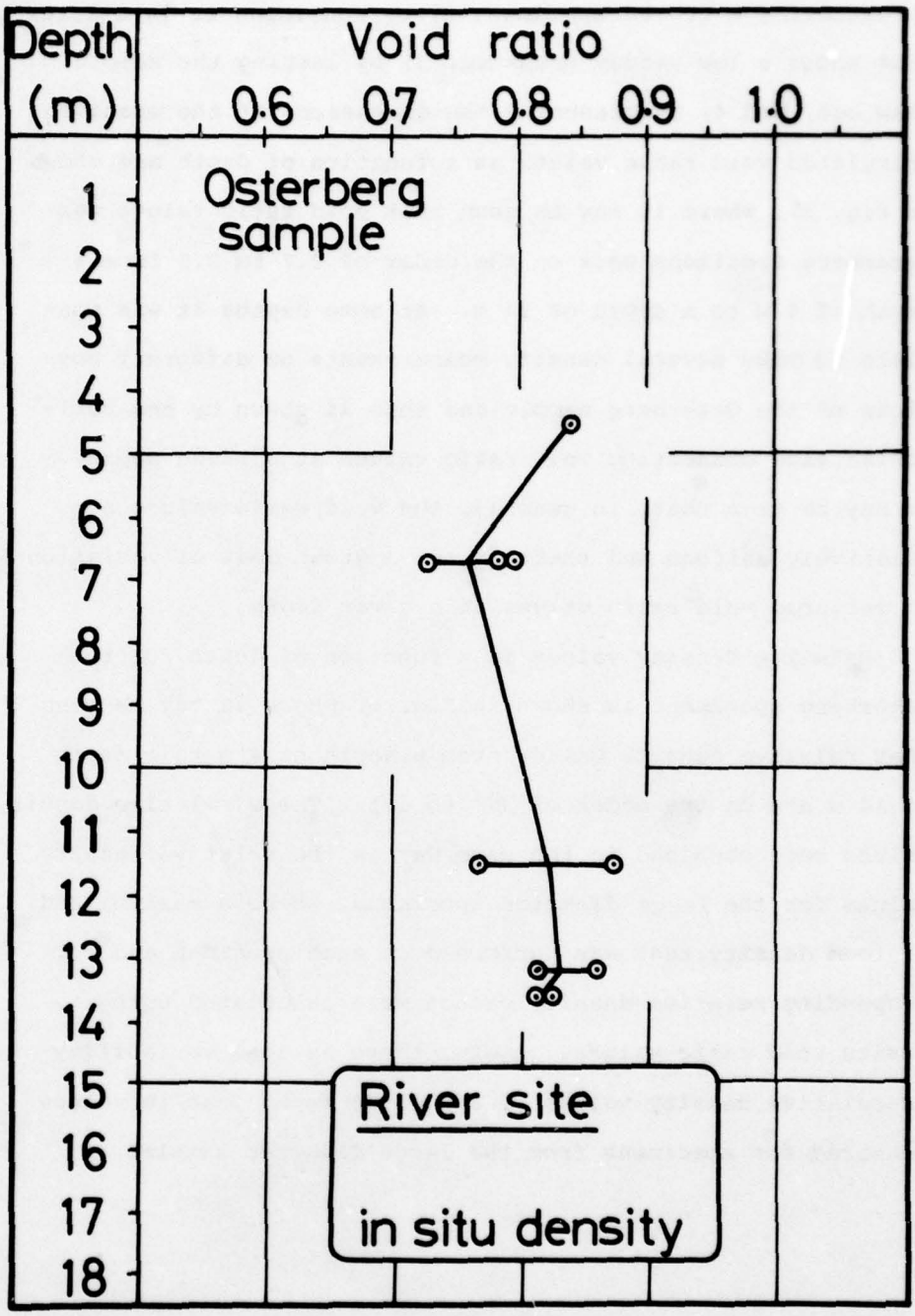

Fig. 35 Insitu Void Ratio Values as a Function of Depth at the River Site - From Osterberg Specimens.

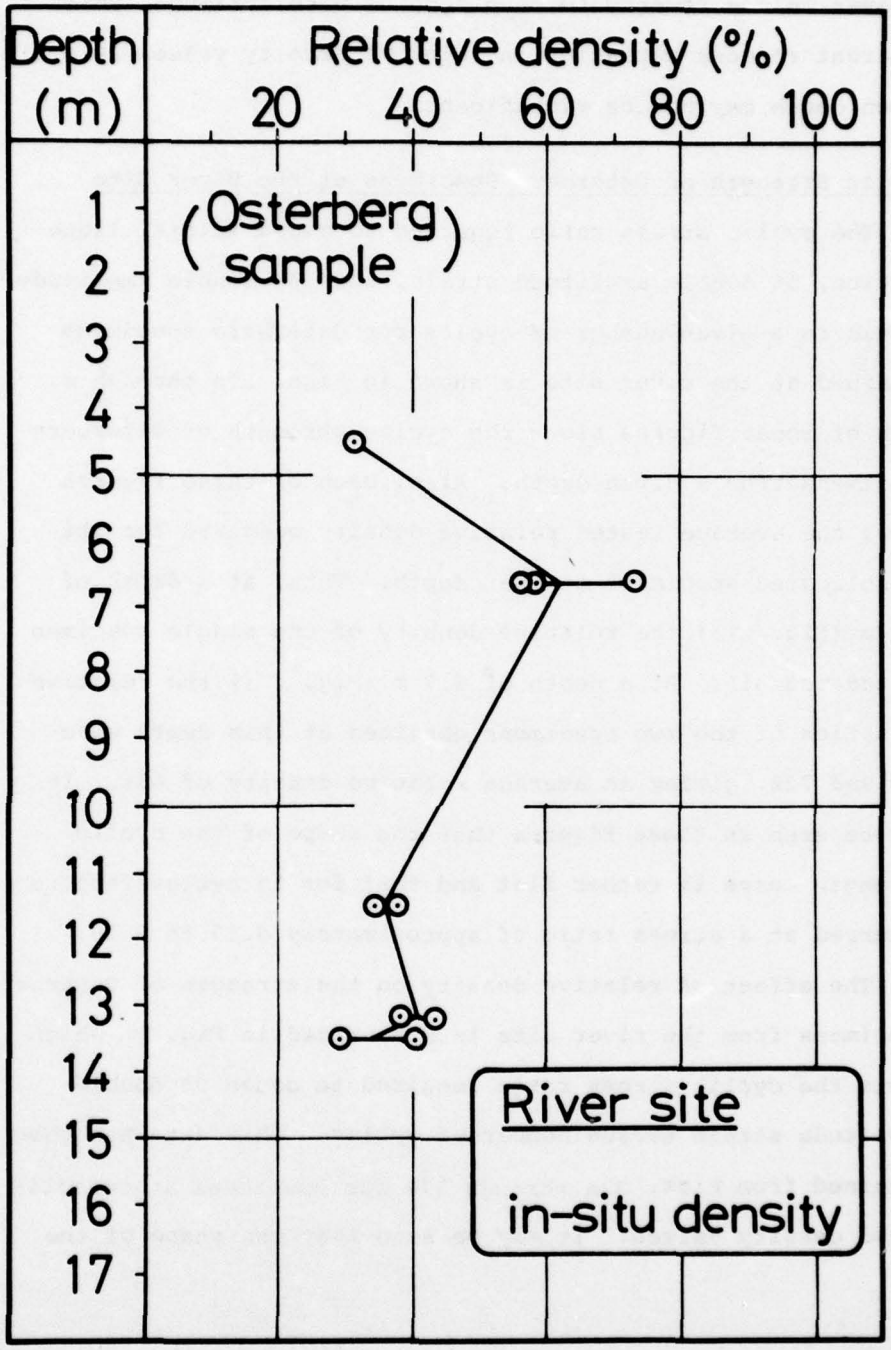

Fig. 36 Insitu Relative Density Values as a Function of Depth at the River Site - From Osterberg Specimens.

However, since fewer Osterberg samples were obtained, this apparent reduced variation in relative density values at a given depth may not be significant.

Cyclic Strength of Osterberg Specimens at the River Site

The cyclic stress ratio required to cause initial liquefaction, 5% double amplitude strain, and 10% double amplitude strain in a given number of cycles for Osterberg specimens obtained at the river site is shown in Figs. 37a through e. Each of these figures plots the cyclic strength of Osterberg specimens from a given depth. Also, each of these figures shows the average tested relative density measured for the consolidated specimens at that depth. Thus, at a depth of 4.2 m (Fig. 37a) the relative density of the single specimen tested was 31%. At a depth of 6.7 m (Fig. 37b) the relative densities of the two specimens obtained at this depth were 56% and 73%, giving an average relative density of 65%. It may be seen in these Figures that the shape of the cyclic strength curve is rather flat and that for 15 cycles failure occurred at a stress ratio of approximately 0.15 to 0.20.

The effect of relative density on the strength of Osterberg specimens from the river site is summarized in Fig. 38 which plots the cyclic stress ratio required to cause 5% double amplitude strain versus number of cycles. This data has been obtained from Figs. 37a through 37e for specimens at consolidated density values. It may be seen that the shape of the

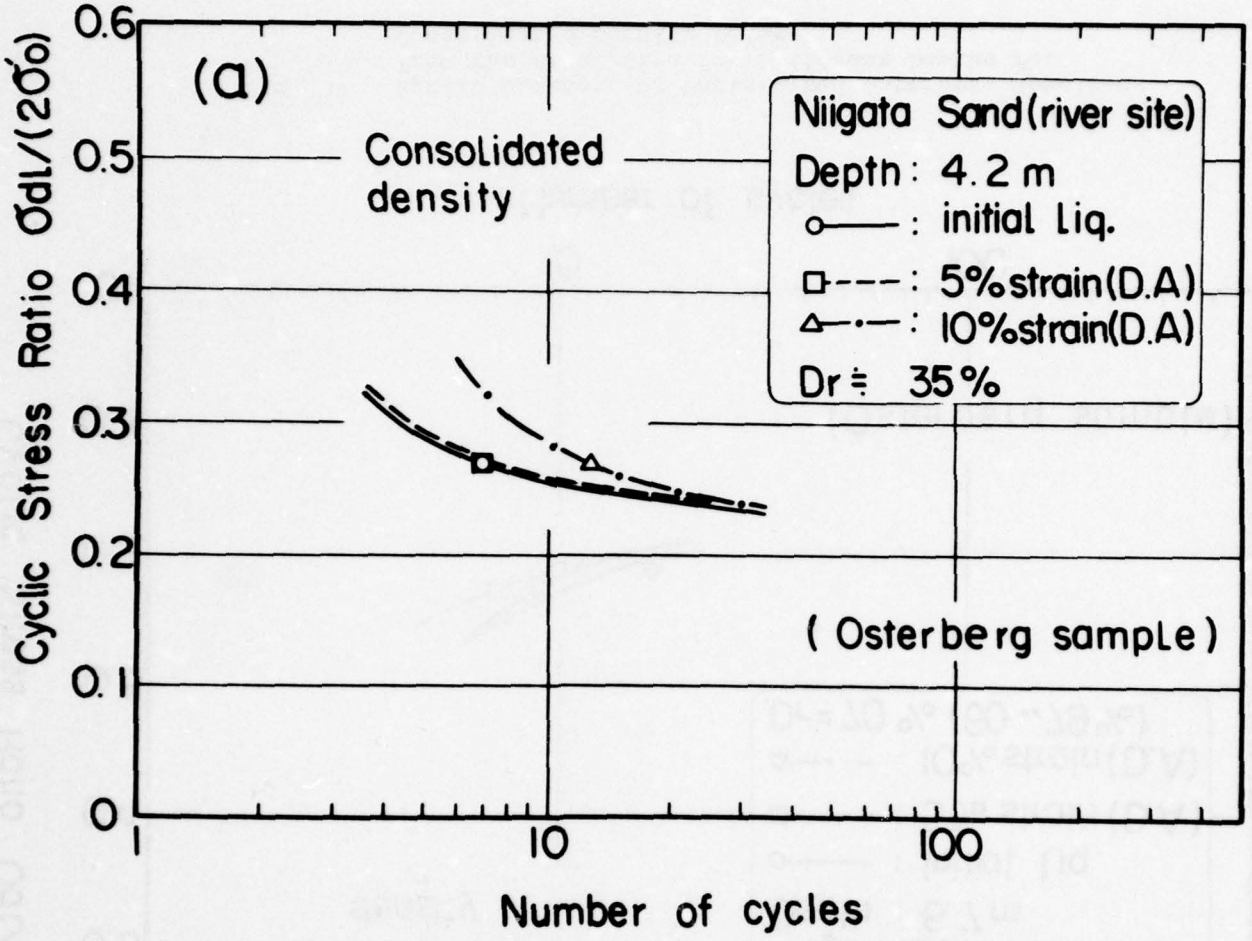

Fig. 37a Cyclic Strength of Undisturbed Osterberg Specimens from the River Site for Different Depths for Consolidated Density Values.

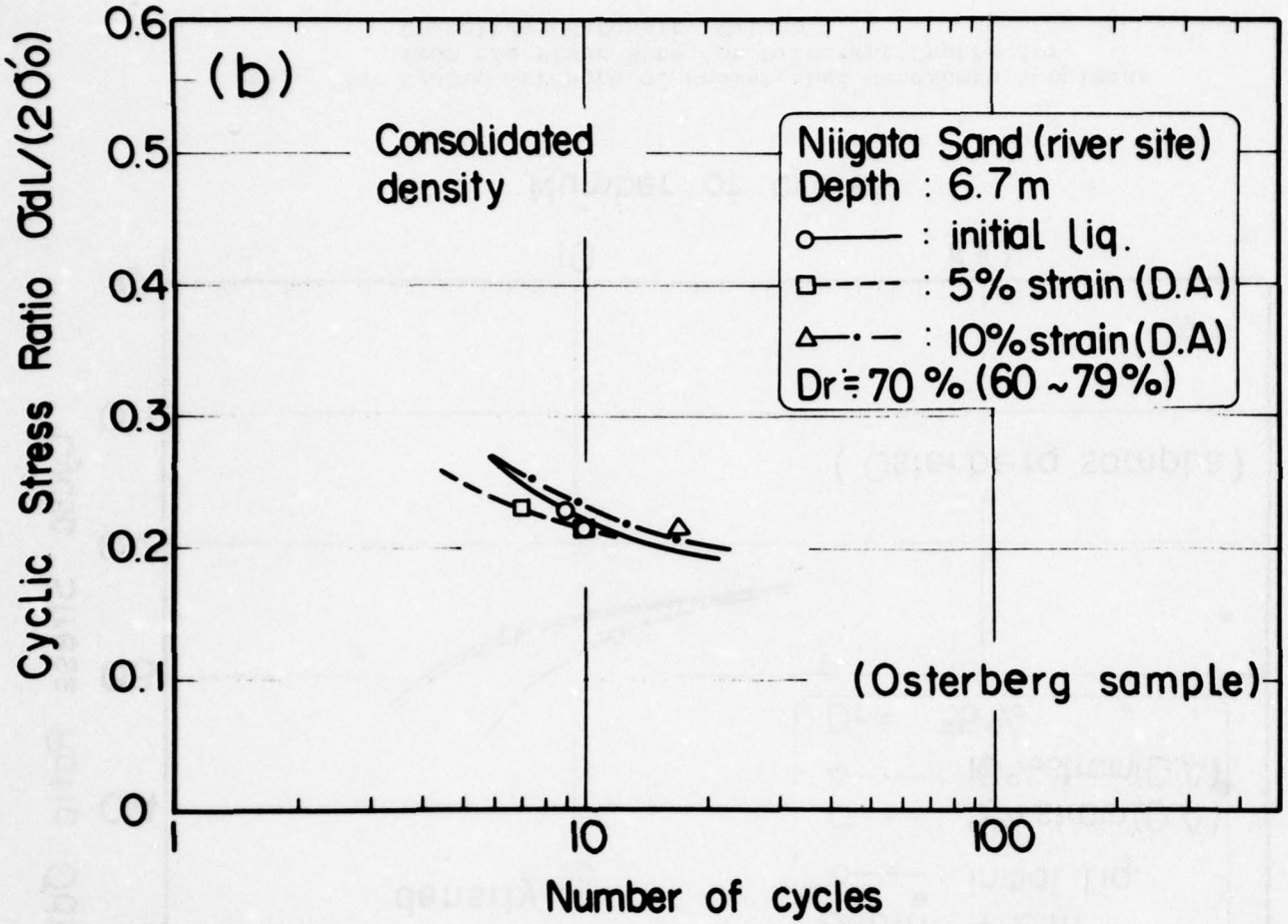

Fig. 37b Cyclic Strength of Undisturbed Osterberg Specimens from the River Site for Different Depths for Consolidated Density Values

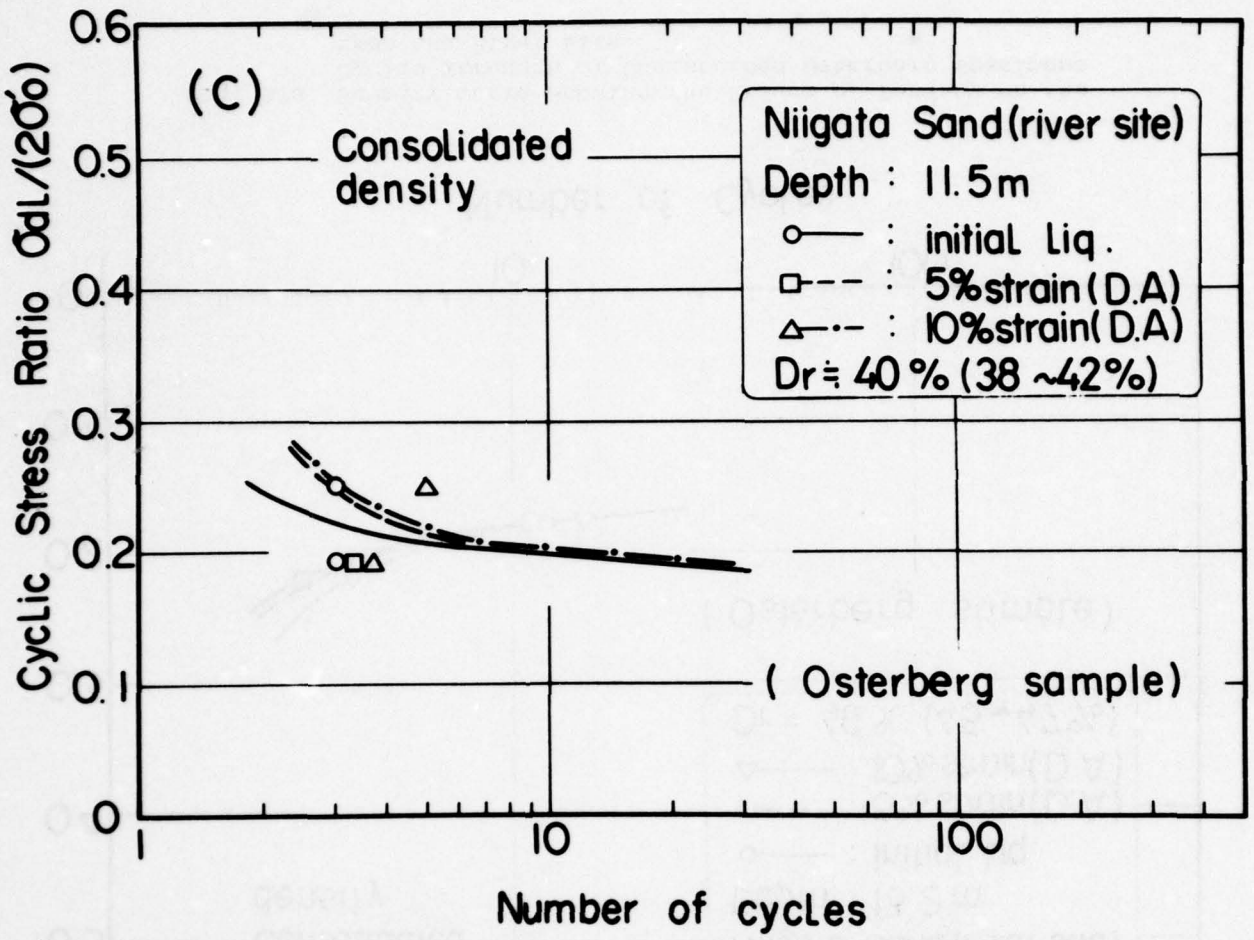

Fig. 37c Cyclic Strength of Undisturbed Osterberg Specimens from the River Site for Different Depths for Consolidated Density Values.

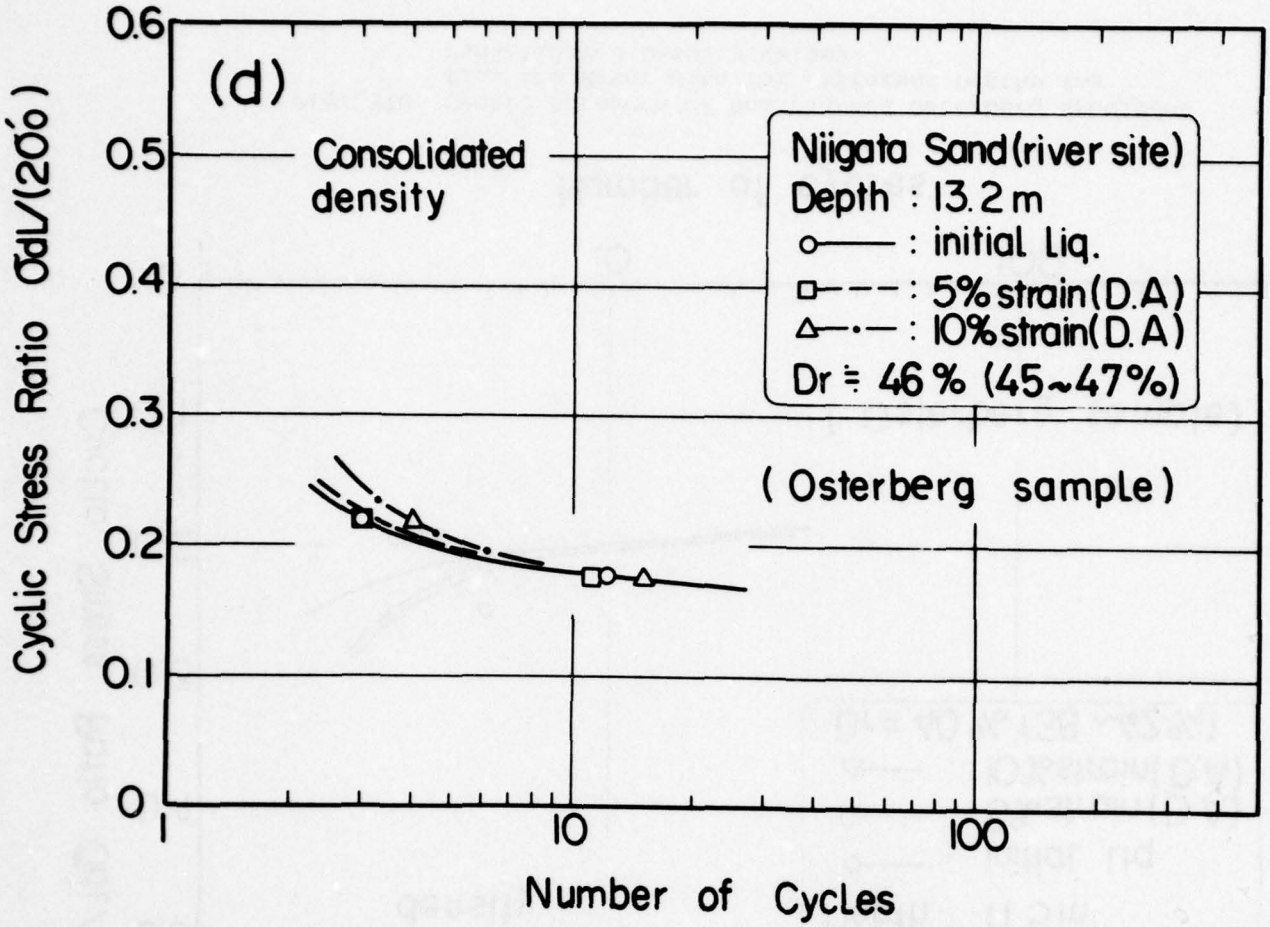

Fig. 37d Summary Curve Showing the Effect of Density on the Cyclic Strength of Undisturbed Osterberg Specimens from the River Site.

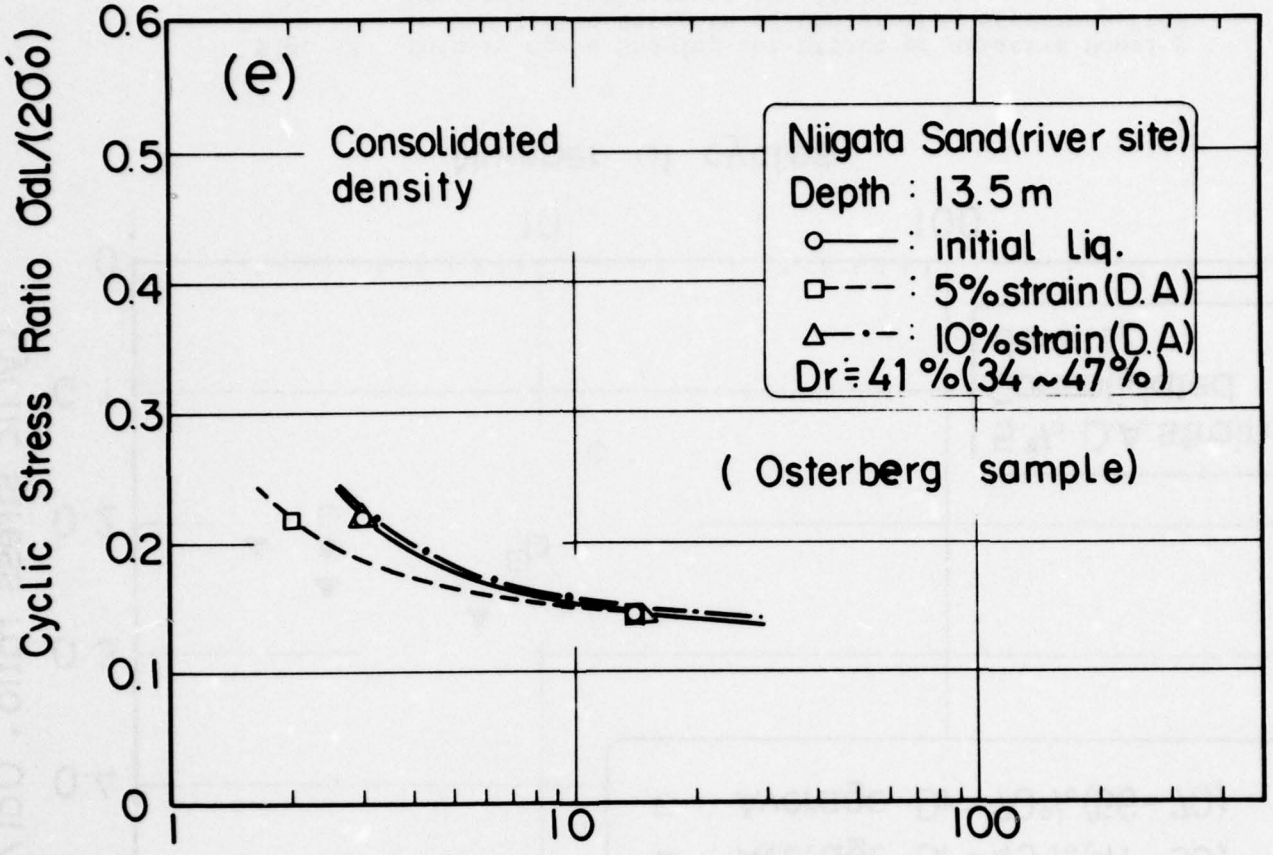

Fig. 37e Summary Curve Showing the Effect of Density on the Cyclic Strength of Undisturbed Osterberg Specimens from the River Site.

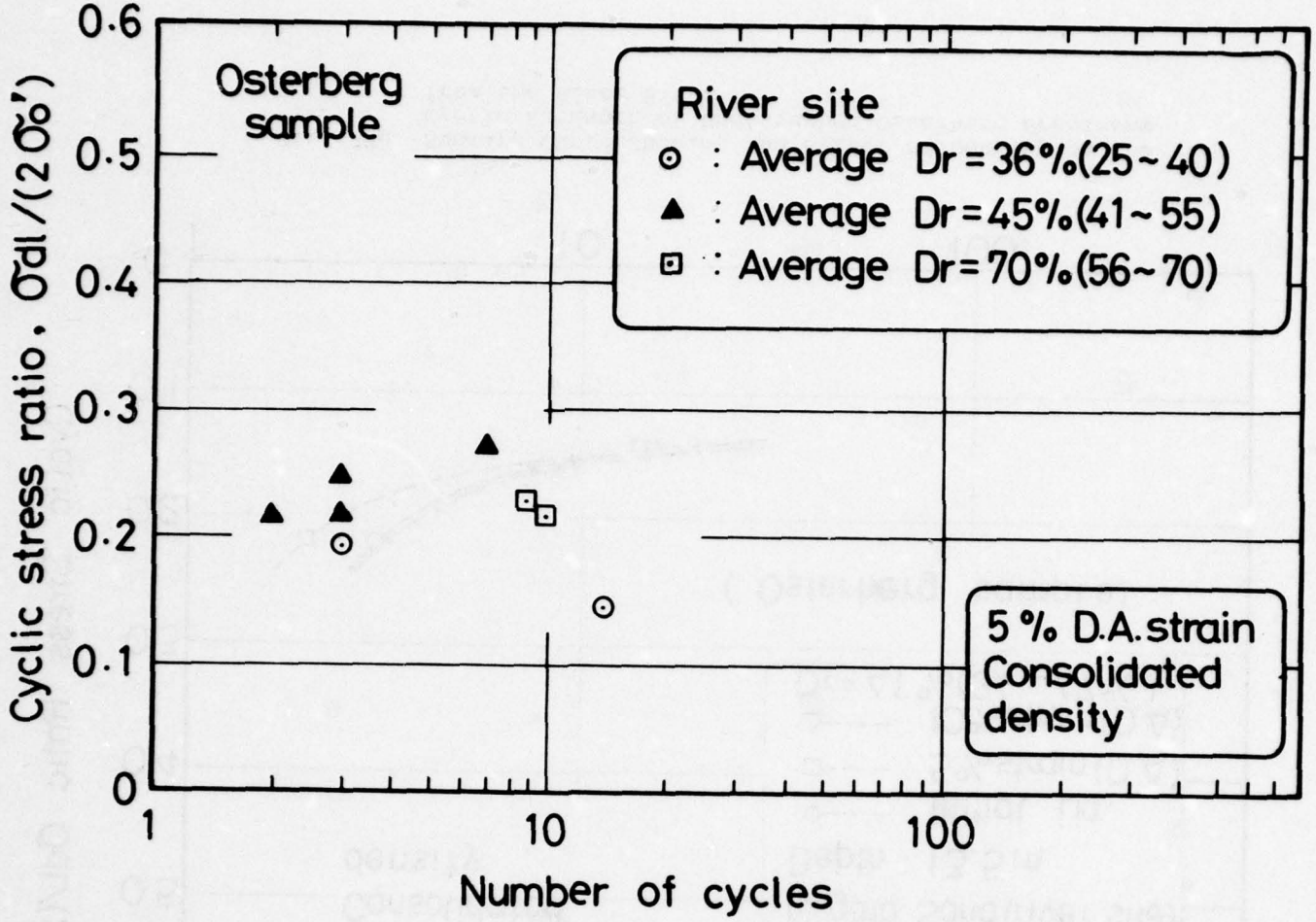

Fig. 38 Summary Curve Showing the Effect of Relative Density on the Cyclic Strength of Undisturbed Specimens from Osterberg Samples from the River Site.

curves is similar to the shape of curves obtained for tests on specimens from large diameter samples.

Insitu Cyclic Triaxial Strength Values

Consolidation of the undisturbed specimens prior to laboratory testing changed specimen density values from the insitu state to the consolidated laboratory state. In general, the change in relative density was approximately 5%. Therefore, in order to estimate the cyclic strength of specimens at their insitu densitites, the test data shown in Fig. 37 was adjusted in the same way as was done for specimens from large diameter samples reflecting the empirical relationship that at approximately 50% relative density, the cyclic strength is directly proportional to the relative density. (Silver and Ishihara, 1978). Since the relative density values were lower for the insitu state, the insitu cyclic triaxial strength curves were slightly lower than the laboratory cyclic strength curves. Nonetheless, the shapes of the curves are similar.

The cyclic triaxial strength of Osterberg specimens as a function of depth at the river site is summarized in Fig. 39 where the stress ratio required to cause failure in 20 cycles is plotted as a function of depth for specimens at estimated insitu density values. It may be seen that the stress ratio required to cause failure is on the order of 0.24 at 4 m and decreases uniformly with depth to a value of approximately 0.18 at a depth of 13 m.

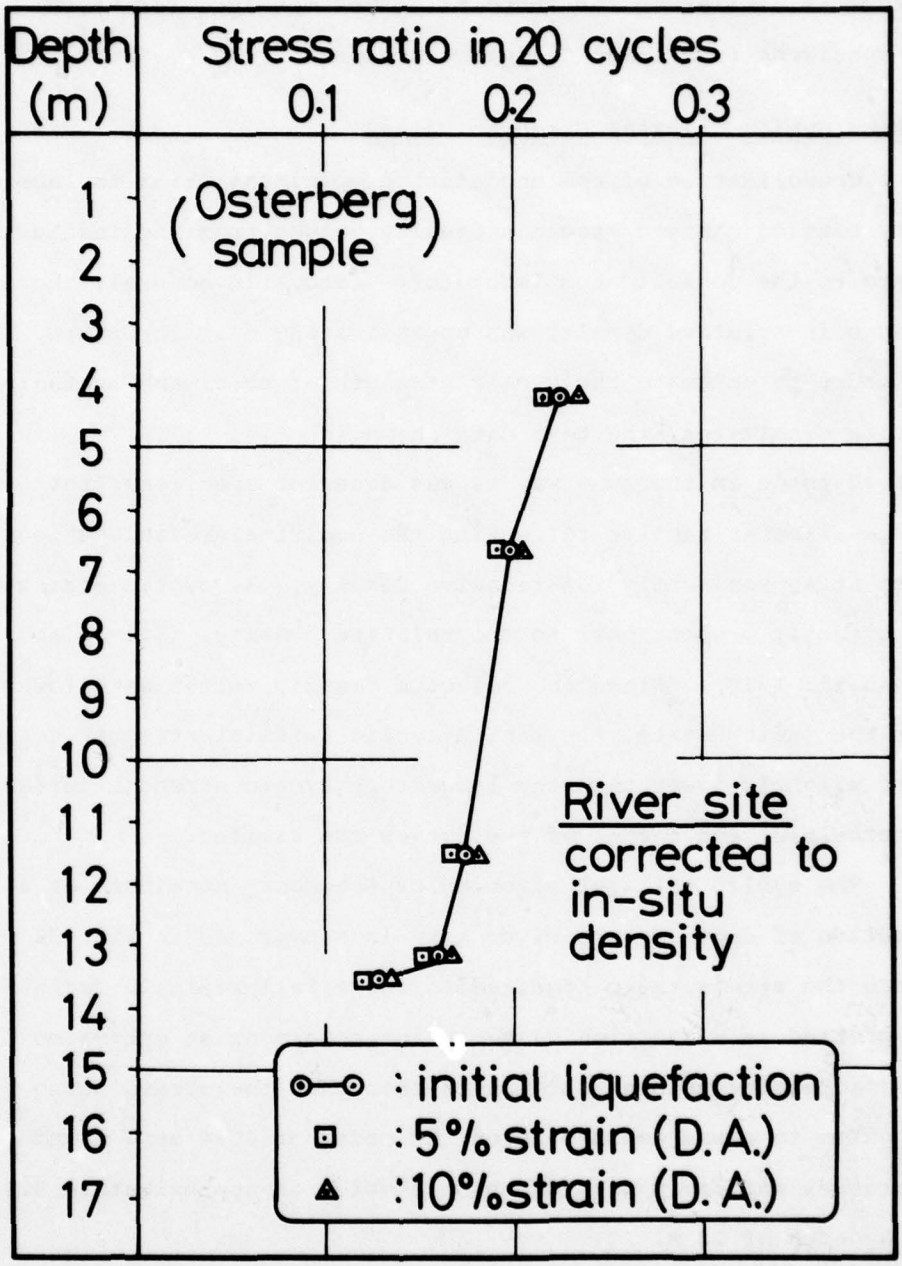

Fig. 39 Insitu Values of Cyclic Triaxial Strength (Failure in 20 Cycles) as a Function of Depth for Specimens from Ostreberg Samples at the River Site.

CHAPTER 7

CYCLIC BEHAVIOR OF SPECIMENS FROM OSTERBERG SOIL SAMPLES FROM THE ROAD SITE

Introduction

The major goal of this study was to compare index property values and cyclic strength values from two adjacent sites; one site which showed serious evidence of liquefaction during the 1954 Niigata earthquake and a second site which showed no surface evidence of liquefaction during the earthquake. The river site, described in previous chapters, provided a sampling location at which surface evidence of liquefaction was noted. The road site, approximately 350 m away, provided a sampling location where the soil profile and the method of soil deposition was similar to the river site, yet at this location no surface evidence of liquefaction was noted. This chapter describes the subsurface conditions at the road site as well as index property values and cyclic strength values obtained from specimens from Osterberg samples taken at the site.

Soil Conditions at the Road Site

Fig. 40 shows the soil profile at the road site. It may be seen that the top 1.5 m consists of surface soil which is underlain to a depth of 4 m with silt and sandy silt. This top 4 m thick layer is a reclaimed deposit which is thought to have been dumped through water in the early part of the

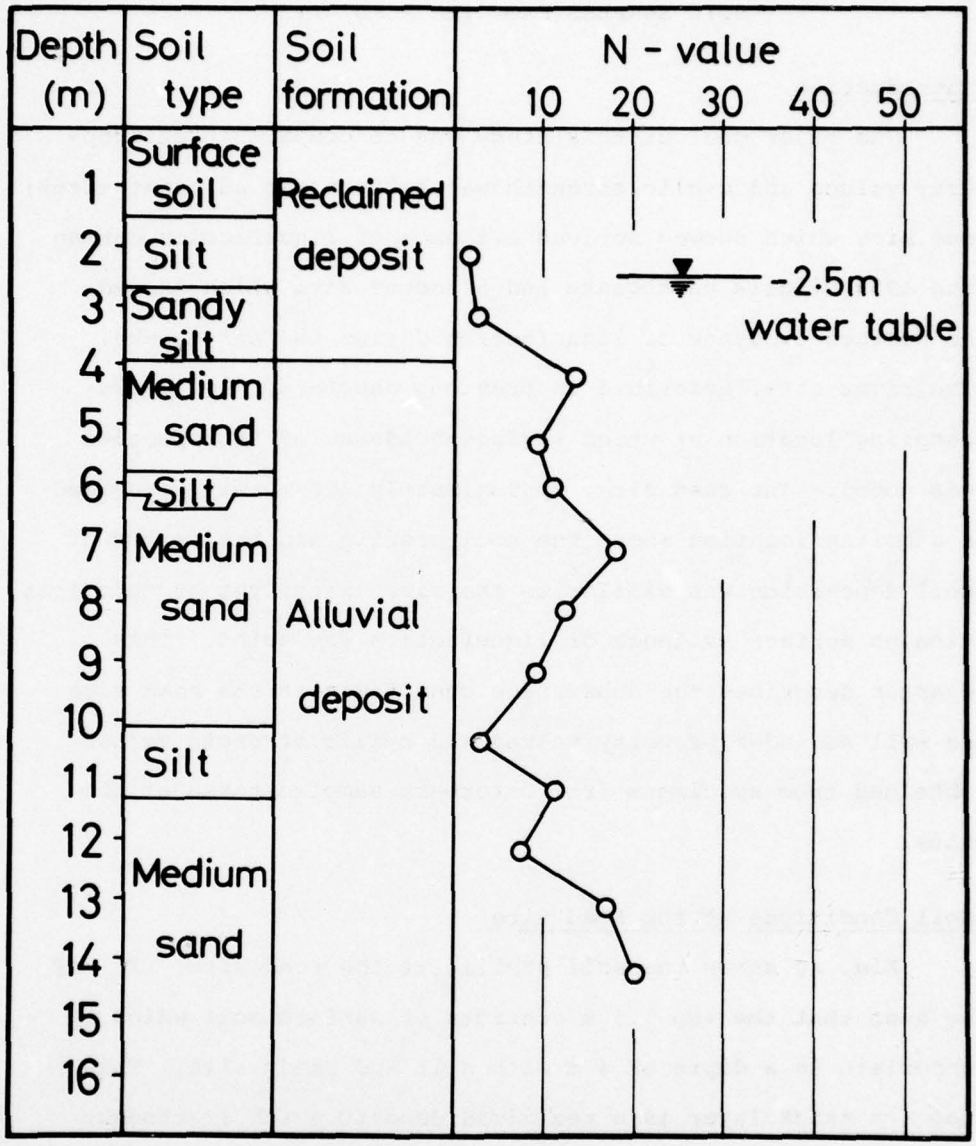

Fig. 40 Soil Profile at the Road Site Showing Soil Type, Method of Soil Deposition and Standard Penetration Test Values.

century to reclaim land from the river bed of the Shinano River. Below 4 m the soil profile consists of alternate layers of medium sand and silt to a depth of 16 m, which was the depth to which soil investigations at the site were taken. These layers are believed to be a natural alluvium deposit made up of stream bed deposits of the meandering Shinano River. Fig. 40 also shows standard penetration test values as a function of depth through the road site deposit. It may be seen that the relative density values in the reclaimed deposit are very low and are on the order of 2 to 3 blows per foot. These N values increase to approximately 10 blows per foot in the alluvial deposit to a depth of 12 m. Below 12 m there seems to be a gradual increase in standard penetration test resistance with N values exceeding 20 blows per foot at a depth of 14 m. It is important to note that between 4 m and 13 m the average blow counts at the road site were on the order of 10, which is on the same order as blow counts recorded at the river site.

Index Property Values at the Road Site

Adjacent to the standard penetration test boring at the road site, a second boring was made in which Osterberg samples were taken almost continuously with depth. No large diameter samples, however, were taken at the road site, and thus the Osterberg samples provide the only basis for evaluating insitu index property values and cyclic strength of soils at the

road site. Table 5 summarizes these values. It may be seen that the 8 Osterberg samples provided 15 specimens for index property testing and cyclic strength testing. At any given depth, on the order of 2 specimens from Osterberg samples were used for index property testing and cyclic strength testing. In general, it was possible to obtain 4 specimens from each Osterberg sample but the remaining two specimens were saved for fabric studies.

The grain size distribution at the road site, obtained from Osterberg samples taken at different depths, are summarized on Fig. 41 which shows the range of particular sizes obtained from all samples taken at the site. It may be seen that the site consists of uniformly graded medium sand with almost no fines.

The mean particle size, D_{50}, and the uniformity coefficient of sands at the site as a function of depth is shown in Fig. 42 where it may be seen that the mean particle size in the natural river bed deposit (below 4 m) is on the order of 0.3. The uniformity coefficient of the sand may be seen to be on the order of 1.5.

Insitu void ratio values for Osterberg specimens at the road site were determined in the same way as the river site. First, the frozen specimen was extruded from the Shelby tube and placed in the triaxial cell under a small effective negative pressure. Then, after the specimen had thawed out, measurements were taken to calculate its insitu density.

TABLE 5

INDEX PROPERTY VALUES AND CYCLIC TRIAXIAL TEST VALUES
OSTERBERG SPECIMENS FROM THE ROAD SITE - NIIGATA, JAPAN

Sample No.	Depth (m)	Gradation		Specific Gravity	Void Ratio		Limiting Void Ratios		Relative Density		$\frac{\sigma d\ell}{2\sigma_o'}$	No. of Cycles		
		D_{50} (mm)	U_c		e_c*	e**	e_{max}	e_{min}	D_{rc}* (%)	D_r** (%)		Init.	5%	10%
B3-S1	4.2	0.63	2.22	2.70	0.910	0.935	1.067	0.661	39	33	0.176	4	4	6
"	"	0.34	1.80	2.68	0.943	0.980	1.103	0.661	36	28	0.219	1	1	2
B3-S3	5.1	0.23	2.45	2.67	1.005	1.047	1.222	0.609	35	29	0.178	7	6	7
B3-S3	6.9	0.36	1.50	2.67	0.939	0.962	1.078	0.565	27	23	0.244	1	2	3
"	"	0.38	1.62	2.68	0.751	0.766	1.059	0.565	62	59	0.188	50	60	70
B3-S4	8.4	0.30	1.83	2.68	-	0.870	1.155	0.589	-	50	-	-	-	-
"	"	0.28	1.58	2.68	0.825	0.840	1.145	0.613	60	57	0.222	8	13	29
B3-S5	9.2	0.34	1.44	2.66	0.940	0.959	1.162	0.668	45	41	0.173	13	13	18
"	"	0.30	1.79	2.65	0.988	1.015	1.184	0.682	39	31	0.193	7	7	10

e, Dr = initial void ratio and relative density of undisturbed specimens

e_c Drc = consolidated void ratio and relative density of undisturbed specimens

Note: All tests performed at an effective confining pressure (σ_c') 1.5 kg/cm^2 (3000 lb/ft^2)

TABLE 5 (Cont.)

Sample No.	Depth (m)	Gradation		Specific Gravity	Void Ratio		Limiting Void Ratios		Relative Density		$\sigma_{d\ell}$	Number of Cycles		
		D_{50} (mm)	U_c		e_c*	e**	e_{max}	e_{min}	D_{rc}*(%)	D_r**(%)	$2\sigma_o'$	init.	5%	10%
B3-S6	11.7	0.36	1.46	2.67	0.882	0.898	1.069	0.619	42	38	0.194	4	4	5
"	"	0.35	1.54	2.68	0.847	0.865	1.082	0.625	51	48	0.164	24	24	28
B3-S7	12.8	0.48	1.67	2.71	0.759	0.772	0.986	0.548	52	49	0.179	18	19	27
"	"	0.48	1.83	2.68	0.753	0.770	1.007	0.564	57	54	0.191	16	17	27
B3-S8	13.8	0.39	1.83	2.66	0.776	0.792	1.071	0.579	60	57	0.192	16	21	25
"	"	0.45	1.92	2.66	0.846	0.867	1.054	0.555	42	38	0.207	8	9	15

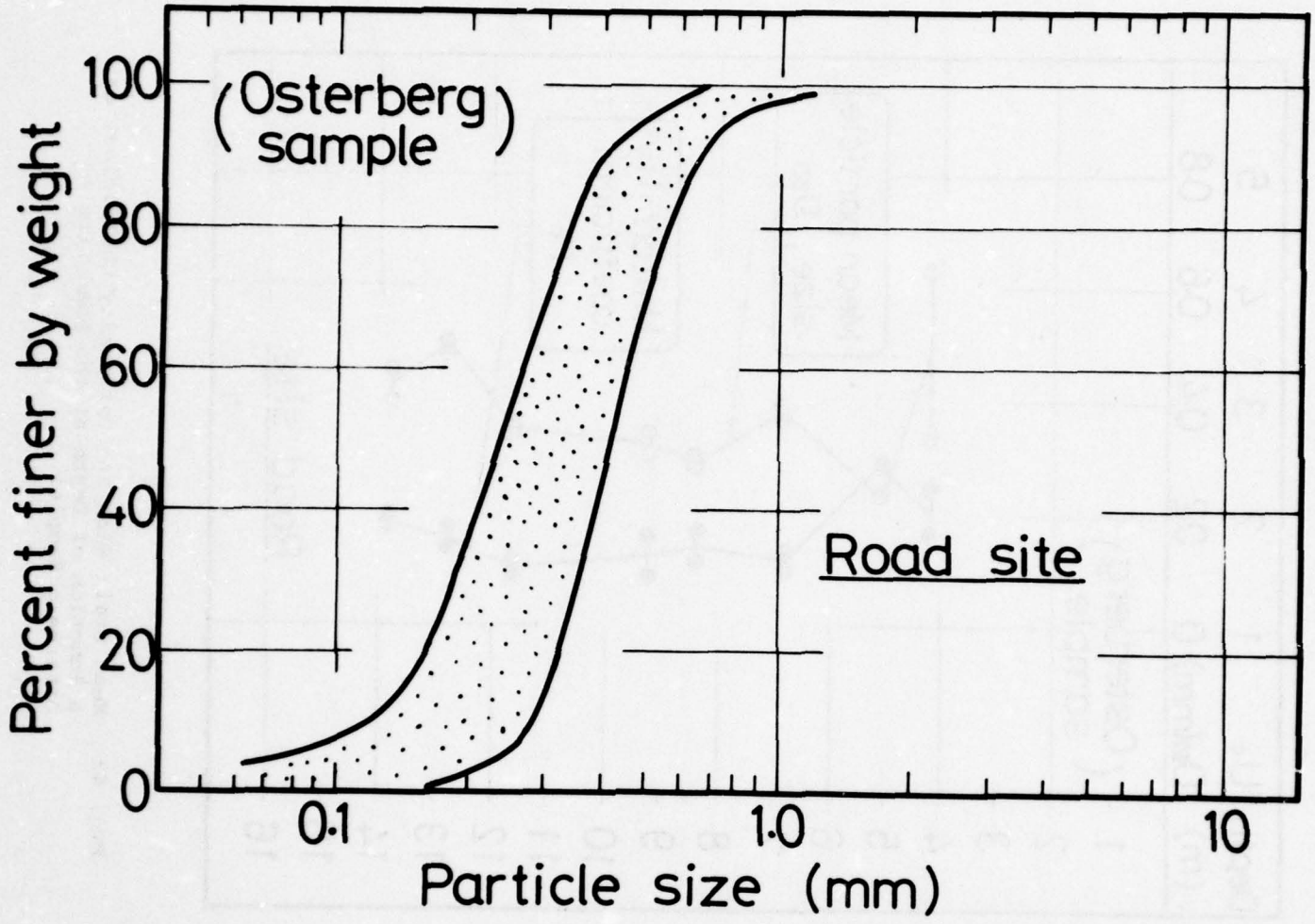

Fig. 41 Summary Curve Showing Grain Size Distribution for Soils at the Road Site - Osterberg Samples.

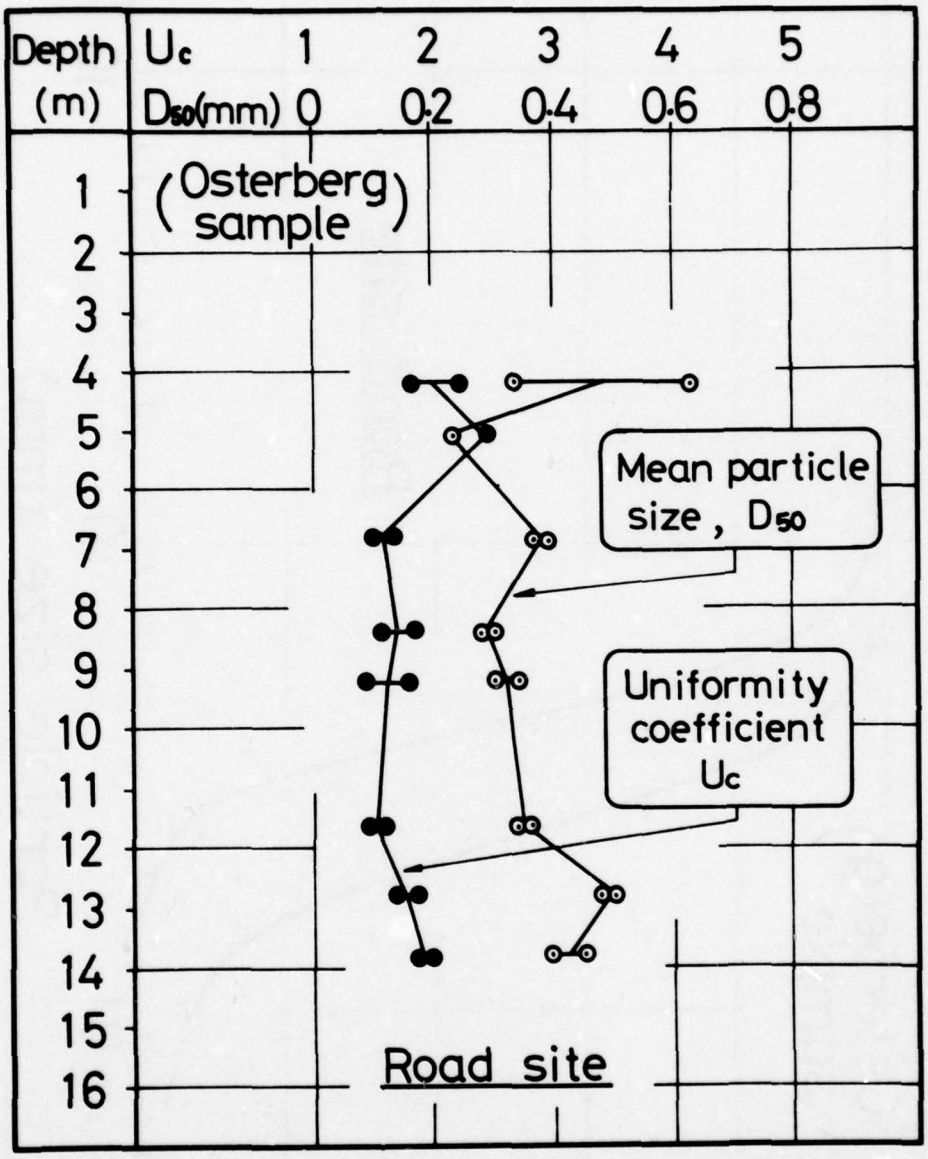

Fig. 42 Mean Grain Size and Uniformity Coefficient as a Function of Depth at the Road Site - Osterberg Samples.

After this, the specimen was consolidated and the resulting density of the specimen was determined and recorded as its tested density.

Insitu void ratio values for Osterberg specimens at the road site as a function of depth are shown in Fig. 43. Multiple data points at the same depth indicated the range of void ratio values from the two specimens obtained from each Osterberg sample. It may be seen that difference in void ratio values between any of the two specimens at the same depth was on the order of 0.05 and that void ratio values in the natural alluvium deposit ranged between 1.0 and 0.75. In general, it was found that the void ratio increased with increasing depth in the natural alluvium deposit.

Maximum and minimum density tests were performed on each specimen, making it possible to calculate the insitu relative density of each specimen. This data is plotted in Fig. 44 which shows insitu relative density values of Osterberg specimens at the road site. As for void ratio values, the range in relative density values for any two specimens at the same depth is low, on the order of 10%. Moreover, it may be seen that average relative density values are on the order of 30% at a dpeth of 4 m and increase to approximately 40% at a depth of 14 m.

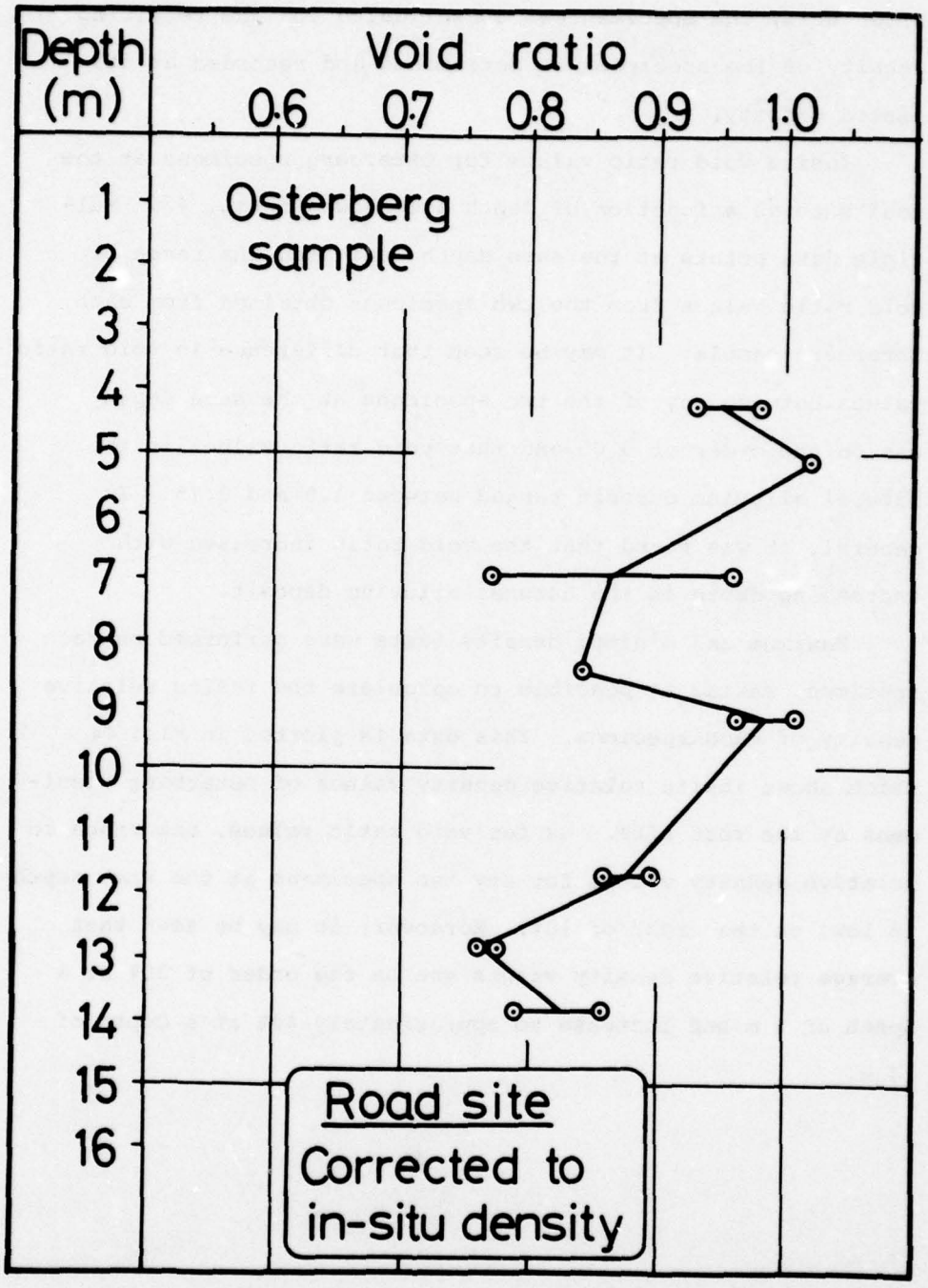

Fig. 43 Insitu Void Ratio Values as a Function of Depth at the Road Site - from Osterberg Specimens.

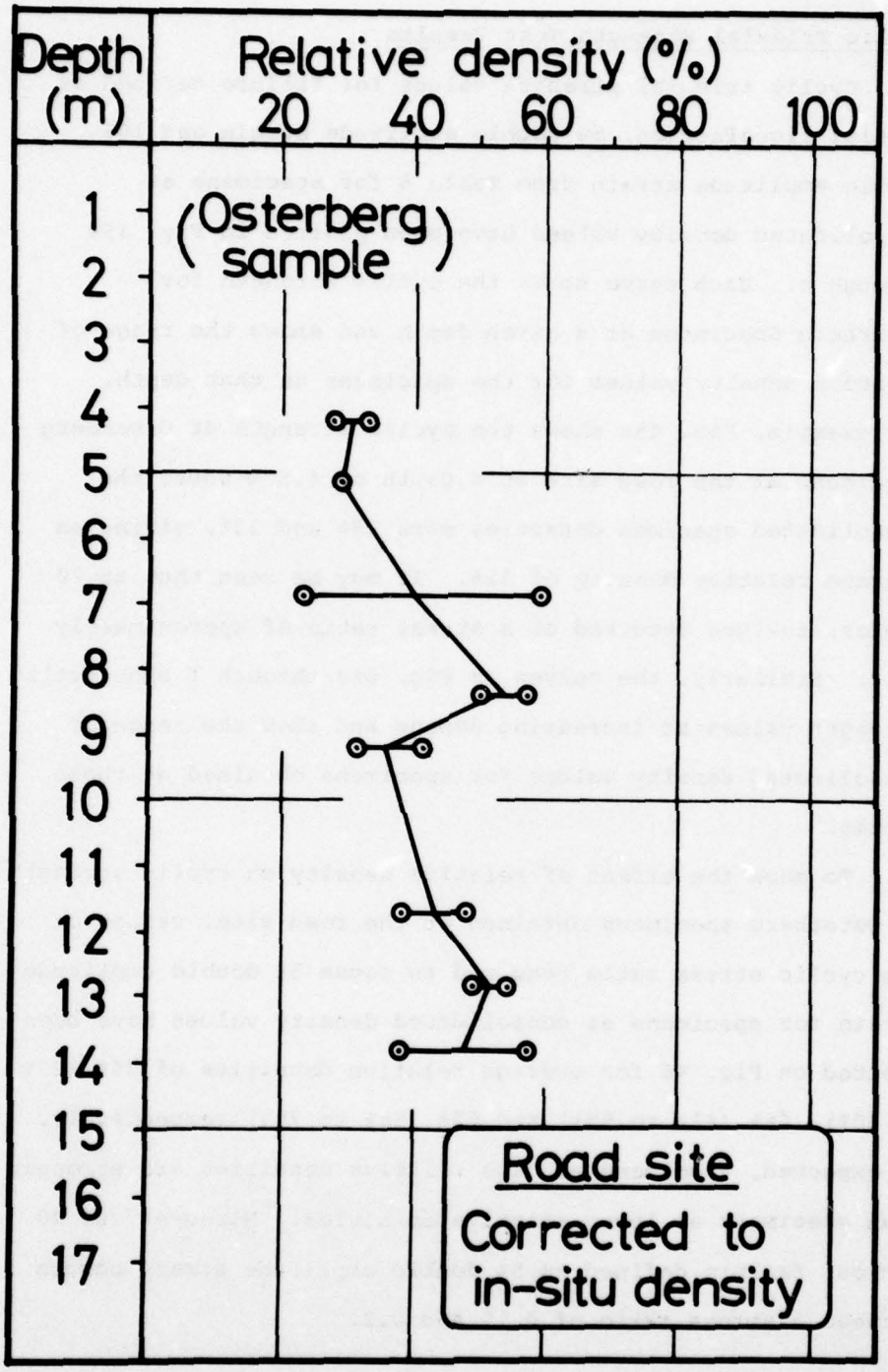

Fig. 44 Insitu Relative Density Values as a Function of Depth at the Road Site - from Osterberg Specimens.

Cyclic Triaxial Strength Test Results

Cyclic triaxial strength values for failure defined as initial liquefaction, 5% double amplitude strain and 10% double amplitude strain from Table 5 for specimens at consolidated density values have been plotted in Fig. 45a through h. Each curve shows the cyclic strength for Osterberg Specimens at a given depth and shows the range of relative density values for the specimens at that depth. For example, Fib. 45a shows the cyclic strength of Osterberg specimens at the road site at a depth of 4.5 m where the consolidated specimen densities were 28% and 33%, giving an average relative density of 31%. It may be seen that at 20 cycles, failure occurred at a stress ratio of approximately 0.18. Similarly, the curves in Fig. 45d through f show cyclic strength values at increasing depths and show the range of consolidated density values for specimens obtained at those depths.

To show the effect of relative density on cyclic strength of Osterberg specimens obtained at the road site, values of the cyclic stress ratio required to cause 5% double amplitude strain for specimens at consolidated density values have been plotted on Fig. 46 for average relative densities of 35% (25% to 40%), 46% (41% to 55%) and 60% (56% to 70%) respectively. As expected, specimens at high relative densities are stronger than specimens at lower relative densities. Moreover, at 20 cycles, failure defined as 5% double amplitude strain occurs between a stress ratio of 0.15 and 0.2.

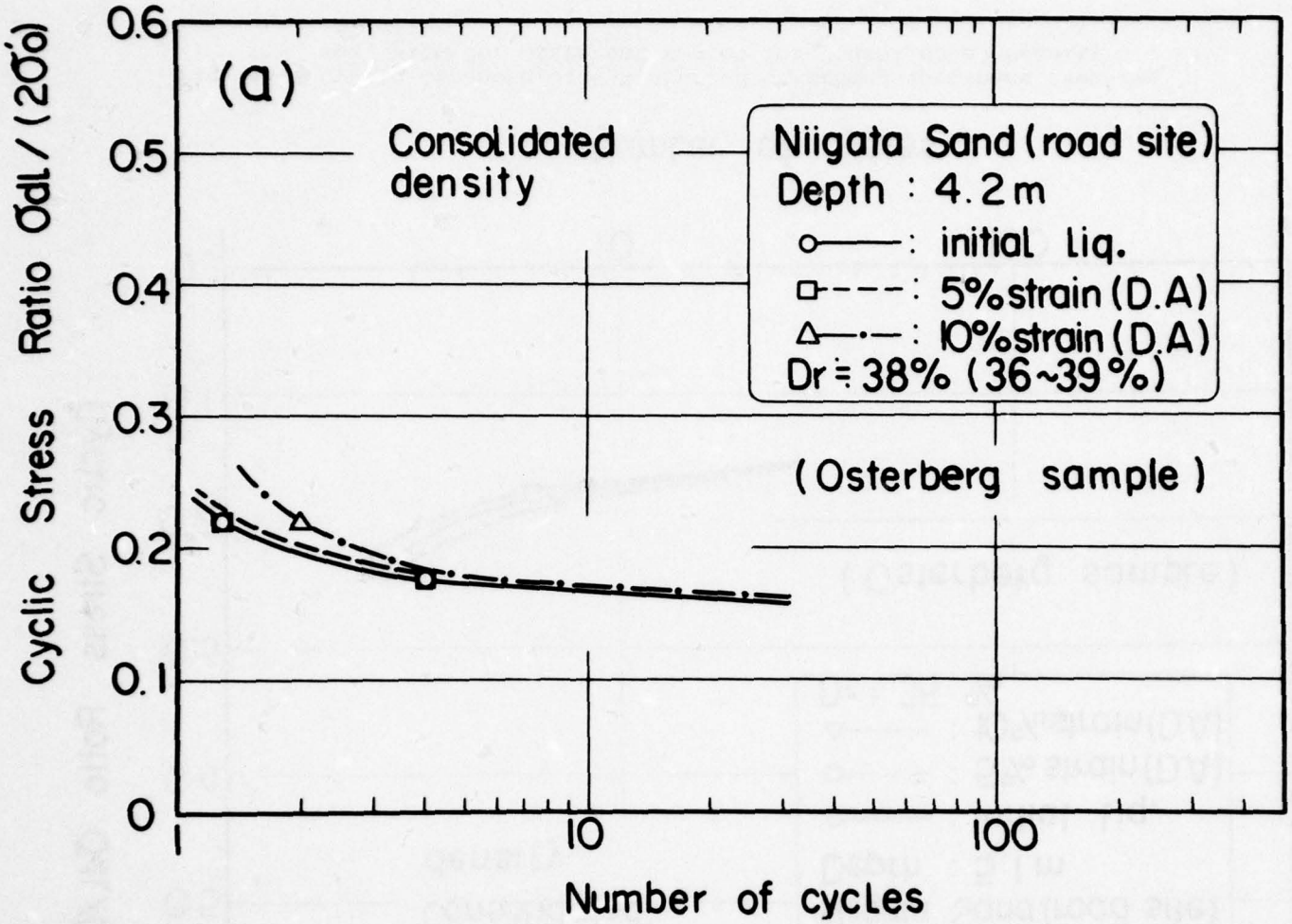

Fig. 45a Cyclic Strength of Undisturbed Osterberg Specimens from the Road Site for Different Depths for Consolidated Density Values.

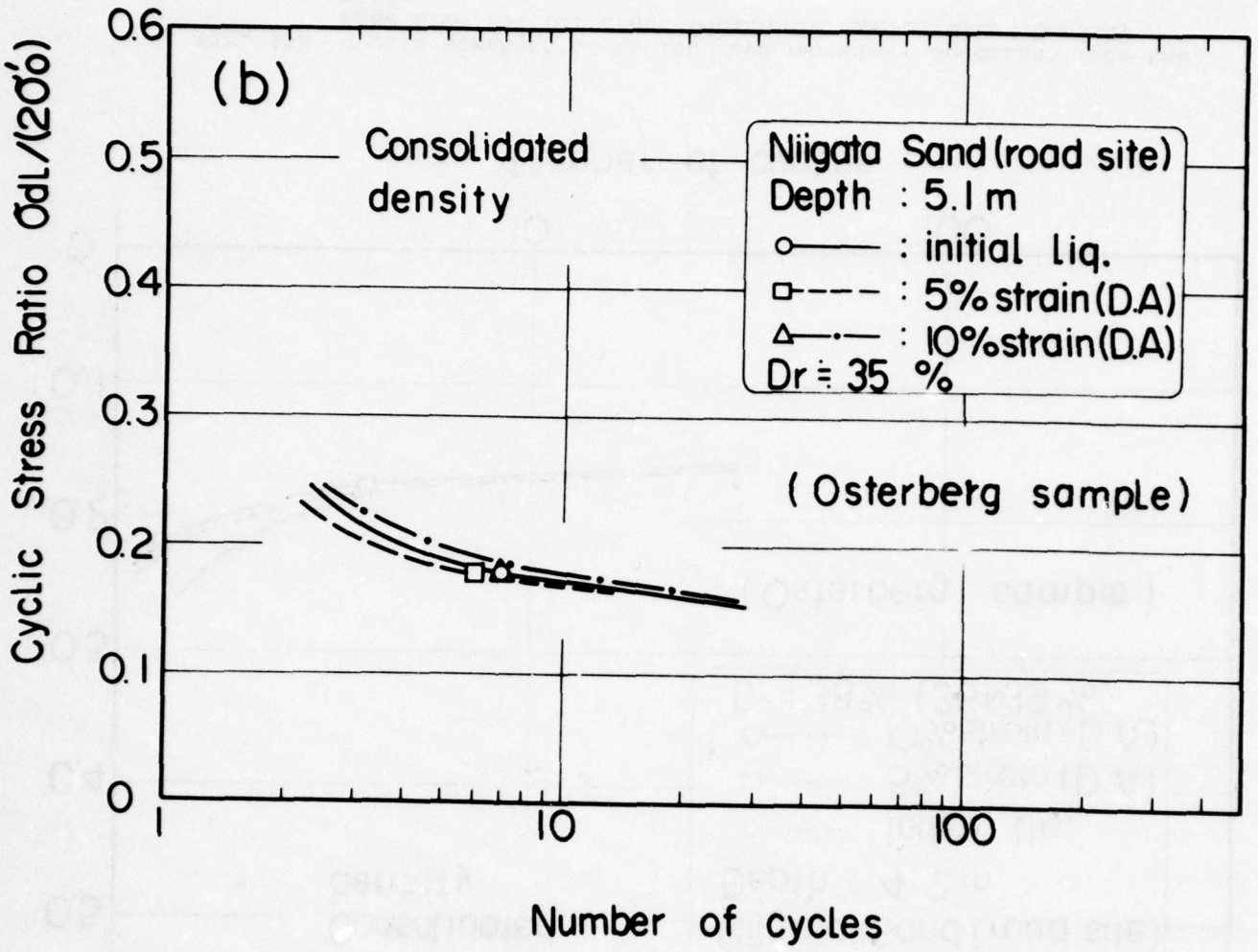

Fig. 45b Cyclic Strength of Undisturbed Osterberg Specimens from the Road Site for Different Depths for Consolidated Density Values.

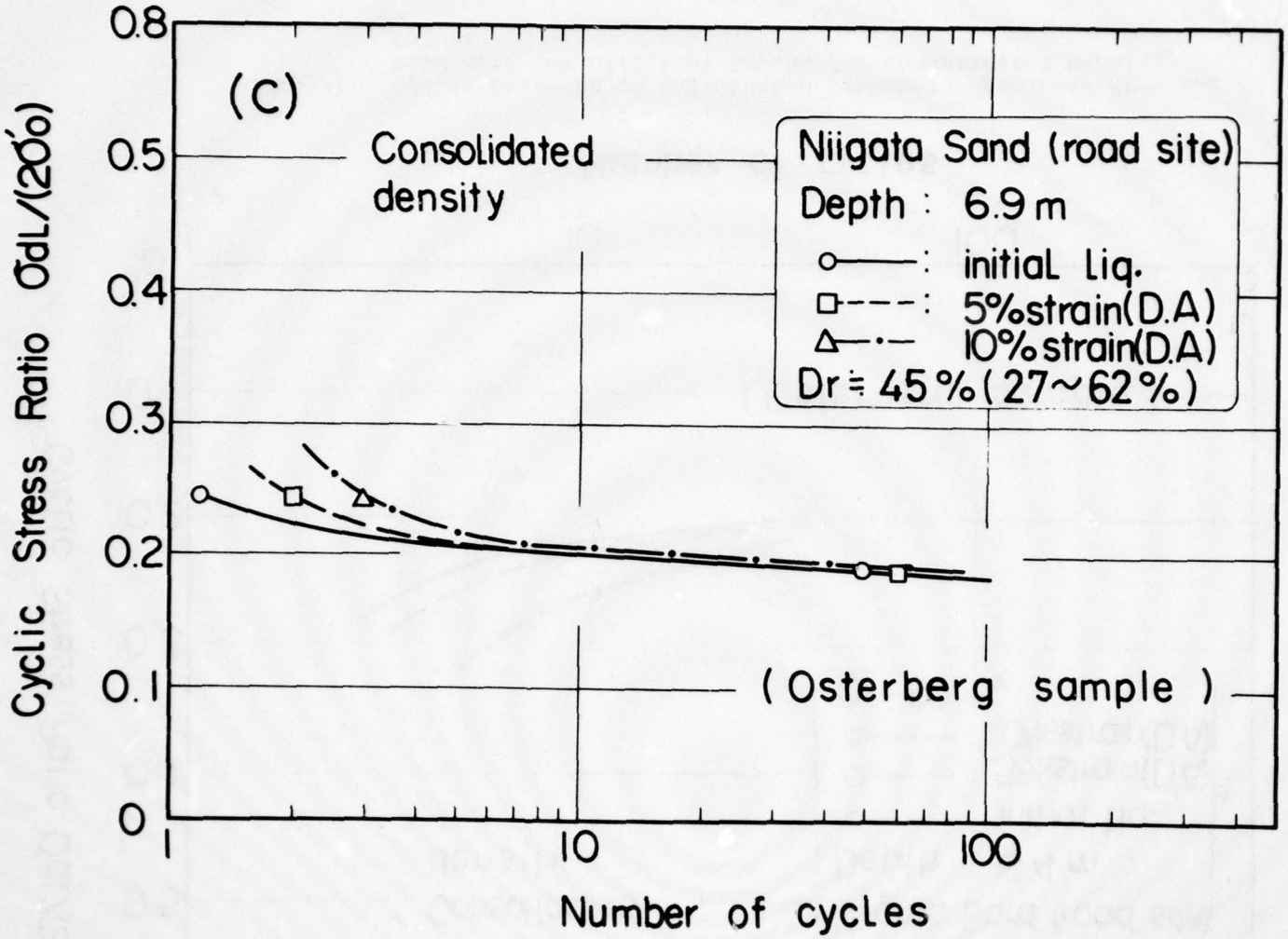

Fig. 45c Cyclic Strength of Undisturbed Osterbeg Specimens from the Road Site for Different Depths for Consolidated Density Values.

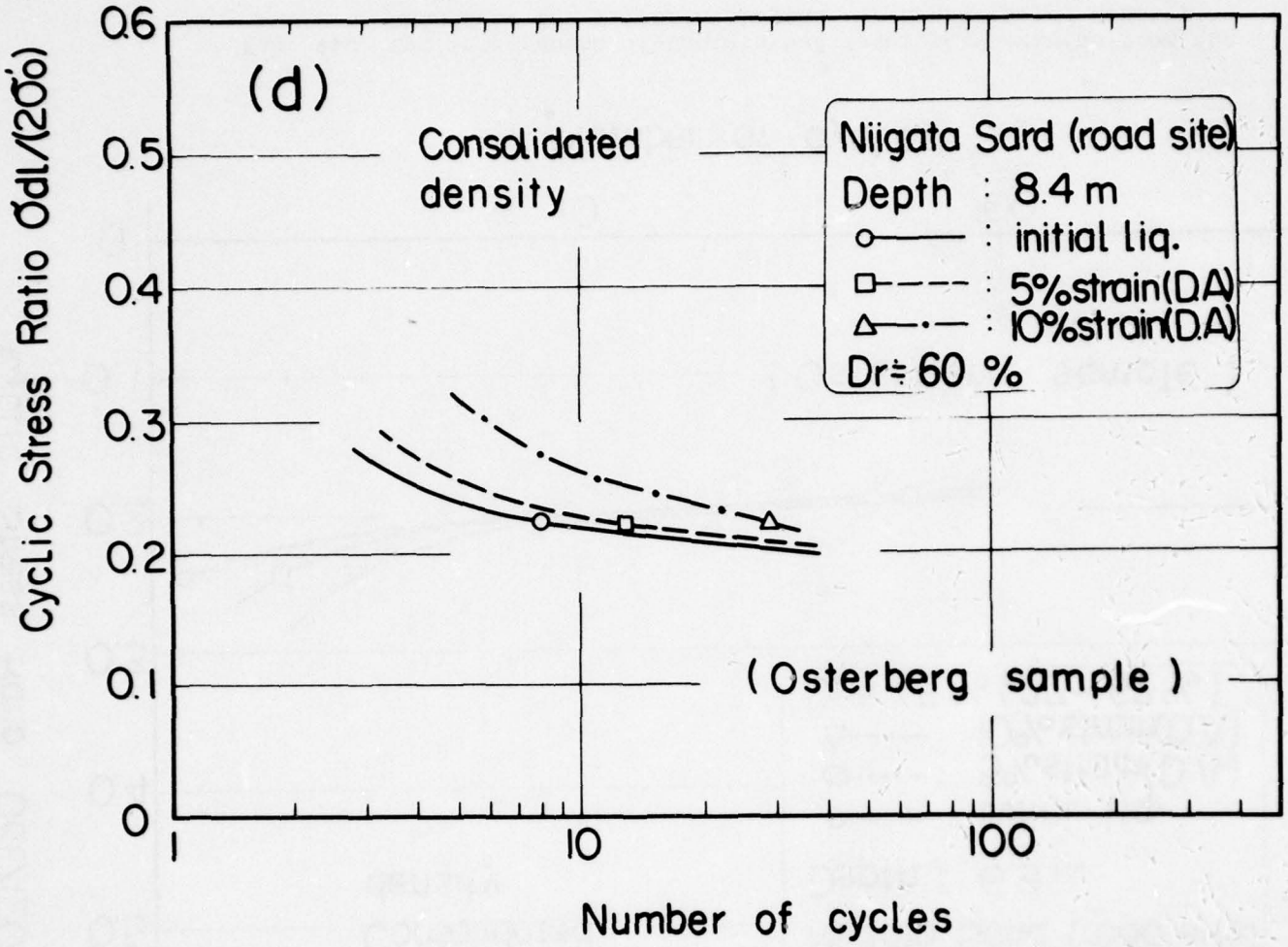

Fig. 45d Cyclic Strength of Undisturbed Osterberg Specimens from the Road Site for Different Depths for Consolidated Density Values.

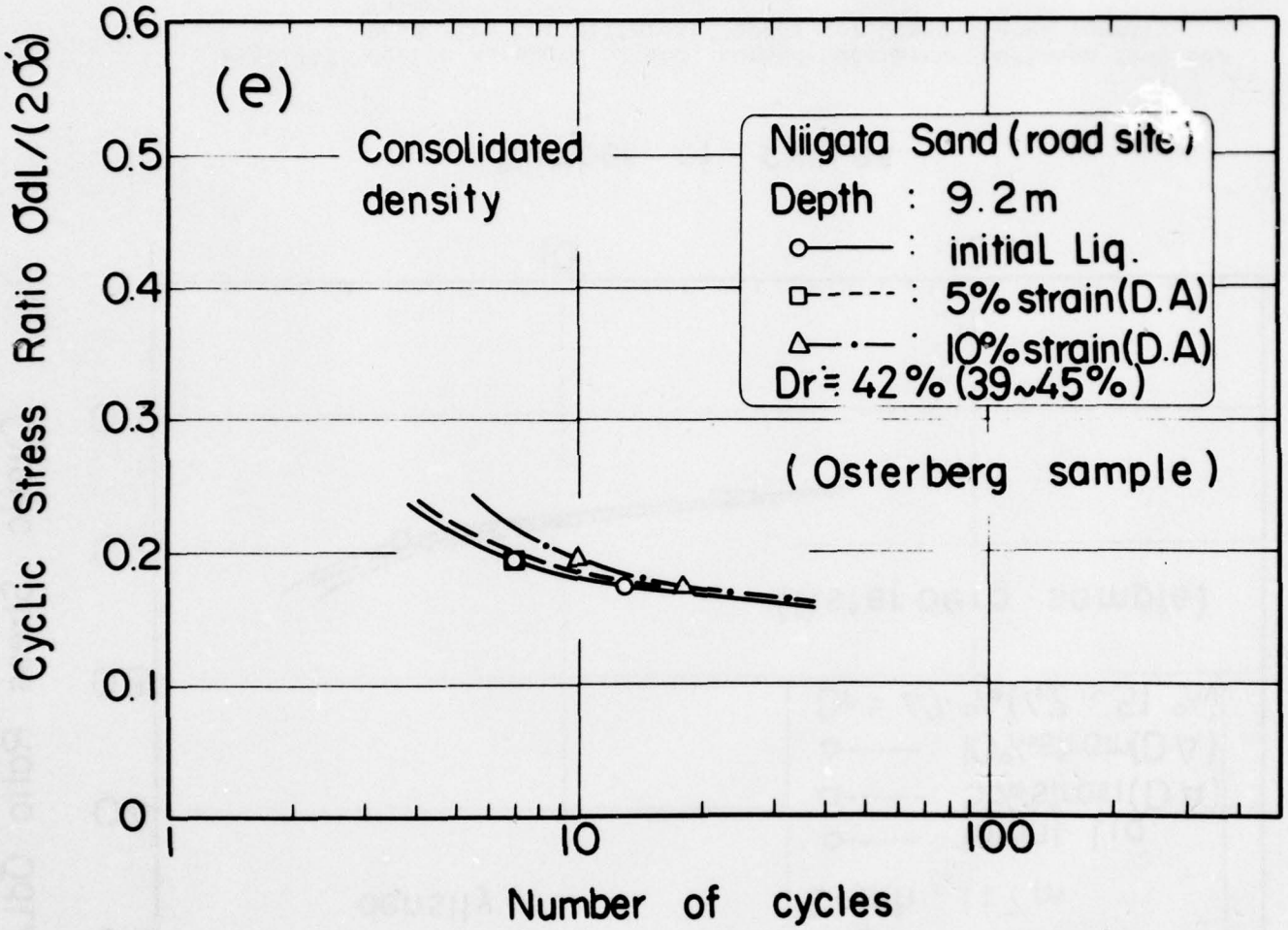

Fig. 45e Cyclic Strength of Undisturbed Osterberg Specimens from the Road Site for Different Depths for Consolidated Density Values.

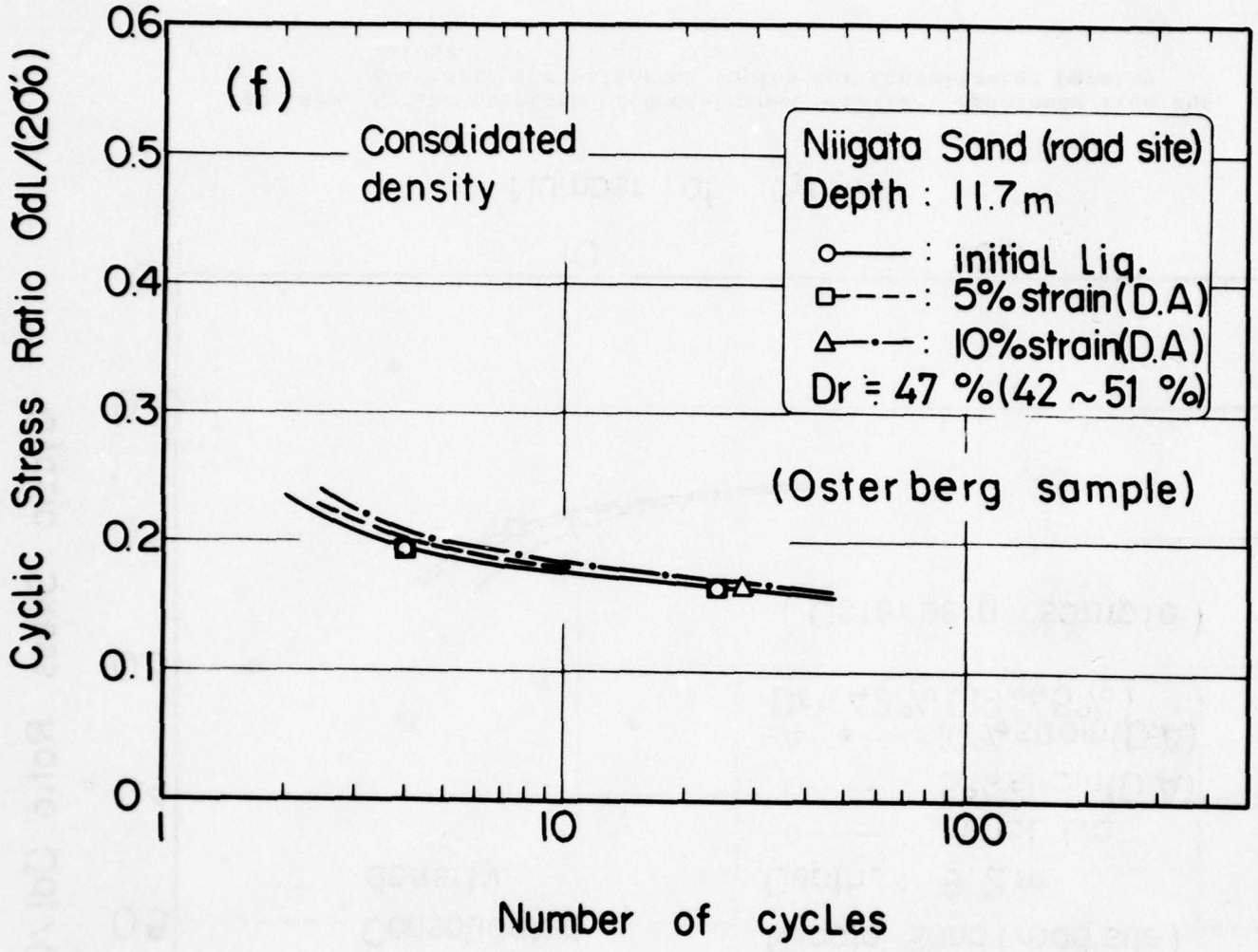

Fig. 45f Cyclic Strength of Undisturbed Osterberg Specimens from the Road Site for Different Depths for Consolidated Density Values.

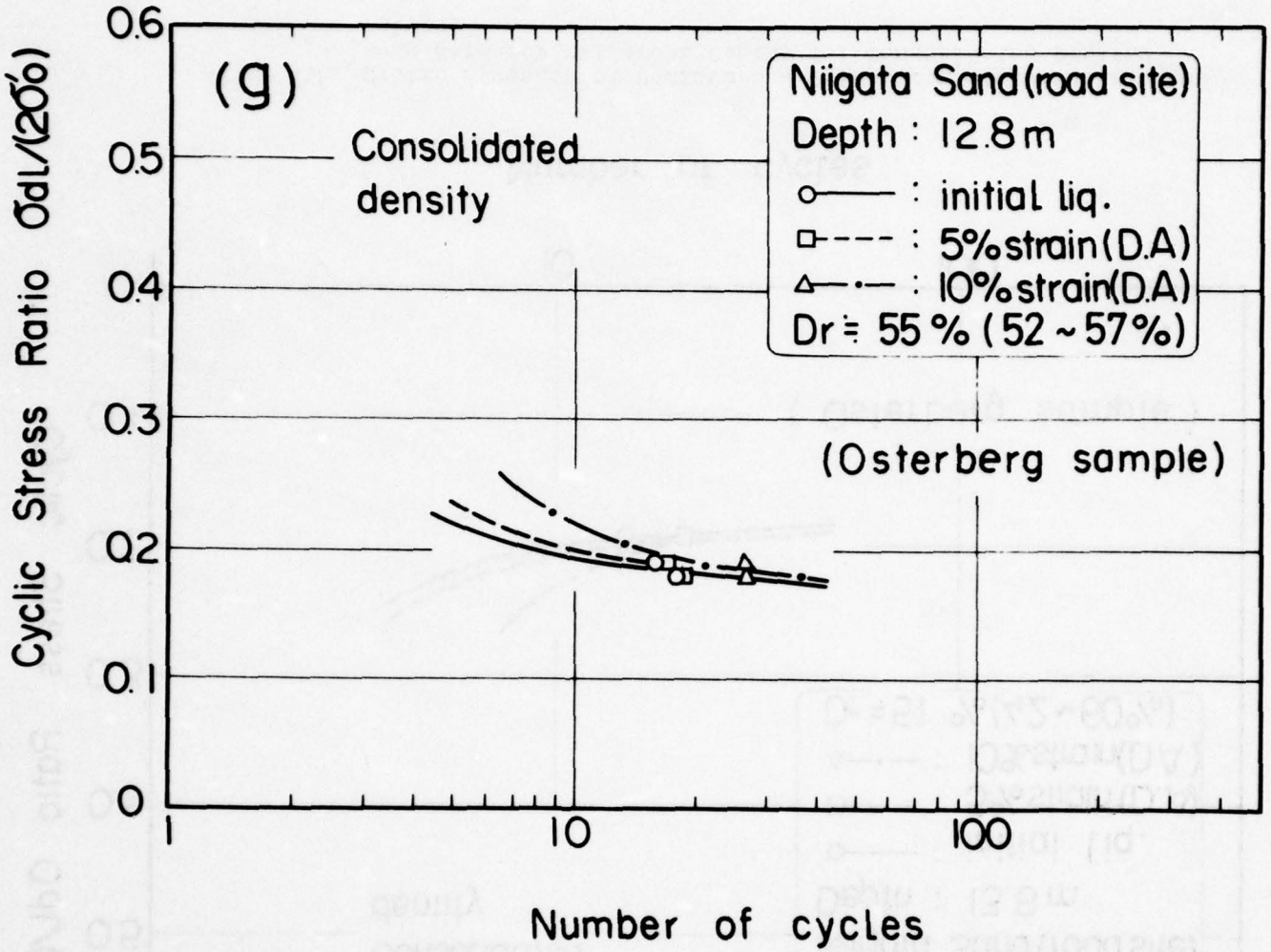

Fig. 45g Cyclic Strength of Undisturbed Osterberg Specimens from the Road Site for Different Depths for Consolidated Density Values.

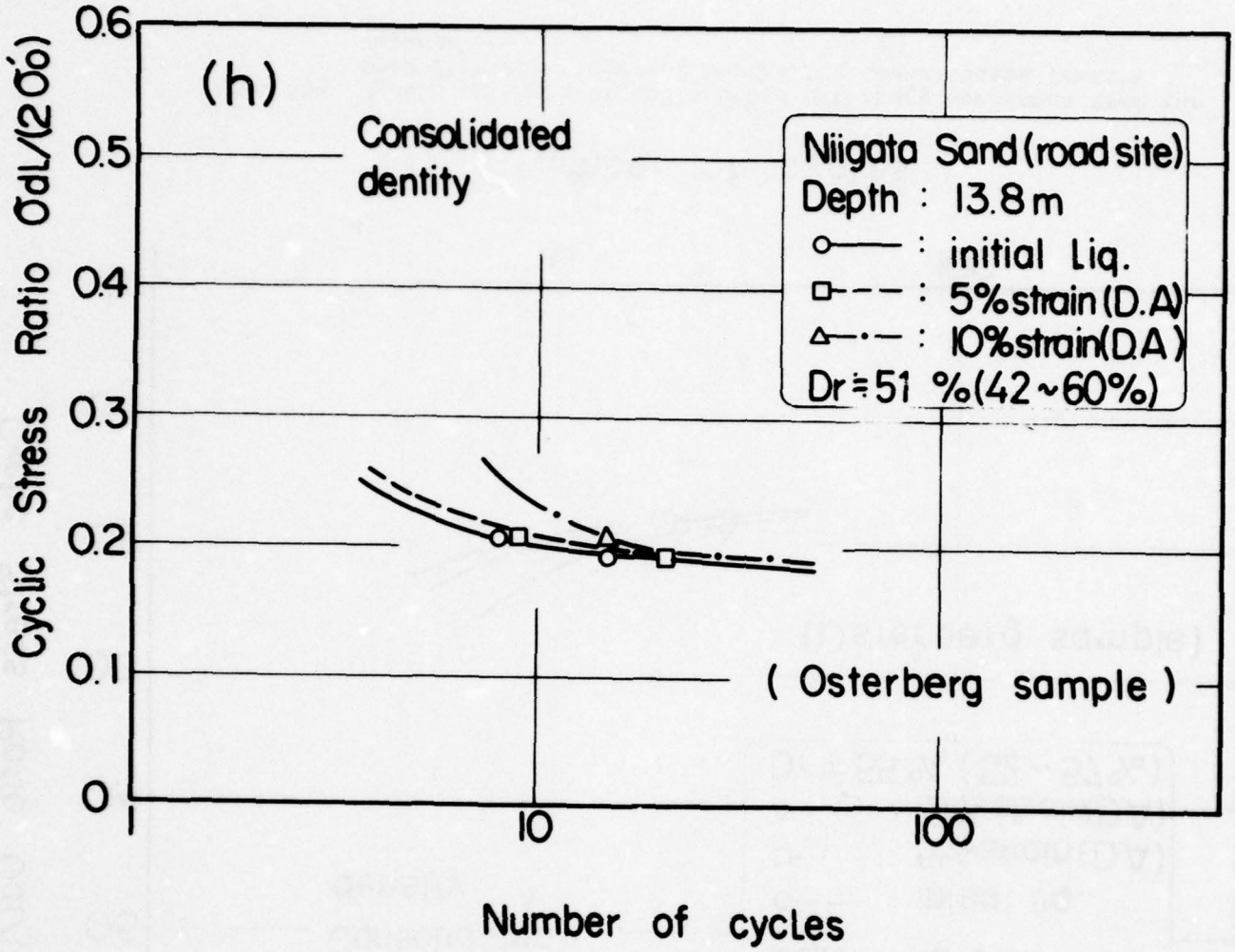

Fig. 45h Cyclic Strength of Undisturbed Osterberg Specimens from the Road Site for Different Depths for Consolidated Density Values.

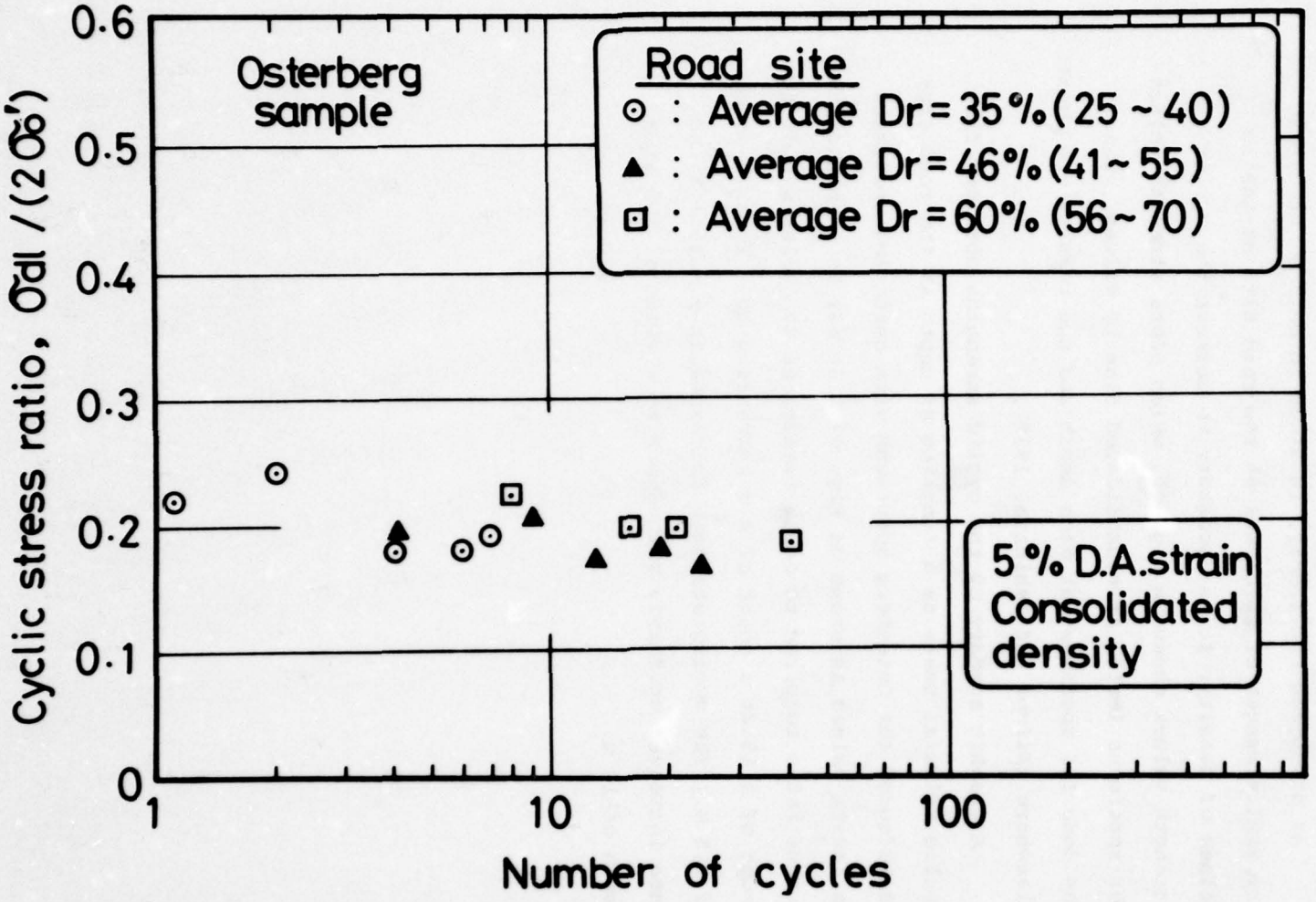

Fig. 46 Summary Curve Showing the Effect of Density on the Cyclic Triaxial Strength of Osterberg Specimens from the Road Site.

Insitu Cyclic Triaxial Strength Values

As discussed previously, in order to define the cyclic triaxial strength of specimens at the road site at insitu values of density, it is necessary to correct the cyclic strength values shown in Fig. 45, which plots strength values for specimens tested at consolidated density values. This was done for specimens at each depth and the results are plotted elsewhere (Silver and Ishihara, 1978).

A graphic summary of the cyclic strengths obtained from cyclic triaxial tests as a function of depth at the road site as measured for Osterberg specimens with densities corrected to insitu values is shown on Fig. 47. It may be seen that the stress ratio required to cause failure at 20 cycles was on the order of 0.15 at a depth of 4 m increasing to 0.2. at a depth of 8.5 m. The cyclic strength decreases at 9 m to 1.5 and then increases uniformly with depth to a value of 0.2 at a depth of 14 m.

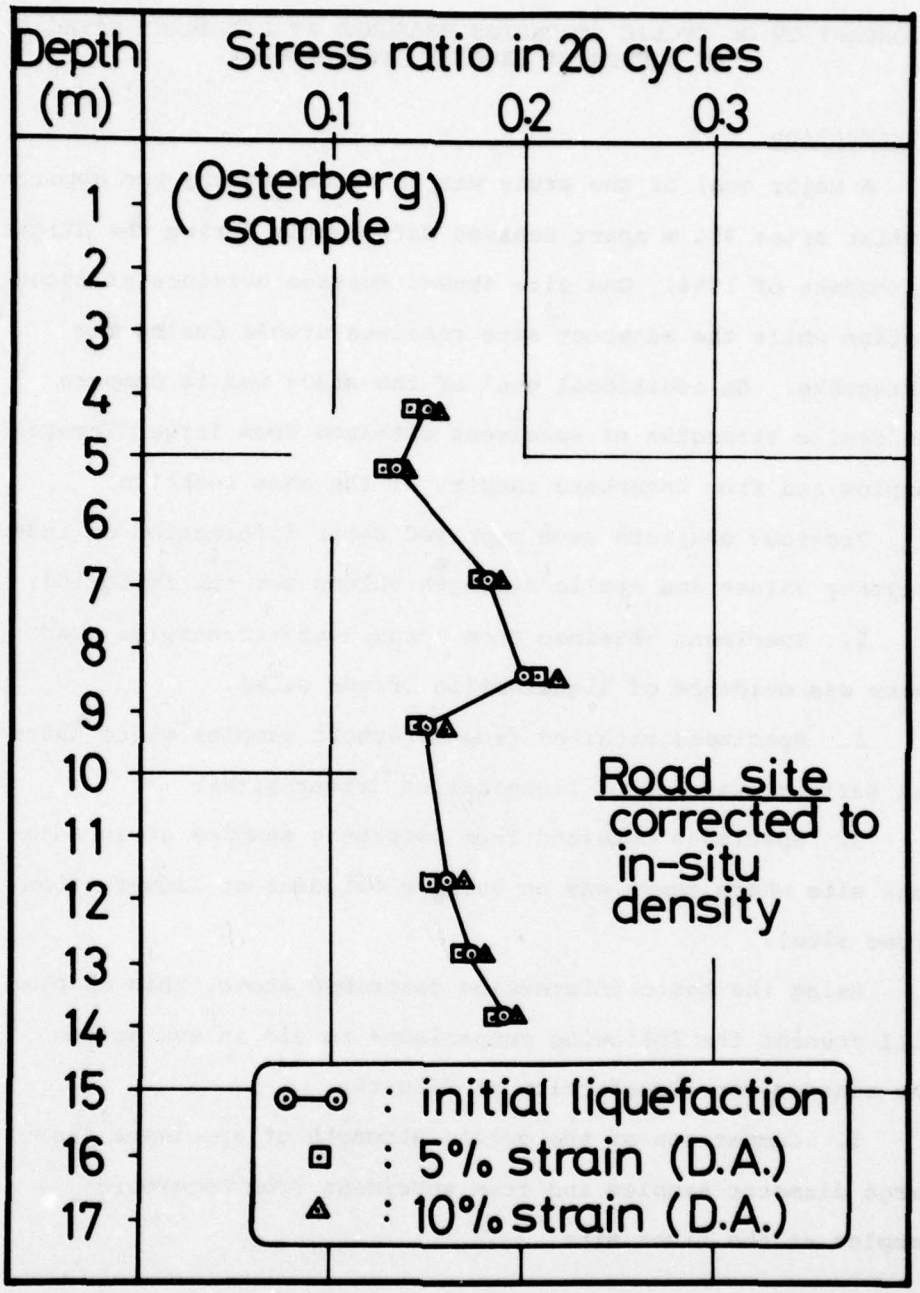

Fig. 47 Insitu Values of Cyclic Triaxial Strength (Failure in 20 Cycles) as a Function of Depth for Specimens from Osterberg Samples at the Road Site

CHAPTER 8

COMPARISON OF CYCLIC STRENGTHS MEASURED AT DIFFERENT SITES BY DIFFERENT SAMPLING TECHNIQUES

Introduction

A major goal of the study was to determine why two apparently similar sites 350 m apart behaved differently during the Niigata earthquake of 1954. One site showed surface evidence of liquefaction while the adjacent site remained stable during the earthquake. An additional goal of the study was to compare the cyclic strengths of specimens obtained from large diameter samples and from Osterberg samples at the same location.

Previous chapters have supplied basic information on index property values and cyclic strength values for the following:

1. Specimens obtained from large diameter samples where there was evidence of liquefaction (river site).

2. Specimens obtained from Osterberg samples where there was surface evidence of liquefaction (river site).

3. Specimens obtained from Osterberg samples at an adjacent site where there was no surface evidence of liquefaction (road site).

Using the basic information described above, this chapter will present the following comparisons to aid in evaluating the reasons for liquefaction at Niigata:

1. Comparison of the cyclic strength of specimens from large diameter samples and from specimens from Osterberg samples at the river site.

2. Comparison of the cyclic strength of specimens from the river site and the road site.

Comparison of Index Property Values for Specimens from Large Diameter Samples and from Specimens from Osterberg Samples at the River Site

One of the most elusive factors required for an understanding of the dynamic behavior of insitu soils is an understanding of insitu density measured as either in place values of void ratio or as in place values of relative density. In previous chapters, insitu void ratio and relative density values at the river site determined from measurements on specimens from large diameter samples were presented on Figs. 26 and 27. Similar data determined from specimens from Osterberg samples were presented on Figs. 35 and 36 Fig. 48 compares the void ratio values as a function of depth measured by these two sampling techniques at the river site. For the limited data, between a depth of 2 m and 7 m, it would appear that specimens from the Osterberg samples are denser than specimens from the large diameter samples. However, at greater depths, on the order of 11 m, it appears that density values for the two types of specimens are more equivalent.

It must be remembered, however, that void ratio values alone may not properly evaluate the engineering properties of soils since insitu void ratio values must be compared with limiting maximum and minimum void ratio values to be able to compare engineering properties for different layers. Therefore,

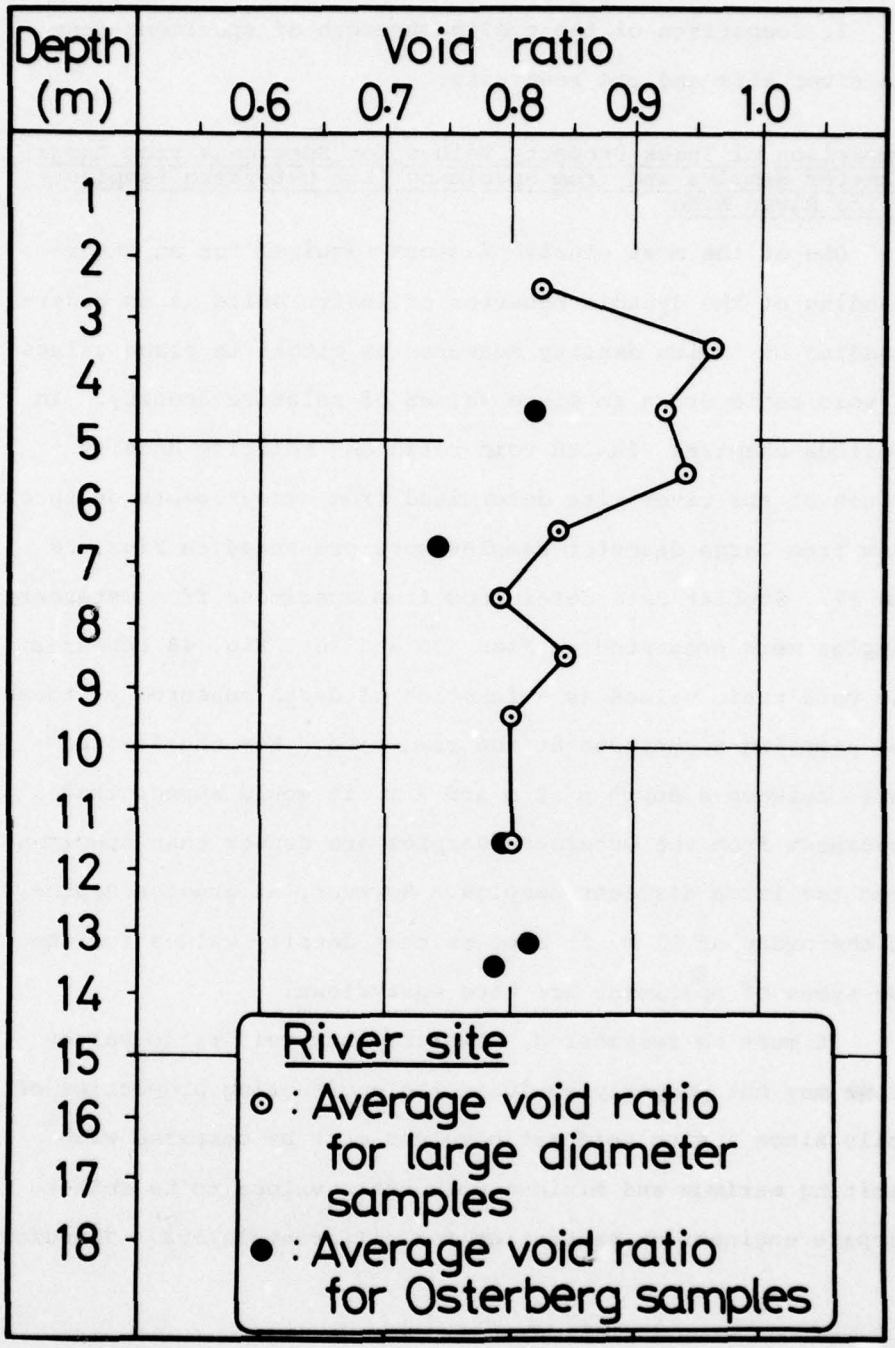

Fig. 48 Comparison of Insitu Void Ratio Values as a Function of Depth for Specimens from Large Diameter Samples and for Specimens from Osterberg Samples at the River Site.

relative density values as a function of depths, have been plotted in Fig. 49 for specimens from large diameter samples and for specimens from Osterberg samples all taken at the river site. To a depth of 10 m the limited available data does not conclusively show whether specimens from Osterberg samples are denser than specimens from large diameter samples. However, at deeper depths, such as at 11 m to 14 m, the trend of both sets of data seems to be similar with relative density values on the order of 40%.

Comparison of Cyclic Strength as Measured on Specimens from Large Diameter Samples and on Specimens from Osterberg Samples

It has previously been shown that because of the rather uniform grain size distribution with depth of the sands at the two sampling sites, it was possible to compare the cyclic strengths of soils from any depth for specimens tested at the same consolidated density. Thus, by comparing the effect of relative density on the strength of specimens from Osterberg samples and the effect of relative density on the strength of specimens from large diameter samples, another check on the effect of sampling may be made. This has been done in Fig. 50 which plots the cyclic stress ratio required to cause 5% double amplitude strain as a function of the number of cycles. The lines in the curve represent cyclic strength values as a function of relative density measured from cyclic triaxial strength tests on specimens from large diameter samples. The data points represent test values from cyclic triaxial strength tests on specimens from Osterberg samples. This data is for

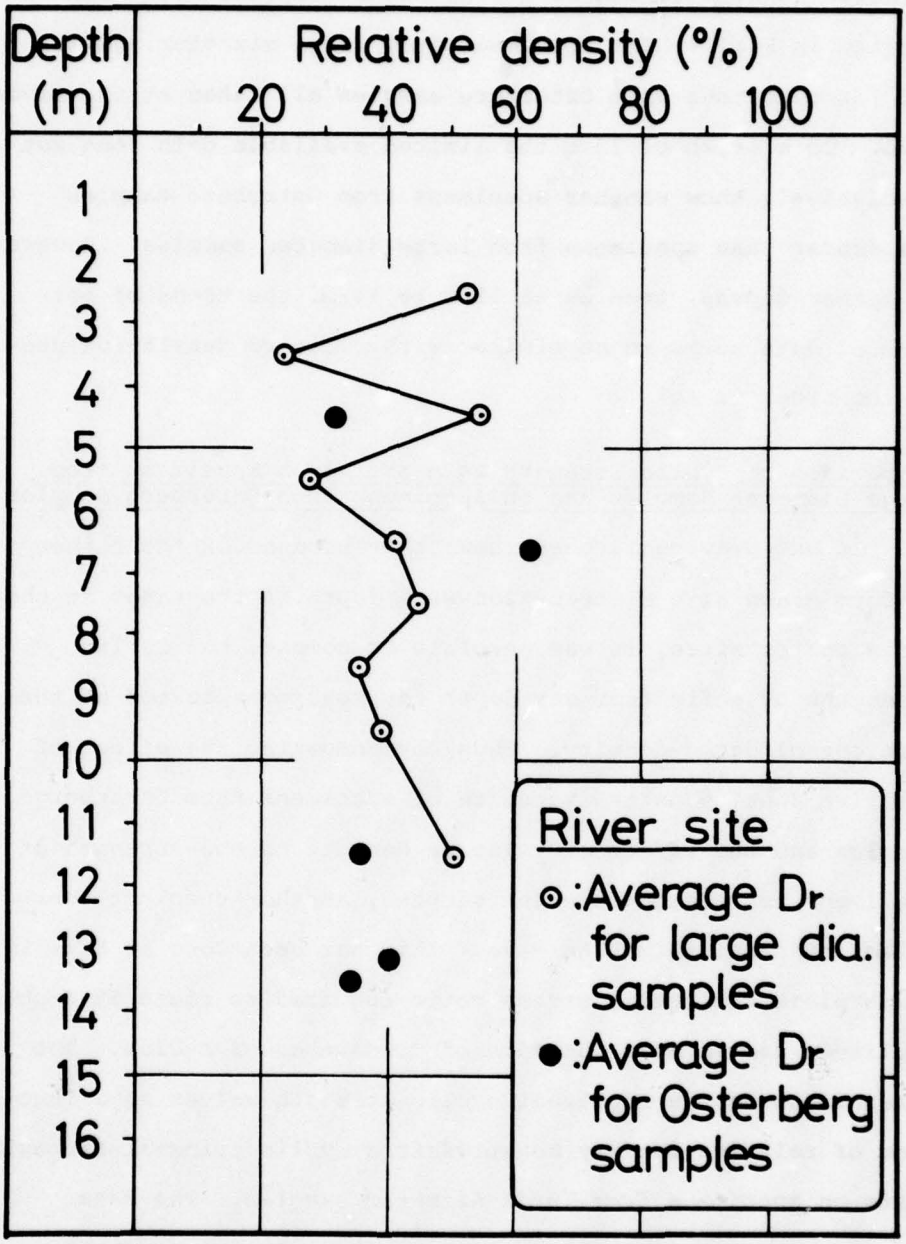

Fig. 49 Comparison of Insitu Relative Density Values as a Function of Depth for Specimens from Large Diameter Samples and for Specimens from Osterberg Samples at the River Site.

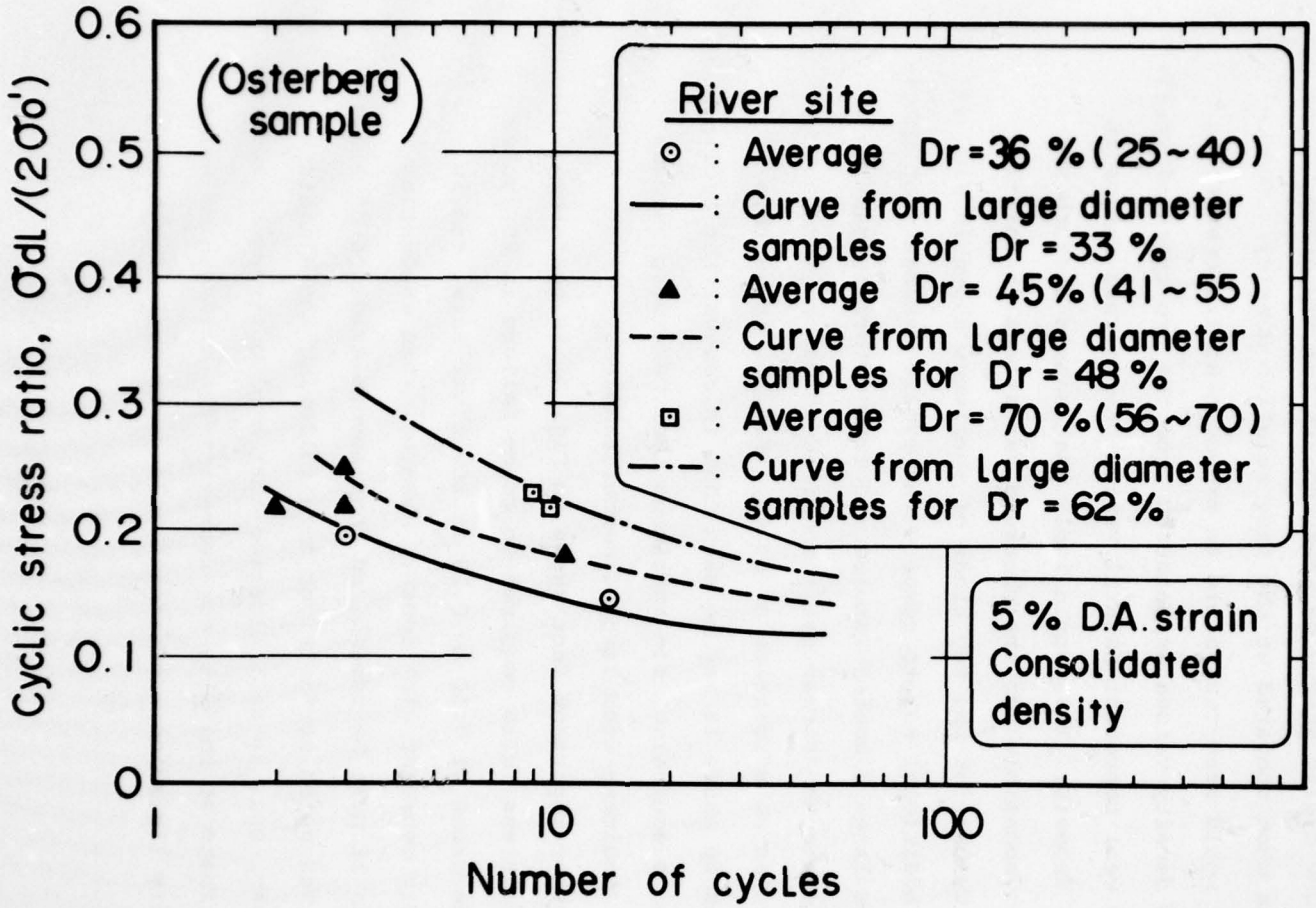

Fig. 50 Comparison of the Cyclic Strength of Undisturbed Specimens from Large Diameter Samples and of Specimens from Osterberg Samples from the River Site for Different Relative Density Values.

laboratory cyclic strength values measured for consolidated specimens. It may be seen that there is very little difference between the cyclic strengths measured for the two kinds of specimens when compared at the same relative density. Therefore, it would seem reasonable to expect that differences in relative density values as measured from the two types of specimens may well represent natural variations in void ratios in the soil deposit. This would imply that sample disturbance was not responsible for the observed variations in relative density values for the two kinds of specimens shown in Fig. 49

An additional way to compare the cyclic strengths of specimens from large diameter samples and from Osterberg samples is to compare the stress ratio required to cause liquefaction in 20 cycles as a function of depth. Fig. 51 shows this relationship where it may be seen that in general the cyclic strength is equivalent for specimens from Osterberg samples and for specimens from large diameter samples.

Another important fact shown in Fig. 51 is that the cyclic triaxial stress ratio required to cause failure in 20 cycles is on the order of 0.10 to 0.15 at the river site, and is relatively constant with depth. However, when evaluating this data it must be remembered that severe evidence of liquefaction was noted at the river site following the Niigata earthquake. This is an indication that cyclic strengths reported for specimens at the site may represent the strength of soils which were liquefied approximately 14 years ago. Moreover,

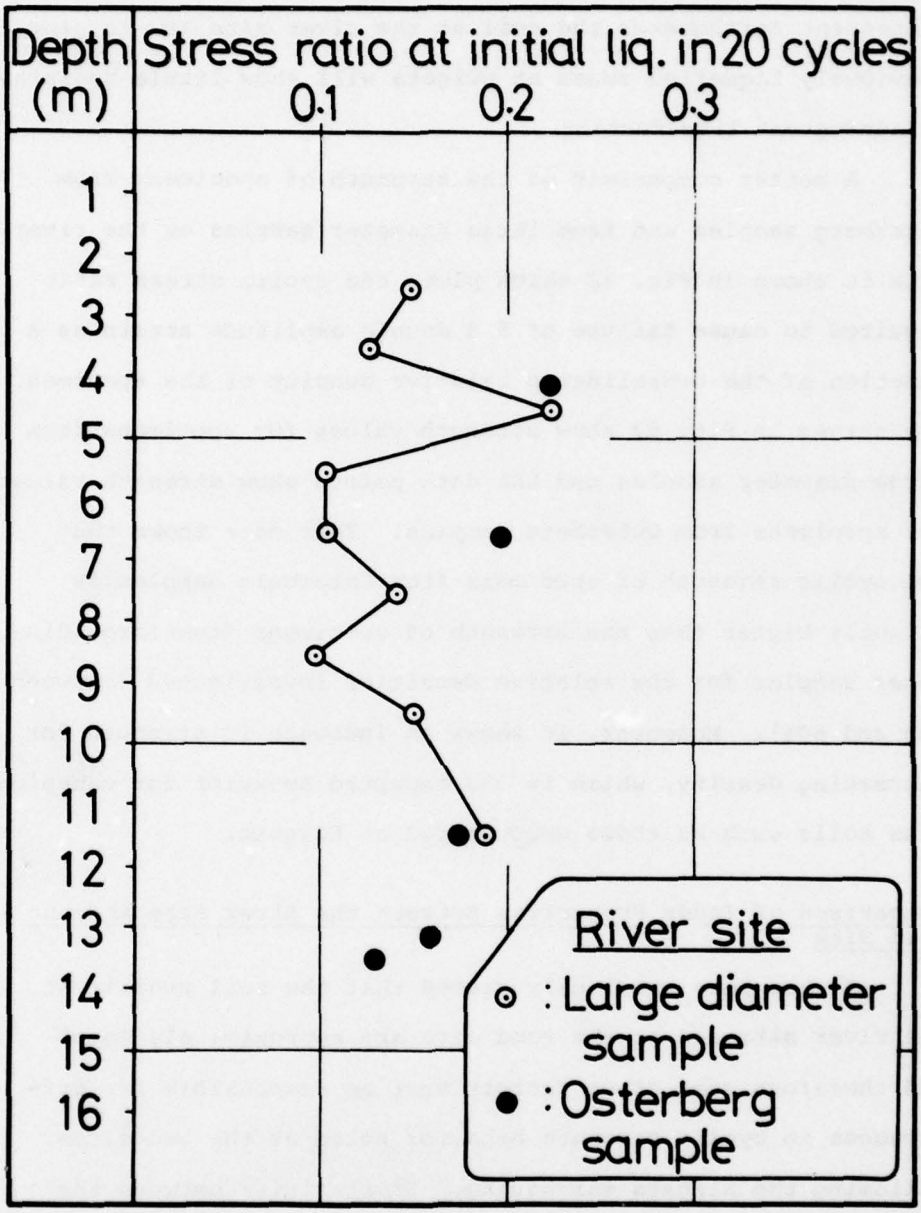

Fig. 51 Comparison of the Stress Ratio Required to Cause Failure in 20 Cycles as Measured in Cyclic Triaxial Strength Tests on Undisturbed Specimens from Large Diameter Samples and on Specimens from Osterberg Samples at the River Site.

these strength values are rather low and would imply that in subsequent earthquakes the soil at the river site and in other previously liquefied zones at Niigata will show little resistance to subsequent liquefaction.

A better comparison of the strength of specimens from Osterberg samples and from large diameter samples at the river site is shown in Fig. 52 which plots the cyclic stress ratio required to cause failure of 5 % double amplitude strain as a function of the consolidated relative density of the specimen. The curves in Fig. 52 show strength values for specimens from large diameter samples and the data points show strength values for specimens from Osterberg samples. This data shows that the cyclic strength of specimens from Osterberg samples is slightly higher than the strength of specimens from large diameter samples for the relative densities investigated (between 30% and 60%). Moreover, it shows an increase in strength for increasing density, which is the expected behavior for cohesionless soils such as those encountered at Niigata.

Comparison of Index Properties Between the River Site and the Road Site

It has been previously stated that the soil profile at the river site and at the road site are approximately equal and therefore some other factors must be responsible for differences in cyclic strength behavior noted at the two sites following the Niigata earthquake. Similarities between the two sites is first shown in Fig. 53 which compares the standard

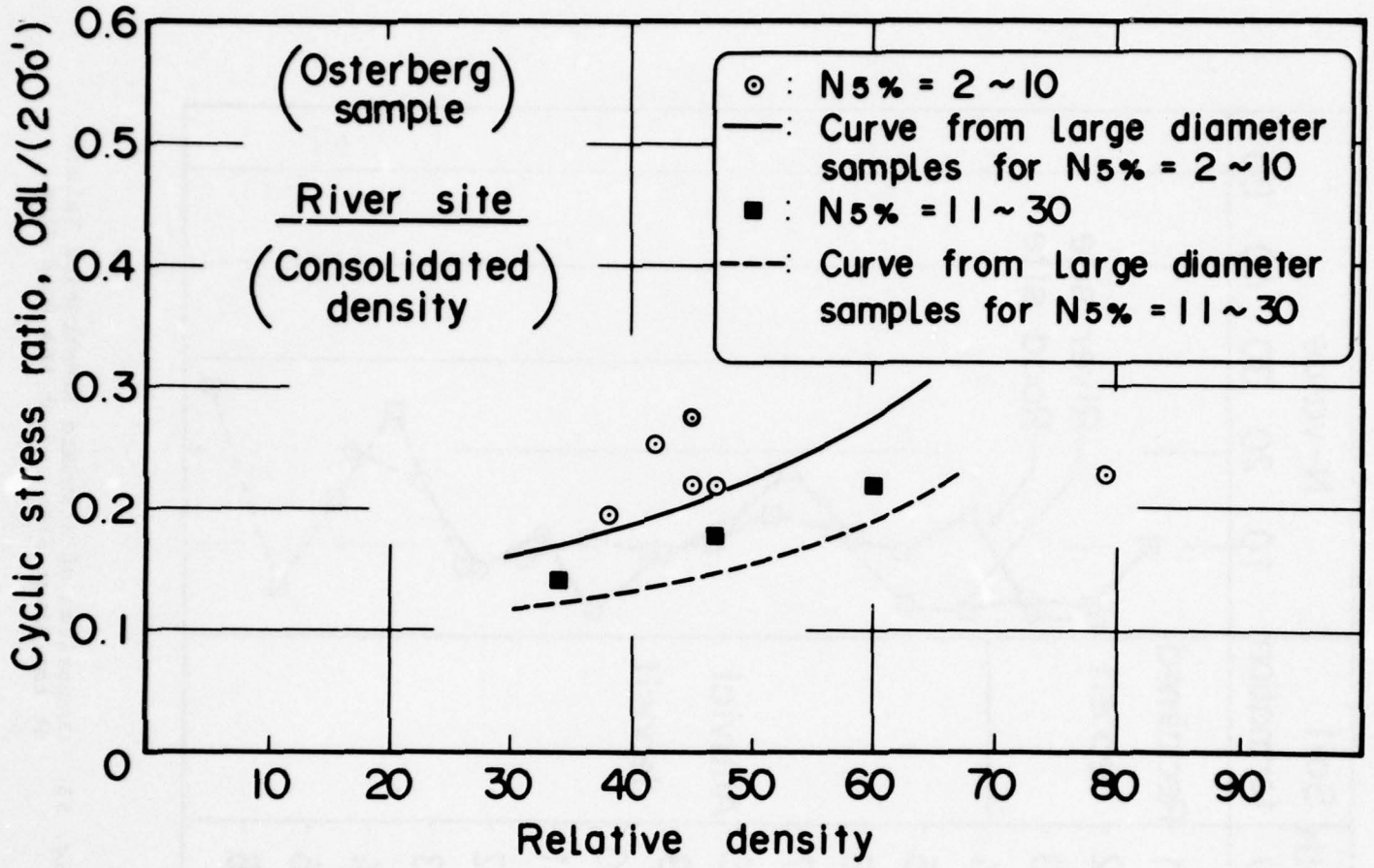

Fig. 52 Comparison Showing the Effect of Relative Density on the Cyclic Triaxial Strength of Specimens from Large Diameter Samples and of Specimens from Osterberg Specimens from the River Site.

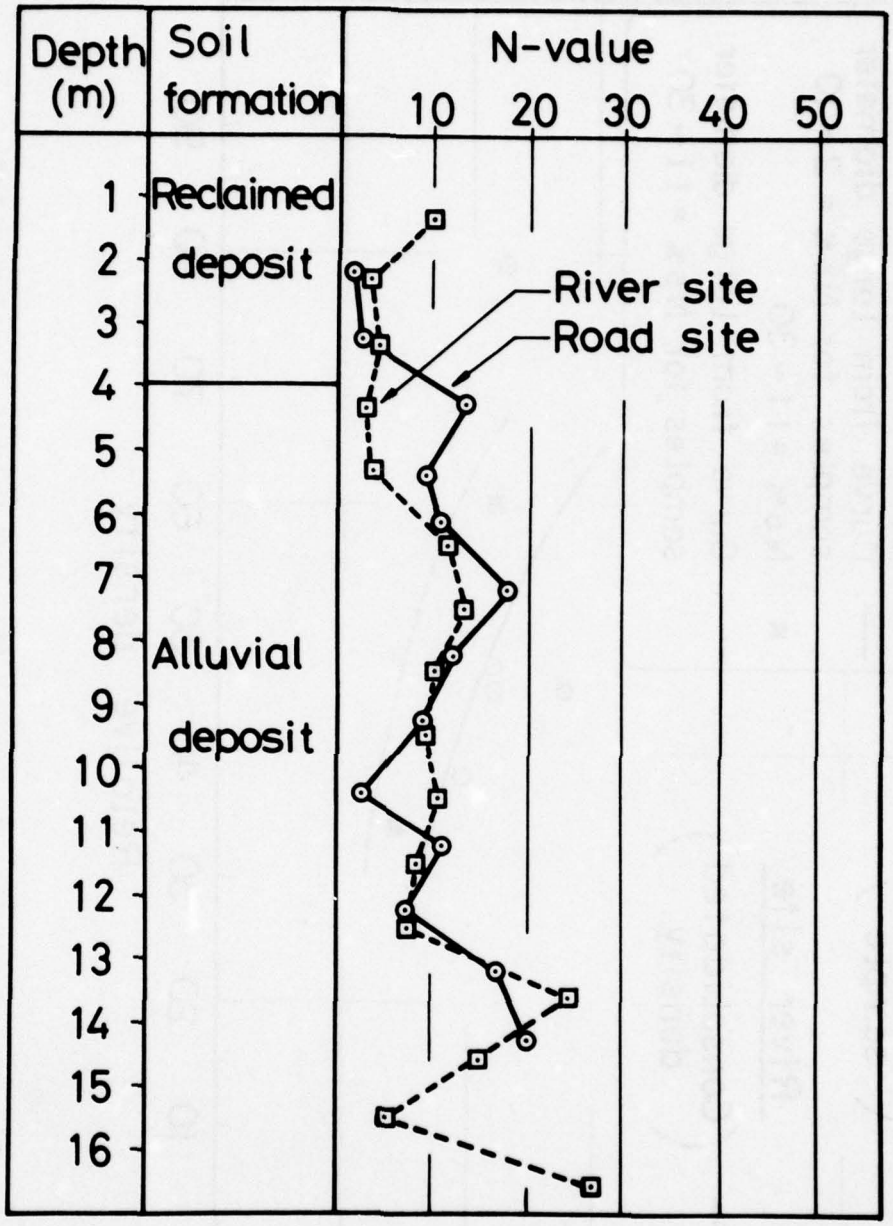

Fig. 53 Comparison of Standard Penetration Values at the River Site and at the Road Site.

penetration values as a function of depth. It should be noted that the surface elevation of the road site was higher than the surface elevation of the river site. Also, the ground water level was 2.5 m lower at the road site than at the river site. Nonetheless, borings indicated that both at the river site and at the road site the boundary between the reclaimed deposit and the alluvial deposit occurred at a depth of 4 m. Therefore, comparisons of standard penetration blow counts and index property values for both sites were made by using the boundary between the reclaimed deposit and alluvial deposit boundary as a marker for both sites.

It may be seen in Fig. 53 that Standard Penetration values are lower at the river site than at the road site to a depth of approximately 8 m. Below this depth, standard penetration values are reasonably equivalent. Since liquefaction is known to have occurred, the decreased penetration resistance at the river site over the road site could possibly be due to the fact that this lower density layer is actually a liquefied layer. Moreover, the equivalent blow counts measured below approximately 9 m may indicate that this zone remained stable both at the river and at the road during the Niigata earthquake.

A further comparison between the river site and the road site is shown first by Fig. 54 which plots the mean soil particle size and second by Fig. 55 which plots the particle

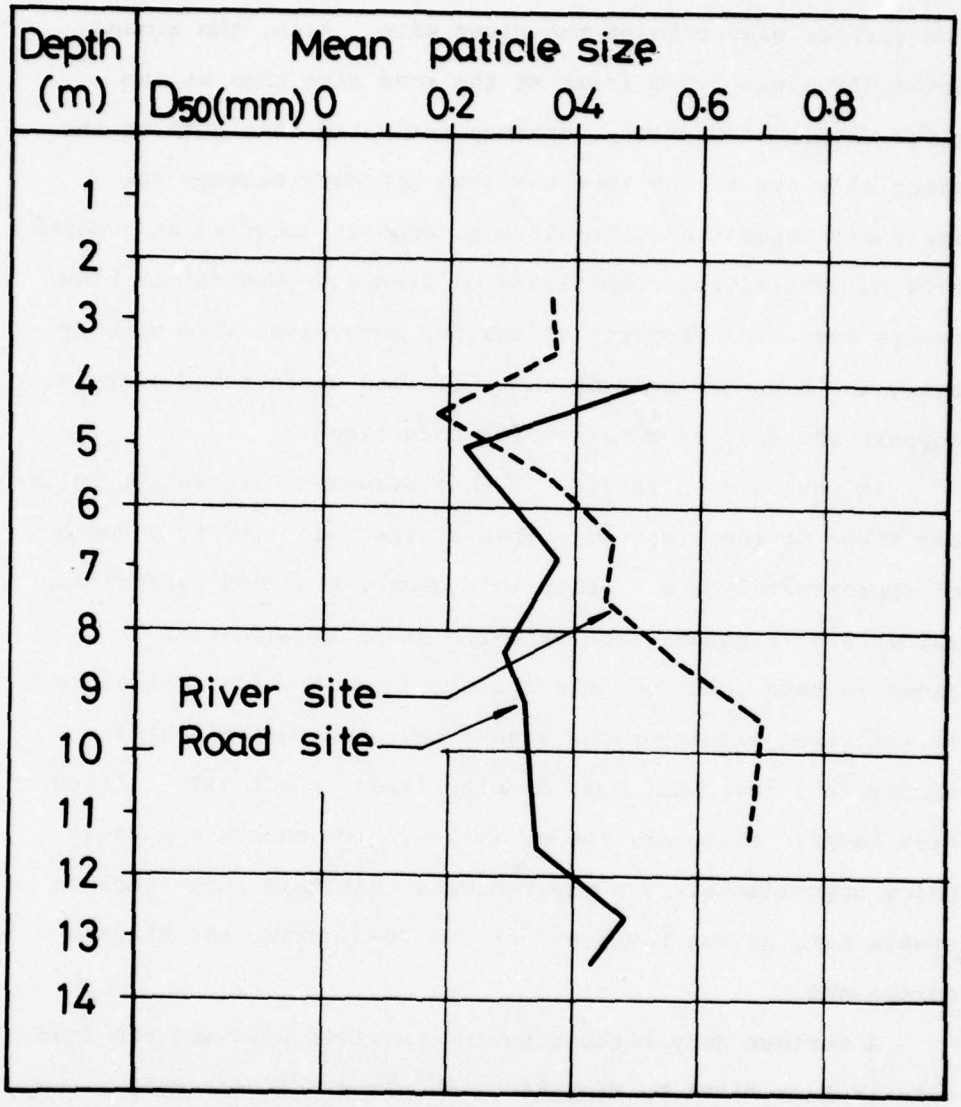

Fig. 54 Comparison of Mean Particle Size with Depth at the River Site and at the Road Site.

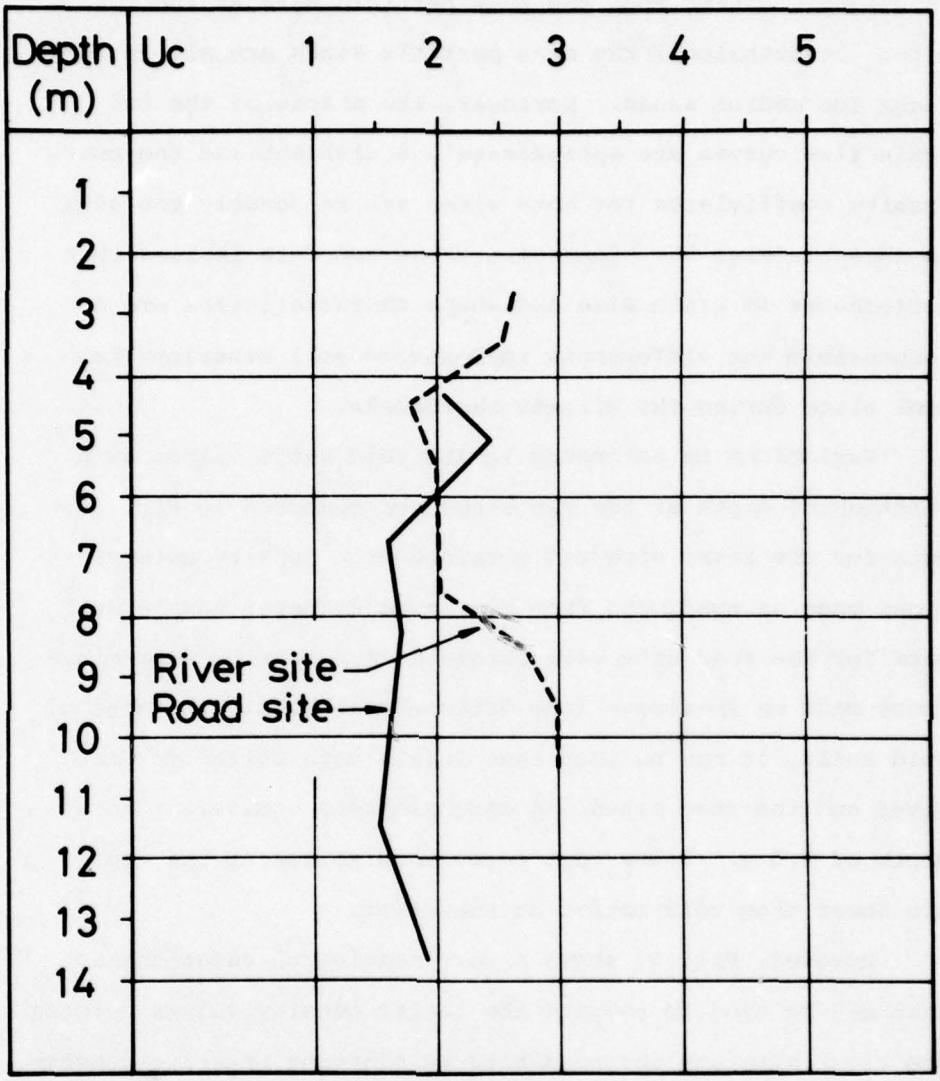

Fig. 55 Comparison of Particle Uniformity Coefficient with Depth at the River Site and at the Road Site.

BLANK PAGE

uniformity coefficient at the two sites as a function of depth. It may be seen that the mean particle size at the river site is slightly higher than the mean particle size at the road site. Nevertheless, the mean particle sizes are all in the range for medium sands. Moreover, the shapes of the two grain size curves are approximately equivalent and the uniformity coefficients for both sites are reasonably the same as shown in Fig. 55. Comparing these two data implies that differences in grain size and shape characteristics are not responsible for differences in measured soil behavior that took place during the Niigata earthquake.

Variations in estimated insitu void ratio values as a function of depth at the two sites are compared in Fig. 56. Data for the river site was obtained from density determinations made on specimens from the large diameter sample while data for the road site were obtained from density determinations made on specimens from Osterberg samples. In terms of void ratio, it may be seen that insitu void ratios for the river and the road sites are approximately equivalent to a depth of 8.5 m. Below that point void ratios at the road are lower than void ratios at the river.

However, Fig. 57 shows a more meaningful relationship that may be used to compare the insitu density values between the river site and the road site by plotting relative density as a function of depth. Here it may be seen that relative

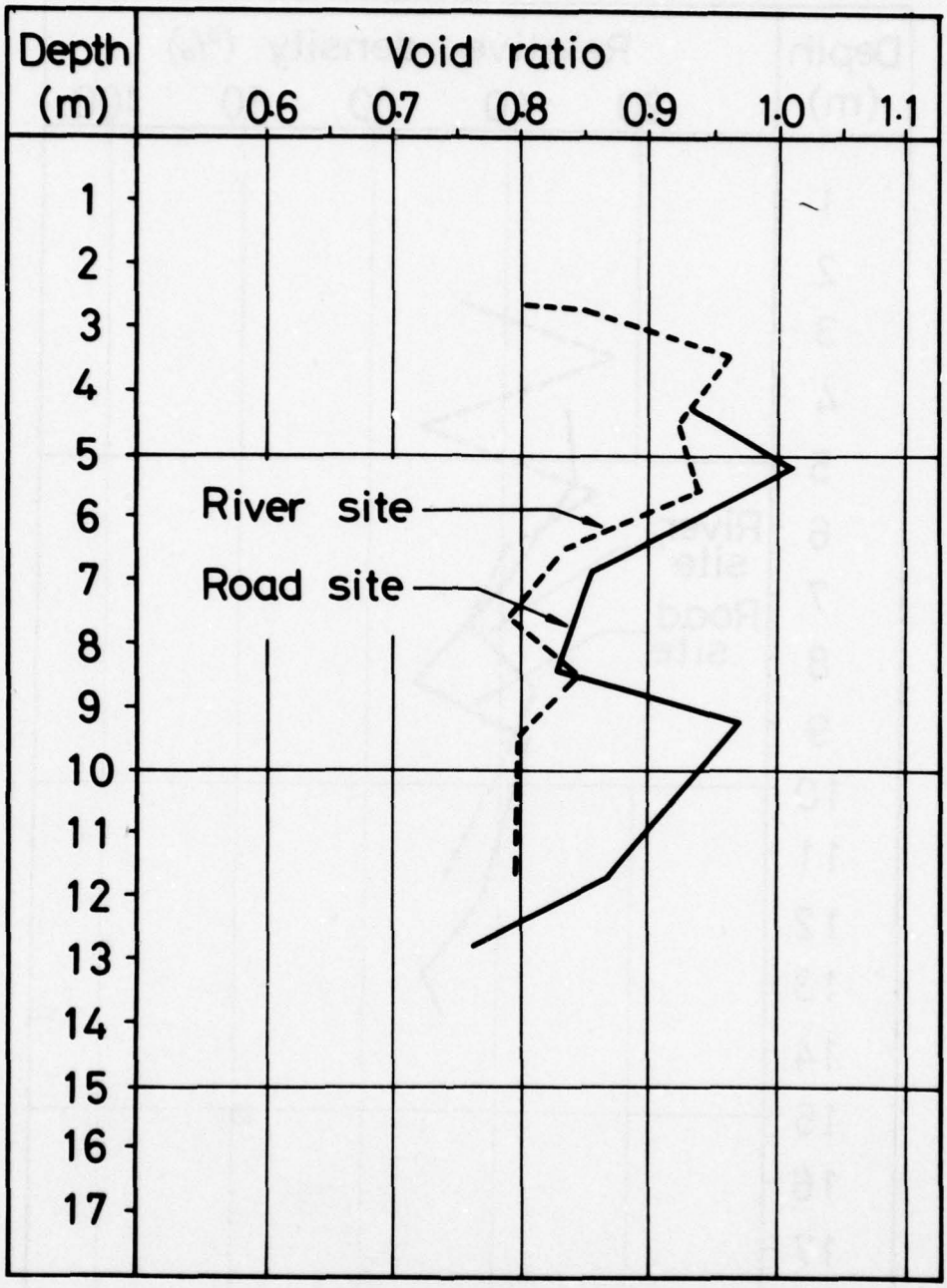

Fig. 56 Comparison of Insitu Void Ratio Values at the River Site and at the Road Site.

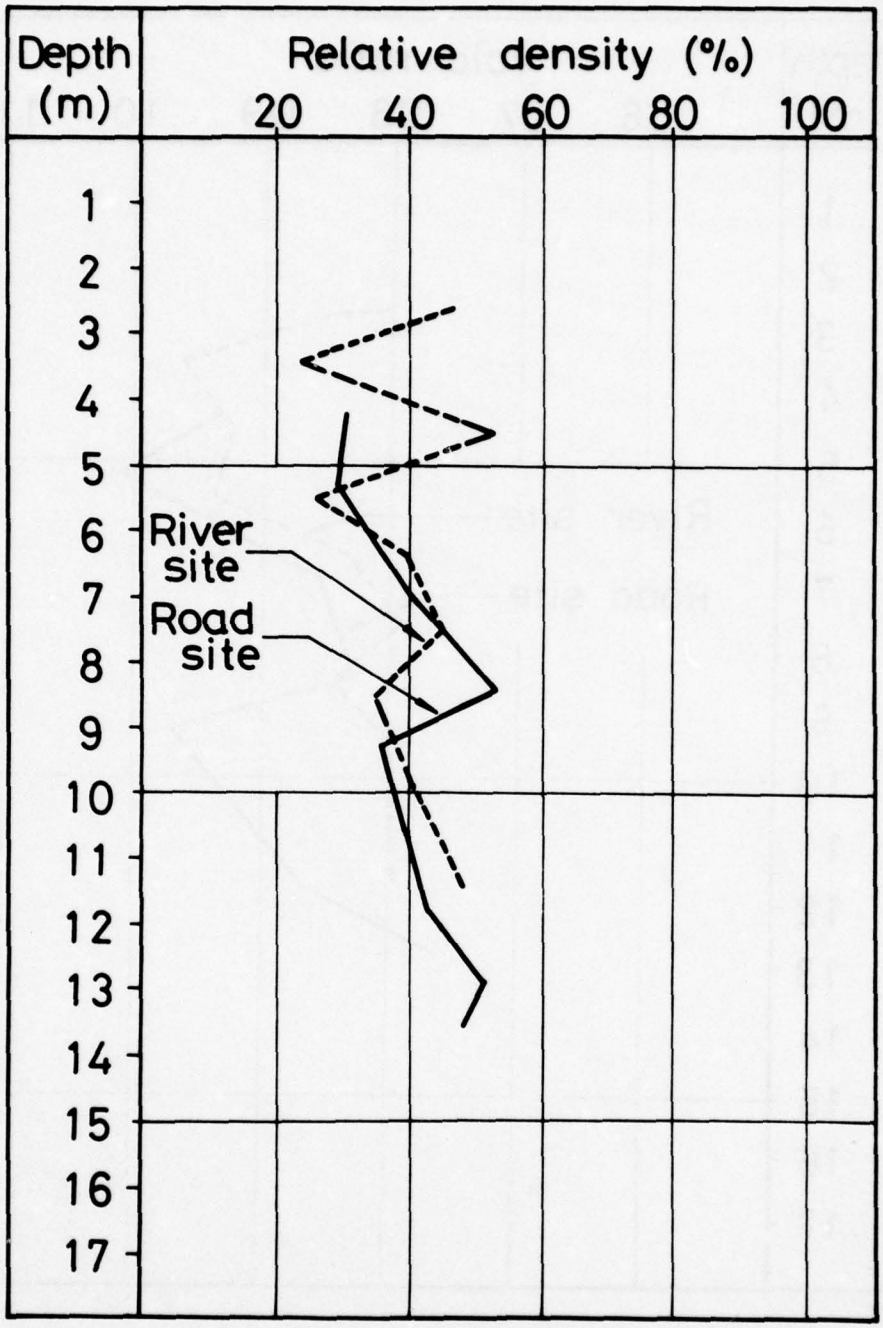

Fig. 57 Comparison of Insitu Relative Density Values at the River Site and at the Road Site.

density values at the road site tend to be a little higher than at the river site. In terms of relative density, both the river and the road seem to have density values on the order of 40%.

Comparison of Cyclic Strength Behavior Between the River Site and the Road Site

The cyclic strength of soil specimens from the road site and from the river site can be compared in a number of ways, such as by comparing the cyclic stress ratios required to cause 5% double amplitude strain as a function of the number of cycles for equivalent values of relative density. This has been done in Fig. 58 which shows that the strength of specimens from both sites are approximately the same at high relative densities (greater than 60%) but that specimens from the road site are stronger at lower relative densities (less than 50%). Nevertheless, the trend is not strong and the difference in strength between the river and the road site does not seem too great.

Another way to compare the strength of specimens from the river site and from the road site is by comparing the stress ratio required to cause failure in a given number of cycles versus the relative density. This has been done in Fig. 59 where it can be clearly seen that specimens from the road site are stronger than specimens from the river site. The reasons for this difference may be due to inherent

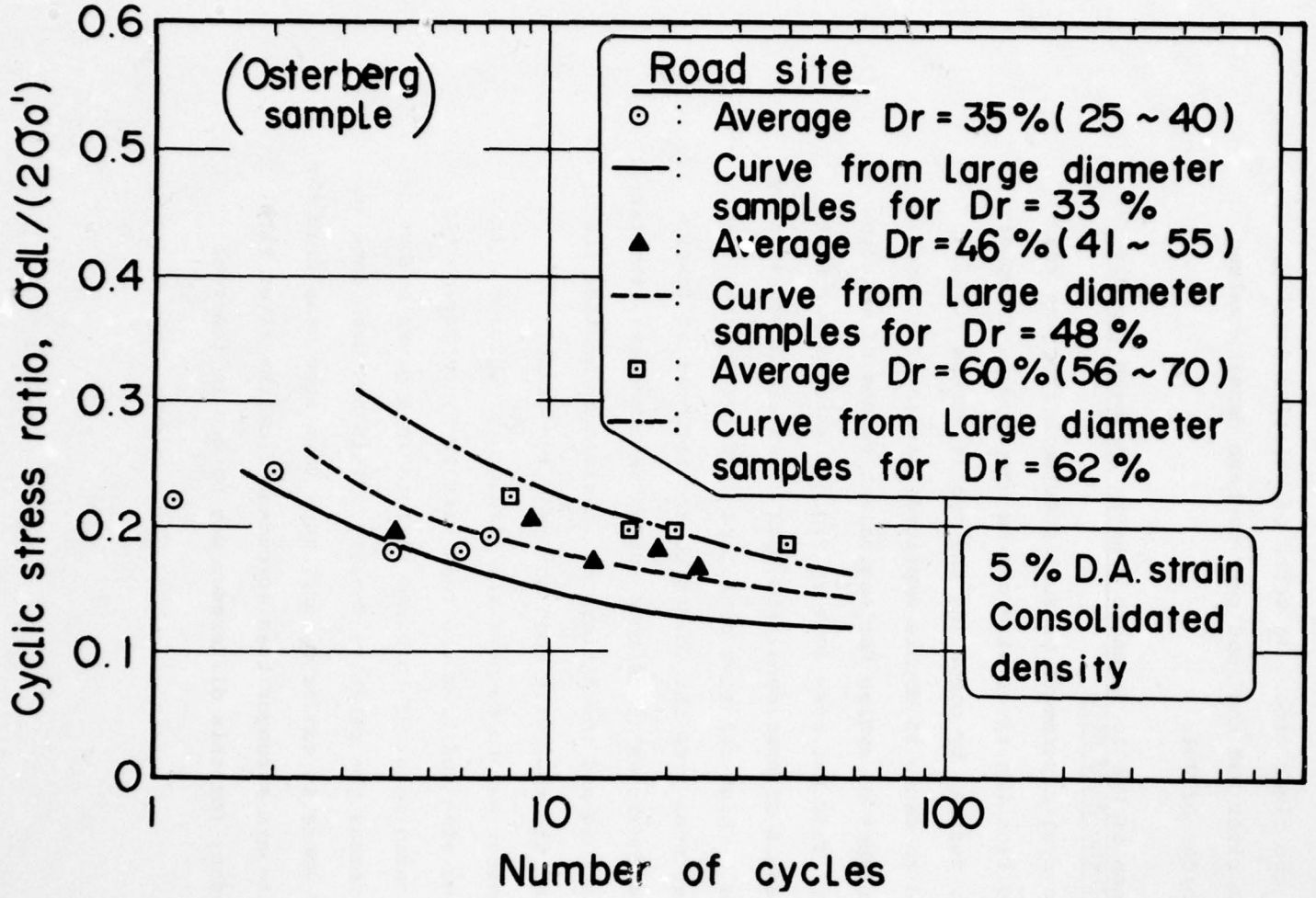

Fig. 58 Comparison of the Cyclic Strength of Undisturbed Specimens from Large Diameter Samples Taken at the River Site and of Specimens Taken from Oesterberg Samples Taken at the Road Site.

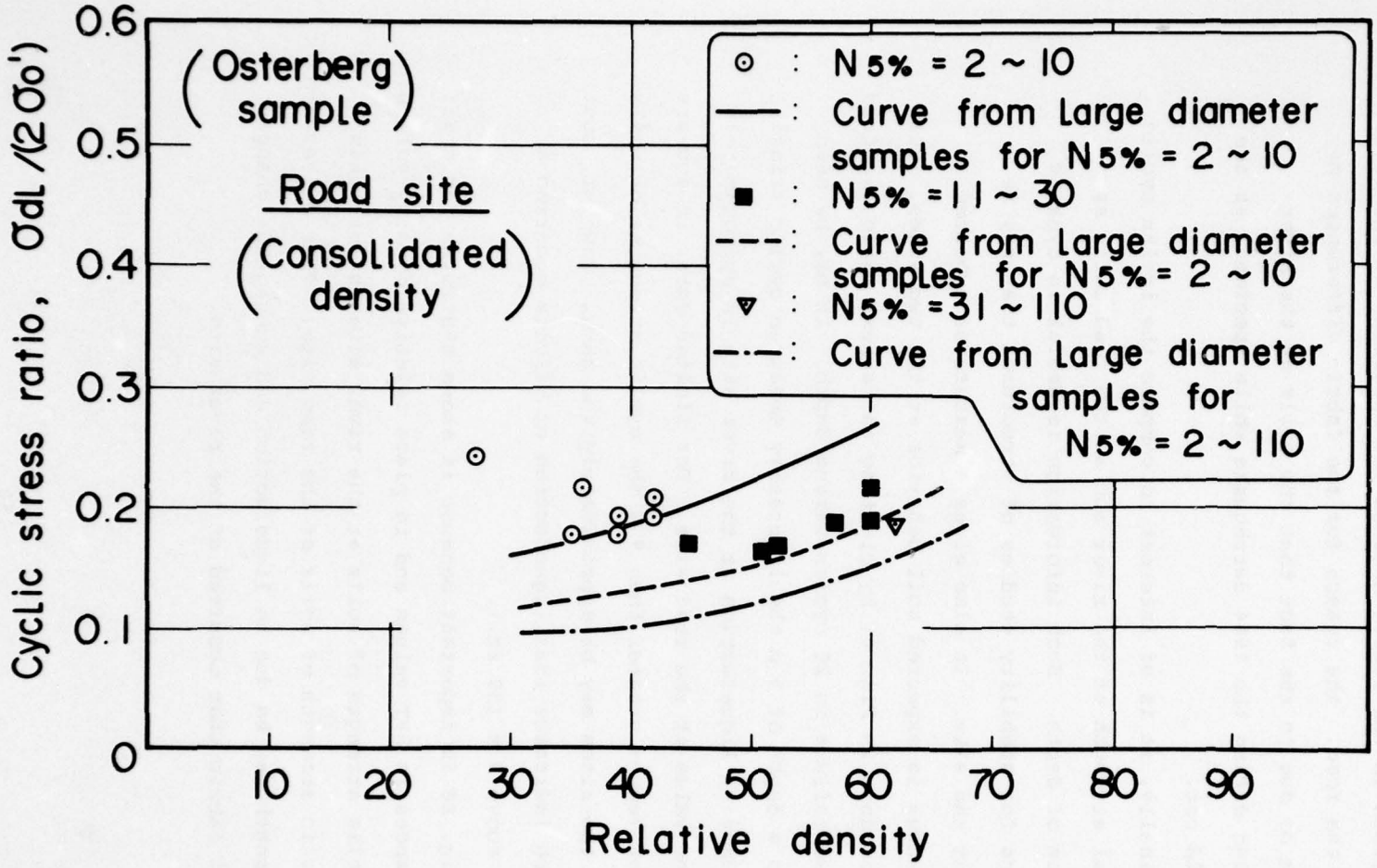

Fig. 59 Comparison Showing the Effect of Relative Density on Cyclic Triaxial Strength of Undisturbed Specimens from Large Diameter Samples at the River Site and of Specimens from Oesterberg Samples at the Road Site.

differences in the fabric between the specimens at the river and at the road. The reason for the fabric differences may in turn be due to the fact that the soils at the river liquefied during the 1964 earthquake while specimens at the road did not.

Finally, it is of interest to compare the insitu cyclic triaxial strength at the river and at the road sites as a function of depth. Such information is useful in dynamic analyses for stability studies of structures that may be built at the site. It also gives a measure of expected differences in expected soil behavior at the two sites. This has been done in Fig. 60 by plotting the stress ratio required to cause failure in 20 cycles versus depth. It may be seen that to a depth of 9 m the laboratory measured cyclic triaxial resistance to liquefaction at the river site is approximately half the value at the road site. For limited data, it appears that for depths greater than 9 m the cyclic strengths of soils at the two sites may be approximately the same. However, most research indicates that liquefaction at Niigata occurred at depths above 9 m (30 ft.).

Fig. 60 is important because it shows that even for small differences in SPT values and in place relative density values, the cyclic strength of soils at the river site is less than the cyclic strength of soils at the road site. This difference in strength may be due to liquefaction and subsequent changes in soil fabric that occurred at the river site.

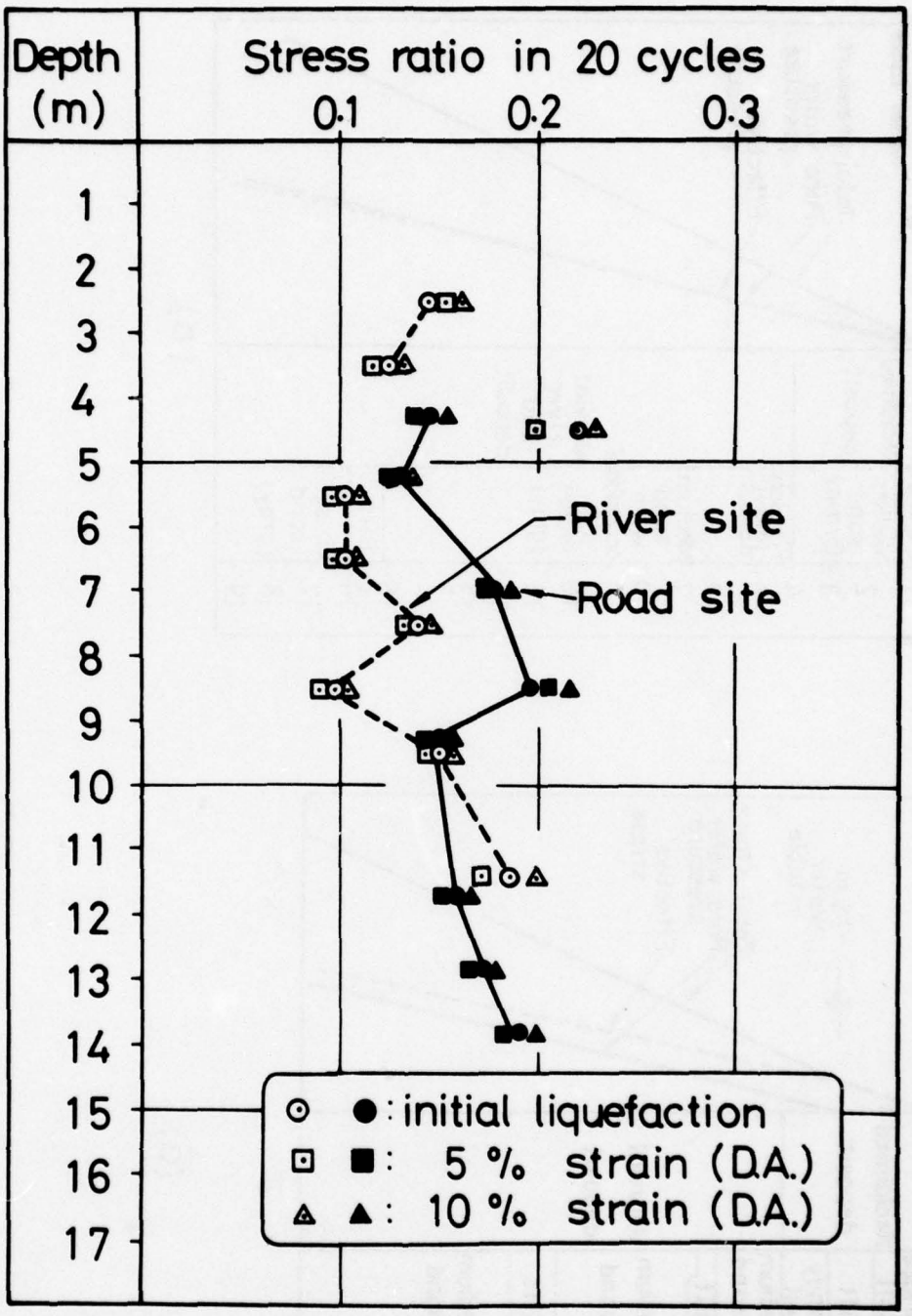

Fig. 60 Comparison of Insitu Cyclic Triaxial Strength (Failure in 20 Cycles) as a Function of Depth at the River Site and at the Road Site.

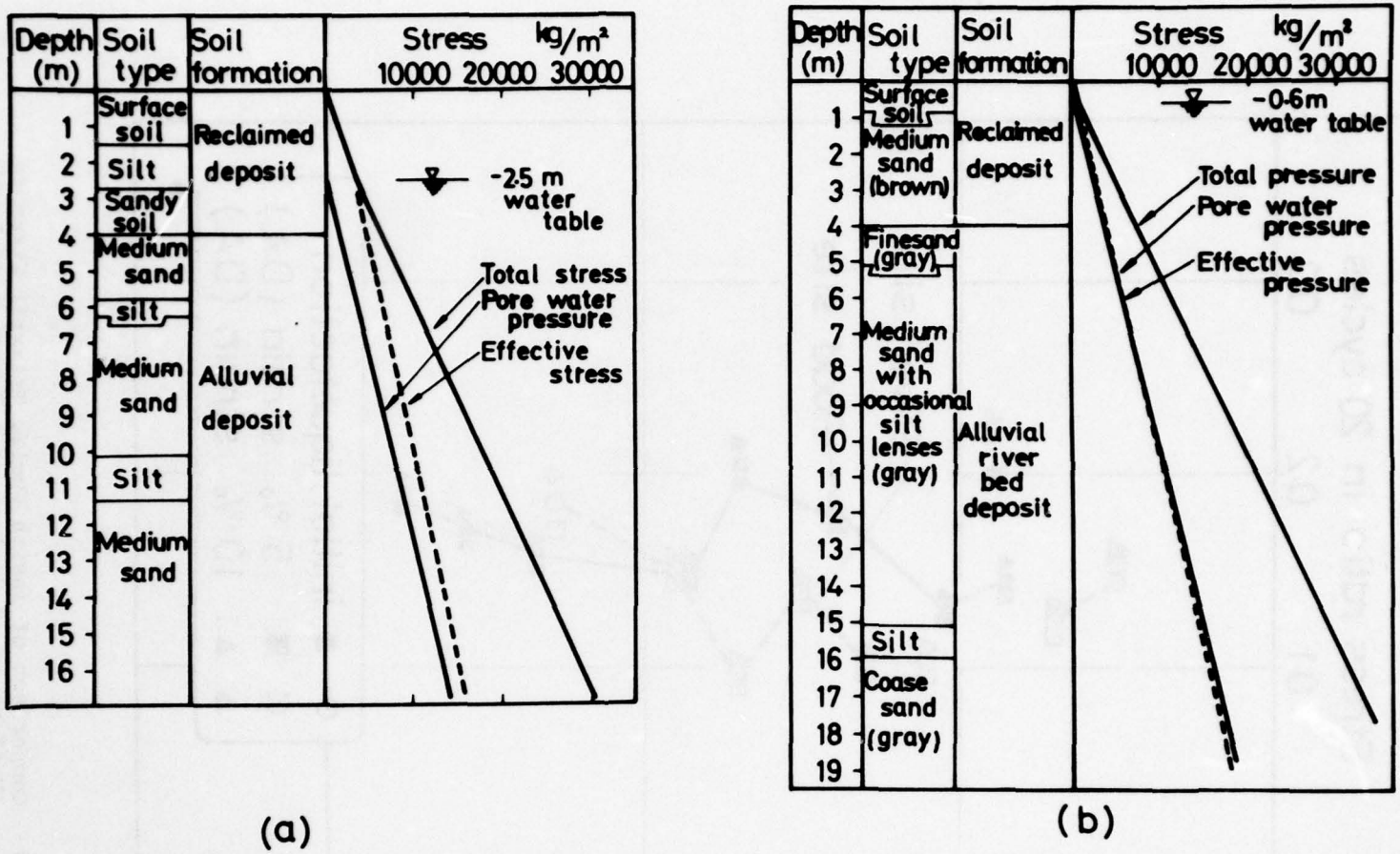

Fig. 61 Distribution with Depth of Total Stress Pore Water Pressure and Effective Stress a) at the Road Site and b) at the River Site.

To further evaluate reasons for the different behavior exhibited by soils at the river site and at the road site, it is important to note that there was a significant difference in ground water elevation at the two sites. This would affect the value of insitu stress as illustrated in Fig. 61 which plots values of total stress, pore water pressure and effective stress with depth both at the road and at the river. Total stresses have been calculated using density values obtained from undisturbed specimens. Pore water pressure values have been calculated assuming that water pressures are hydrostatic.

The effective stress values given in Fig. 61 have been multiplied times the stress ratio required to cause 5% strain in 20 stress cycles given in Fig. 60 for any depth. The resulting values in Fig. 62 plot the value of cyclic axial stress in triaxial tests ($\sigma_{d\ell}$) required to cause failure (5% double amplitude strain) in 30 cycles. The curve clearly shows the effect of confining pressure at the two sites and confirms the initial conclusion of Seed and Idriss (1967) that differences in ground water levels or differences in the height of overburden significantly influenced liquefaction behavior at Niigata.

Correction of SPT Values

It is now generally recognized that it is difficult to compare together SPT values from different sites without

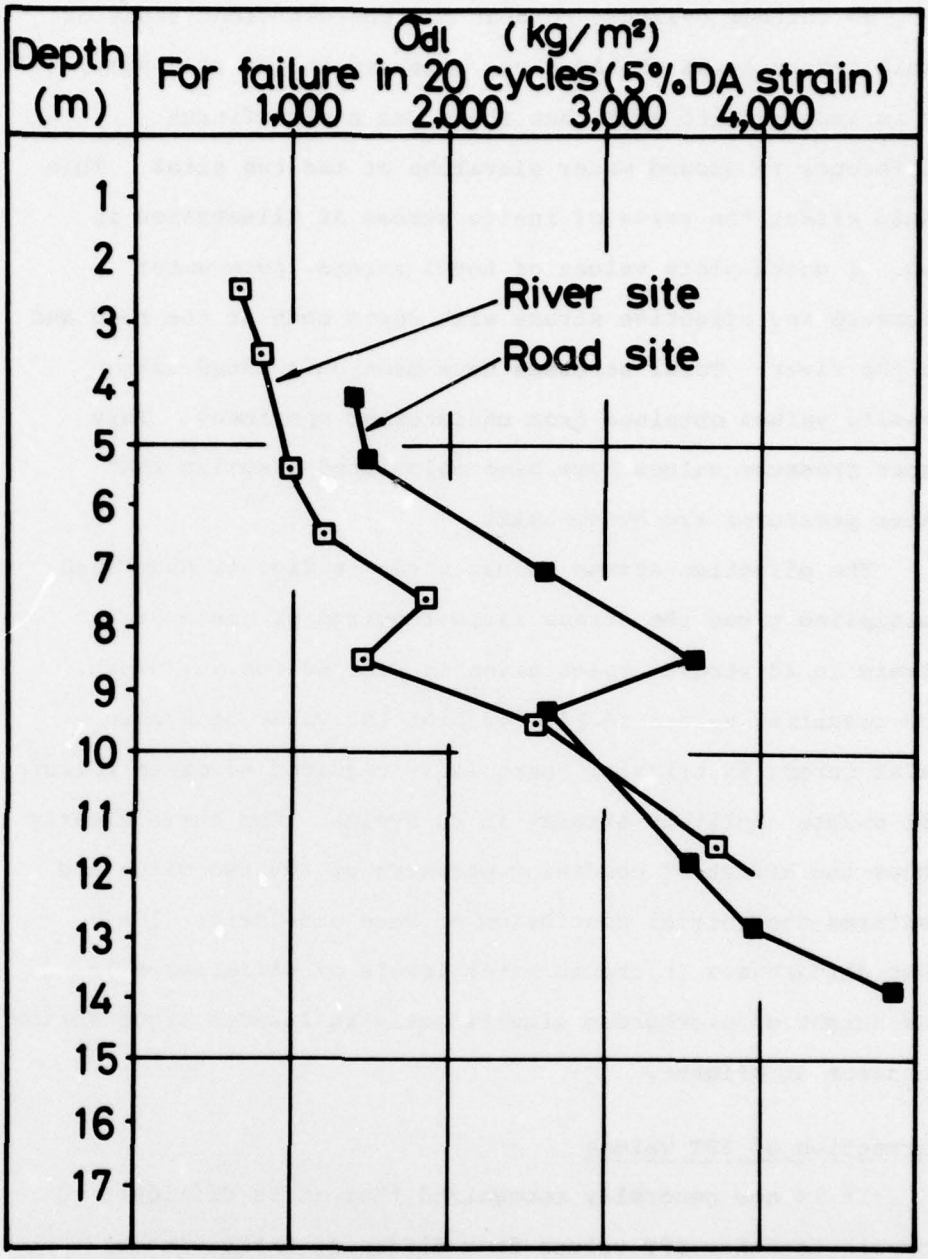

Fig. 62 Comparison with Depth of Cyclic Triaxial Axial Stress Required to Cause Failure in 20 Cycles (5% Double Amplitude Strain) for the Road Site and the River Site.

recognizing that N values are influenced by 1) the field procedures used; 2) the type of soil being sampled and 3) the overburden pressure (Bowles, 1968). However, at both the river site and at the road site, SPT values were obtained by the same boring crew using the same procedure in essentially the same soil deposit. Therefore, any influence of factors 1) and 2) on N values can be ignored.

However, Fig. 61 shows that effective stress with depth at the two sites was not the same because of differences in the ground water level. Moreover, Gibbs and Holtz (1957) have shown that for two cohesionless soils of the same density, the one with the greatest overburden pressure has the higher penetration number. Based on this finding, the following N value correction was proposed

$$N' = N \frac{50}{\sigma_v' + 10}$$

where N' is the corrected SPT test blow count, N is the actual blow count and σ_v' is the effective overburden pressure in lb/in^2.

Both actual N values (blow count) and corrected N values as a function of depth for the river site and for the road site have been plotted in Fig. 63. The effect of overburden pressure is to magnify the small difference in actual N values to become large differences in corrected N values down to about 9 m. At greater depths, both actual and corrected N values are more or less equivalent.

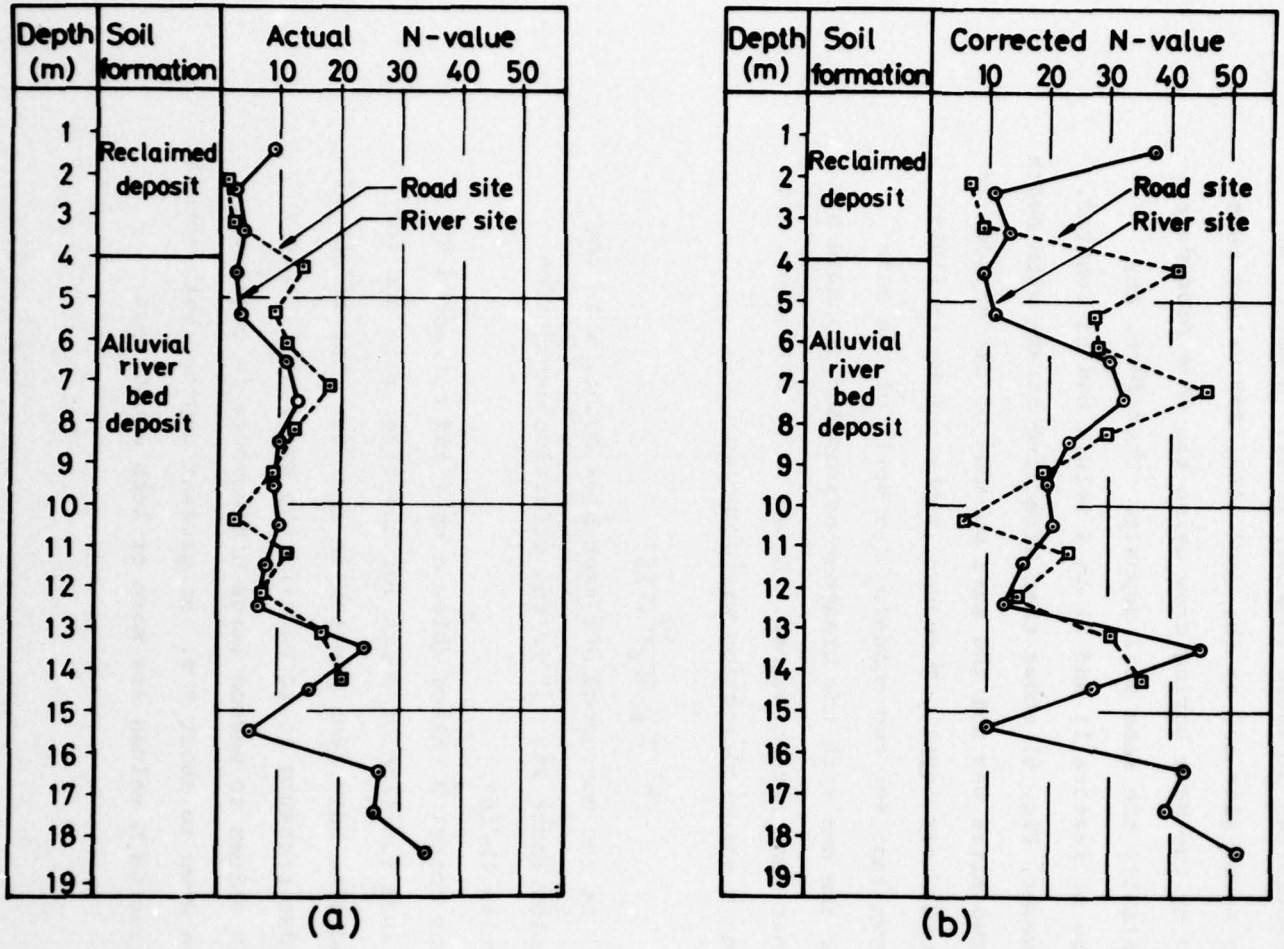

Fig. 63 Comparison of (a) Actual N Values and (b) Corrected N Values at the River Site and at the Road Site.

CHAPTER 9

DISCUSSION, SUMMARY AND CONCLUSIONS

Standard Penetration Tests, undisturbed field sampling, laboratory index property tests and laboratory cyclic triaxial strength tests were performed on cohesionless soils from Niigata, Japan, to determine why some soil deposits failed by liquefaction while apparently similar deposits remained stable during the 1964 earthquake. A further goal of the study was to determine if previously liquefied soils would be more or less susceptible to liquefaction in subsequent earthquakes.

Undisturbed samples for testing were obtained from two relatively close together sites underlain by essentially the same soil layer: a "river site" where there was severe surface evidence of liquefaction following the 1964 earthquake and a "road site" where surface evidence of liquefaction was not observed.

Undisturbed soil sampling was performed with a newly designed Japanese large diameter sampler. The appearance of samples taken with the large diameter sampler were found to be of high quality. Samples showed precise layering with almost no disturbance of lenses of silt or coarse sand. Thus, one of the advantages of this sampling technique is the ability to obtain a large volume of undisturbed sand from below the water table.

One of the disadvantages of using the large diameter sampler is the need for earth anchors to provide a reaction for the sampling process. However, the cost of these anchors may be justified for important projects where large good quality samples are required.

Undisturbed soil samples were also obtained with a U.S. Osterberg sampler so that U.S. and Japanese sampling procedures could be compared.

Field procedures for obtaining small diameter specimens from a large diameter sample were shown to be a meaningful way to avoid sample handling problems. This is especially true if field freezing is also used to immobilize the fabric of the soil. It was found that field freezing with liquid nitrogen and storage of the samples in dry ice was a convenient way to handle and store both large and small specimens. In relatively clean soils which are not susceptible to frost heave, such freezing does not seem to significantly alter the soil fabric or sampled density.

Comparison of standard penetration test values, index property values, and cyclic triaxial strength test values for soils from the two sites showed the following:

1. Insitu relative density values were low at both sites ranging between 20% and 60%. The trend was for relative density values to increase with depth.

2. Cyclic triaxial strength values for undisturbed soil

specimens were not high. Cyclic stress ratios ($\Delta\sigma_{d\ell}/2\sigma'_c$) required to cause failure (defined as 5% double amplitude strain) for 20 stress cycles were on the order of 0.2 for soil specimens at an average relative density of 62% and on the order of 0.14 for soil specimens at an average relative density of 33%.

3. There was an increase in the cyclic strength of undisturbed soil specimens with an increase in relative density. For an increase in relative density from 30% to 60%, the cyclic strength (defined as the stress ratio required to cause 5% double amplitude strain in a given number of cycles) was approximately doubled.

4. At the river site where there was evidence of liquefaction in the 1964 earthquake, there was a tendency for cyclic triaxial strengths to increase for samples from increasing depths. This behavior is consistent with the measured increase in blow counts and the increase in relative density with depth. Further, the site shows low SPT values, low calculated relative density values and low cyclic triaxial strength values. It can therefore be concluded that the river site, if unimproved, will show little resistance to liquefaction in future earthquakes.

5. Based on somewhat limited data, it appears that the cyclic triaxial strength of specimens from large diameter samples and for specimens from Osterberg samples are reasonably equivalent when test results were compared at the same value

of relative density.

6. There was no significant difference in cyclic strength for specimens from either the river site or the road site when test results were compared at the same value of relative density. Nevertheless, even though SPT resistance and insitu density values were not too different at the two sites, the laboratory measured cyclic strength at the river site was about one half the strength at the road site to a depth of about 9 m (30 ft.) (Fig. 67). It is generally believed that liquefaction occurred above this depth. This is indirect evidence that the soil fabric at the river site was different and more susceptable to earthquake induced liquefaction than the soil fabric at the road site.

7. SPT values and relative density values are slightly higher for the road site than for the river site. However, the measured differences were not large. Nevertheless, sand boils, cracking and other surface indications gave clear evidence that soil at the river site liquefied and soil at the road site did not liquefy during the 1964 earthquake. This difference in behavior may in fact be due to higher effective stress with depth at the river site, resulting from a lower water table at the road site than at the river site.

8. In reviewing historical records, it appears that most of the severe earthquake damage from liquefaction at Niigata occurred in areas that have been reclaimed by dumping sand through water.

9. In performing this study, it became clear that any

form of sampling, sample handling, or specimen preparation for relatively clean cohesionless soils weakens the soil by some amount. Therefore, the test results reported herein may be considered as a lower bound on expected field behavior of soils from Niigata.

REFERENCES

Ambraseys, N.N. and Sarma, S., (1969), "Liquefaction of Soils Induced by Earthquakes," Bulletin, Seismological Society of America, Vol. 59, No. 2, April, pp. 651-664.

Bishop, A.W. (1948), "A New Sampling Tool for use in Cohesionless Sands Below the Water Table," Geotechnique, Volume II, pp. 125-131.

Bowles, E., (1968), Foundation Analysis and Design, McGraw-Hill Book Company, New York.

Castro, G., (1969), "Liquefaction of Sands," Harvard Soil Mechanics Series, No. 81, January.

Coffey, D.P., (1967), "Methods of Advancing Boreholes and Taking Disturbed Samples," Proceedings Site Investigation Symposium, Civil Engineering Transactions (Australia), Vol. CEG:1, April, pp. 5-9.

Dixon, S.J. and Burke, J.W., (1973), "Liquefaction Case History," Journal of the SM & FE Div., ASCE, Vol. 99, No. SM 11, November, pp. 921-238.

Fletcher, G.F.A., (1965), "Standard Penetration Test - Its Uses and Abuses," Journal of the SM & FE, ASCE, Vol. 91, No. SM 4, July, pp. 67-75.

Gibbs, H.J. and Holtz, W.G., (1957), "Research on Determining the Density of Sand by Spoon Penetration Testing," Proceedings, 4th International Conference on SM & FE, London, England, Vol. 1, pp. 35-39.

Hanzawa, H. and Matsuda, E, (1978), "Density of Alluvial Sand Deposits Obtained from Sand Sampling," Specialty Session No. 2 on Soil Sampling, Ninth International Conference on Soil Mechanics and Foundation Engineering, Tokyo, Japan, pp. 7-14.

Hvorslev, M.J., (1949), "Subsurface Exploration and Sampling of Soils for Civil Engineering Purposes, SM & FE Division, ASCE.

Ishihara, K, and Silver, M.L., (1977), "Large Diameter Sand Sampling to Provide Specimens for Liquefaction Testing," Soil Sampling, 9th International Conference on Soil Mechanics and Foundation Engineering, Tokyo, pp. 1-6.

Kishida, H., (1969), "Characteristics of Liquefied Sands During Mino Owari, Tohnankai and Fukui Earthquakes," Soils and Foundations (Japan), Vol. 9, No. 1, March, pp. 75-92.

Kuribayashi, E. and Tatsuoka, F., (1975), "Brief Review of Liquefaction During Earthquakes in Japan," Soils and Foundations, Vol. 15, No. 4, December, pp. 81-92.

Ladd, R., (1974), "Specimen Preparation and Liquefaction of Sands," Journal of the Geotechnical Engineering Division, ASCE Vol. 100, No. GT 10, October, pp. 1180-1184.

Lee, K.L. and Seed, H.B., (1967), "Cyclic Stress Conditions Causing Liquefaction of Sand," Journal of the SM & FD, ASCE, Vol. 93, No. SM 1, January 1967, pp. 47-70.

Mulilis, J.P., Horz, R.Z., and Townsend, F.C., (1976), "The Effects of Cyclic Triaxial Testing Techniques on the Liquefaction Behavior of Monterrey No. 0 Sand," Miscellaneous Paper, U.S. Army Corps of Engineers, Waterways Experiment Station, Vicksburg, Mississippi.

Newmark, N.M., (1965), "Effects of Earthquakes on Dams and Embankments," Geotechnique, Vol. 15, No. 2, June, pp. 137-160.

Osterberg, J.O., (1952), "New Piston-Type Soil Sampler," Engineering News Record, April 24, pp. 77-78.

Pan American Conference on Soil Mechanics and Foundation Engineering (1973), Fourth, San Juan, Puerto Rico, Vol. 1-3, ASCE, (Eleven Articles on Insitu Testing and Density Determinations).

Seed, H.B., (1968), "Landslides During Earthquakes," Journal of the Soil Mechanics and Foundations Division, ASCE, Vol. 94, No. SM 5, September, pp. 1053-1122.

Seed, H.B., (1976), "Evaluation of Soil Liquefaction Effects on Level Ground During Earthquakes," Preprint 2752, ASCE Annual Meeting, Philadelphia, Pennsylvania.

Seed, H.B., and Idriss, I.M., (1967), "Analysis of Soil Liquefaction in Niigata Earthquake," Journal of the Soil Mechanics and Foundation Division, ASCE, Vol. 93, No. SM 3, May, pp. 83-108.

Seed, H.B. and Idriss, I.M., (1971), "Simplified Procedures for Evaluating Soil Liquefaction Potential, Journal of the Soil Mechanics and Foundation Division, ASCE, Vol. 97, SM9, pp. 1249-1273.

Seed, H.B., Lee, K.L. and Idriss, I.M., "Analysis of Sheffield Dam Failure," Journal of the Soil Mechanics and Foundation Division, ASCE, Vol. 95, No. SM6, November, pp. 1453-1490.

Seed, H.B., Lee, K.L., Idriss, I.M., and Makdisi, R., "Analysis of Slides in the San Fernando Dams During the Earthquake of February 9, 1971," Report No. EERC 73-2, Earthquake Engineering Research Center, University of California at Berkeley, Berkeley, California, June.

Silver and others (1976), "Cyclic Triaxial Strength of Standard Test Sand," Journal of the Geotechnical Division, ASCE, Vol. 102, No. GT5, May, pp. 511-523.

Silver, M.L., (1977), "Laboratory Triaxial Testing Procedures to Determine the Cyclic Strength of Soils," NUREG 31, U.S. Nuclear Regulatory Commission, Washington, D.C.

Silver, M.L. and Ishihara, K., (1978), "Sampling and Testing of Undisturbed Sands from Niigata, Japan, to Evaluate Insitu Liquefaction Behavior," Report to the U.S. National Science Foundation, Grant No. FJ-1130, Geotechnical Engineering Laboratory, University of Illinois at Chicago Circle, Chicago, Illinois.

U.S. Geological Survey, (1966), "The Alaska Earthquake, March 27, 1964," Geological Survey Professional Paper, 542 A, B, C, D, Washington.

Valera, J.E., and Donovan, N.C., (1977), "Soil Liquefaction Procedures - A Review," Journal of the Geotechnical Engineering Division, ASCE, Vol. 103, No. GT6, Proceedings Paper 12996, June, pp. 607-625.

In accordance with letter from DAEN-RDC, DAEN-ASI dated 22 July 1977, Subject: Facsimile Catalog Cards for Laboratory Technical Publications, a facsimile catalog card in Library of Congress MARC format is reproduced below.

Silver, Marshall L
Cyclic strength of undisturbed sands from Niigata, Japan / by Marshall L. Silver, Department of Materials Engineering, University of Illinois at Chicago Circle, Chicago, Ill. Vicksburg, Miss. : U. S. Waterways Experiment Station ; Springfield, Va. : available from National Technical Information Service, 1978.
xiii, 164 p. : ill. ; 27 cm. (Technical report - U. S. Army Engineer Waterways Experiment Station ; S-78-10)
Prepared for Office, Chief of Engineers, U. S. Army, Washington, D. C., under Contract No. DACW39-76-M-2407.
References: p. 162-164.

1. Cohesionless soils. 2. Cyclic load tests. 3. Dynamic loads. 4. Earthquake engineering. 5. Liquefaction (Soils). 6. Niigata, Japan. 7. Sands. 8. Soil samplers. 9. Soil tests (Laboratory). 10. Standard penetration tests. 11. Undisturbed sampling. I. University of Illinois at Chicago Circle. Dept. of Materials Engineering. II. United States. Army. Corps of Engineers. III. Series: United States. Waterways Experiment Station, Vicksburg, Miss. Technical report ; S-78-10.
TA7.W34 no.S-78-10